NASA
Technical
Paper
2652

February 1987

Piloted Simulator Study of Allowable Time Delays in Large-Airplane Response

William D. Grantham,
Paul M. Smith,
Lee H. Person, Jr.,
Robert T. Meyer,
and Stephen A. Tingas

NASA

NASA Technical Paper 2652

1987

Piloted Simulator Study of Allowable Time Delays in Large-Airplane Response

William D. Grantham
Langley Research Center
Hampton, Virginia

Paul M. Smith
PRC Kentron, Inc.
Hampton, Virginia

Lee H. Person, Jr.
Langley Research Center
Hampton, Virginia

Robert T. Meyer
and Stephen A. Tingas
Lockheed-Georgia Company
Marietta, Georgia

National Aeronautics
and Space Administration

Scientific and Technical Information Branch

Summary

A piloted simulation was performed to determine the permissible time delay and phase shift in the flight control system of a specific transport-type airplane. The joint venture between NASA, the Naval Air Development Center, and the Lockheed-Georgia Company was conducted with the six-degree-of-freedom ground-based Langley Visual/Motion Simulator (VMS) and a math model similar to an advanced Lockheed L-1011 wide-body jet transport. Time delays in a discrete and lagged form were incorporated into the longitudinal, lateral, and directional control systems of the airplane. Three experienced pilots flew simulated approaches and landings with random localizer and glide-slope offsets during instrument tracking as their principal evaluation task. Pilot work load (defined in this report as pilot control activity), performance, and opinion data were collected and analyzed from a total of 355 landings in calm air, crosswinds, and turbulent air conditions.

The results indicated that the MIL-F-8785C criteria governing allowable control system time delay and phase shift are somewhat restrictive for level 1 (satisfactory) handling qualities when applied to the tested transport-size airplane. Past tests had also shown current criteria to be much too stringent. The roll axis appears to be more critical than the pitch and yaw axes in the approach and landing phase and should be characterized by a quicker response to cockpit commands. Present military criteria fail to differentiate between axes for any pilot rating level of handling qualities (level 1—satisfactory, level 2—acceptable but unsatisfactory, and level 3—unacceptable) for time delay and phase shift. Results of the present study suggest a level 1 handling qualities limit for an effective time delay of 0.15 sec in both the longitudinal and lateral axes, as opposed to a 0.10-sec limit of the present specification for both axes. Also, results of the present study suggest a level 2 handling qualities limit for an effective time delay of 0.82 sec and 0.57 sec for the longitudinal and lateral axes, respectively—as opposed to 0.20 sec of the present specifications. In the area of phase shift between cockpit input and control surface deflection, the present specification states that the response of the control surfaces in flight shall not lag the cockpit control force inputs by more than 15° for a level 1 handling qualities airplane in the approach and landing flight phase. Results of the present study, flown in turbulent air, suggest less severe phase shift limitations for the approach and landing task—approximately 50° in pitch and 40° in roll.

Although airplane control systems are characterized by a combination of delays in both discrete (pure) and lagged forms, it was interesting to note the effect of each on handling qualities. It appears that pilots are better able to manage a lag than a discrete delay because with a lag the pilot can detect an airplane response as soon as an input command is made, whereas with a discrete delay the total airplane response is delayed for a prescribed length of time. Not surprisingly, it was found that there is a direct relationship between the work load required to perform a certain task and the pilot opinion ratings. The harder the pilot had to work in tracking glide slope and localizer, the lower his opinion became of the handling qualities.

Introduction

The present military specification (ref. 1) is recognized as being inadequate in the designation of requirements and criteria for handling qualities of large class III (transport) airplanes; and recent efforts by the National Aeronautics and Space Administration (NASA) and the Department of Defense (DOD) include studies in specific areas related to this problem. The requirements of reference 1 are, in general, based on data that were acquired prior to the mid-1960's when large-airplane data (in terms of current large-airplane size and weight) were virtually nonexistent. Since the majority of data available were for small airplanes, it was inevitable that the specifications would reflect primarily small-airplane characteristics; and in many cases, requirements were developed to ensure that objectionable characteristics, discovered in small airplanes, would not appear in new airplanes.

An inadequate data base for large airplanes has led to some problem areas—one of which is *allowable time delays in airplane response.* Early airplanes had a direct mechanical link between the cockpit controller and the control surface. The system was quite fast with the principal sources of lag being friction, free play, and cable stretch. With the advent of fully powered, highly augmented control systems, lags introduced by the dynamics of the control system became important.

It is known that control system dynamics, as well as open-loop airplane dynamics, affect the handling qualities of the closed-loop pilot and airplane combination. (See ref. 2.) The effect of control system dynamics is to raise the order of the airplane response to pilot control inputs. For example, the basic (open-loop, unaugmented) longitudinal airplane response (angle of attack, pitch attitude, normal acceleration, etc.) are fourth order for elevator control inputs. However, the dynamics of the elevator response to

control stick displacements and the response of stick displacements to stick forces will increase the order of the airplane response to pilot stick force inputs—and these characteristics affect the pilot's closed-loop control significantly and alter his evaluation of particular airplane characteristics. Furthermore, the characteristic digital computation delays of advanced fly-by-wire control systems compound the problem even further.

The pilot-induced oscillation (P.I.O.) tendencies produced by these additional control system delays have led to a military specification (ref. 1) limiting the amount of time delay in a flight control system. For example, the maximum allowed time delay in the flight control system of an airplane (regardless of airplane size or intended mission) for level 1 (satisfactory) handling qualities is 0.1 sec. Many current large airplanes having good flying qualities have transport lags much greater than 0.1 sec. In addition, previous industry and government experiments (refs. 3 and 4) utilizing large airplanes have indicated that time delays much greater than 0.1 sec could be experienced before pilot ratings deteriorated beyond the *satisfactory* region. It is therefore believed that the present criteria for maximum allowable time delay are too stringent when applied to large airplanes, whose large inertias result in maneuvering requirements and piloting tasks markedly different from those of fighter-class airplanes, and that this needless imposition of structural and actuation capabilities on these large airplanes can make their design expensive and operationally inefficient.

Piloted simulation appeared to be an effective and cost-efficient method of obtaining the large amount of data necessary to determine what limits of permissible control system time delay should be imposed on large class III airplanes. Therefore, the objective of this study was to build on the existing large-airplanes data base in the area of control system delays and to utilize the results as the basis for suggested allowable response time delays for the various levels of handling qualities. The present criteria for allowable phase shift between cockpit input and control surface deflection (ref. 1) also appear to be too stringent when compared with previous studies of large airplanes and are, therefore, also addressed in this study. A comparison of the results of the present study with those from previous experiments on the pilot opinion of allowable flight control system delays is presented in this paper.

Symbols and Terminology

Measurements and calculations were made in U.S. Customary Units, and all calculations are based on the airplane body axes. Dots over symbols denote differentiation with respect to time.

A	dead band for aileron-to-rudder interconnect
b	span, ft
C_L	lift coefficient
C_{L_α}	lift-curve slope per unit angle of attack
C_l	rolling-moment coefficient
C_m	pitching-moment coefficient
C_n	yawing-moment coefficient
C_X	longitudinal-force coefficient
C_Y	side-force coefficient
C_Z	vertical-force coefficient
$\bar{c}$	mean aerodynamic chord, ft
F_c	column force, lbf
f	cockpit-control input frequency, rad/sec
g	acceleration due to gravity, $1g \approx 32.17$ ft/sec^2
h	altitude, ft
K_A	gain for aileron-to-rudder interconnect
K_r	yaw-damper gain
K_s	feel-spring gain
L_α	$= C_{L_\alpha}\left(\frac{\bar{q}S}{mV}\right)$, per second
m	airplane mass, slugs
n/α	steady-state normal acceleration change per unit change in angle of attack for incremental horizontal-tail deflection at constant airspeed, g units/rad
P_d	period of Dutch roll oscillation, sec
P_{ph}	period of longitudinal phugoid oscillation, sec
P_{sp}	period of longitudinal short-period oscillation, sec
p, q, r	rolling, pitching, and yawing angular velocities, respectively, rad/sec
$\bar{q}$	dynamic pressure, lbf/ft^2
s	Laplace operator
t	time, sec

t_1 effective time delay, intersection of pitch-rate-response maximum-slope tangent line and zero amplitude line, sec

t_{s_2} time to double amplitude of spiral mode, sec

u, v, w components of resultant velocity along longitudinal, lateral, and vertical body axes, respectively

V airspeed, knots

α angle of attack, deg

β angle of sideslip, deg

δ_a aileron deflection, positive for right roll command, deg

$\delta_{a,s}$ asymmetric deflection of spoilers for roll control, driven by aileron deflection and positive for right roll command, deg

δ_c total column deflection, in.

δ_{col} software stick position, in.

δ_e elevator deflection with elevator geared to horizontal tail (pilot flies horizontal tail), deg

δ_f trailing-edge flap deflection, deg

δ_H horizontal-tail deflection with elevator geared to horizontal tail (pilot flies horizontal tail), deg

δ_{HT} horizontal-tail deflection, deg

δ_p pedal deflection, deg

δ_r rudder deflection, deg

δ_s spoiler deflection, deg

δ_w control-wheel deflection, deg

ζ_d Dutch roll mode damping ratio

ζ_{ph} longitudinal phugoid-mode damping ratio

ζ_{sp} longitudinal short-period mode damping ratio

θ angle of pitch, deg

ρ correlation coefficient

σ standard deviation

τ time constant, sec

τ_R roll-mode time constant, sec

ϕ angle of roll, deg

ψ heading angle, deg

ω_d undamped natural frequency of Dutch roll oscillation, rad/sec

ω_{ph} undamped natural frequency of phugoid mode, rad/sec

ω_{sp} longitudinal short-period undamped natural frequency, rad/sec

ω_ϕ undamped natural frequency appearing in numerator quadratic of ϕ/δ_a transfer function, rad/sec

Derivatives:

$$C_{L_{\dot\alpha}} = \frac{\partial C_L}{\partial \frac{\dot\alpha \bar c}{2V}} \qquad C_{\imath_\beta} = \frac{\partial C_\imath}{\partial \beta}$$

$$C_{m_{\dot\alpha}} = \frac{\partial C_m}{\partial \frac{\dot\alpha \bar c}{2V}} \qquad C_{\imath_{\delta_r}} = \frac{\partial C_\imath}{\partial \delta_r}$$

$$C_{Y_{\delta_a}} = \frac{\partial C_Y}{\partial \delta_a} \qquad C_{Z_{\delta_H}} = \frac{\partial C_Z}{\partial \delta_H}$$

$$C_{Y_{\delta_{a,s}}} = \frac{\partial C_Y}{\partial \delta_{a,s}} \qquad C_{Z_{\delta_e}} = \frac{\partial C_Z}{\partial \delta_e}$$

$$C_{Y_\beta} = \frac{\partial C_Y}{\partial \beta} \qquad C_{\imath_p} = \frac{\partial C_\imath}{\partial \frac{pb}{2V}}$$

$$C_{Y_{\delta_r}} = \frac{\partial C_Y}{\partial \delta_r} \qquad C_{\imath_r} = \frac{\partial C_\imath}{\partial \frac{rb}{2V}}$$

$$C_{X_{\delta_H}} = \frac{\partial C_X}{\partial \delta_H} \qquad C_{n_{\delta_a}} = \frac{\partial C_n}{\partial \delta_a}$$

$$C_{X_{\delta_e}} = \frac{\partial C_X}{\partial \delta_e} \qquad C_{n_{\delta_{a,s}}} = \frac{\partial C_n}{\partial \delta_{a,s}}$$

$$C_{Y_p} = \frac{\partial C_Y}{\partial \frac{pb}{2V}} \qquad C_{n_\beta} = \frac{\partial C_n}{\partial \beta}$$

$$C_{Y_r} = \frac{\partial C_Y}{\partial \frac{rb}{2V}} \qquad C_{n_{\delta_r}} = \frac{\partial C_n}{\partial \delta_r}$$

$$C_{L_q} = \frac{\partial C_L}{\partial \frac{q \bar c}{2V}} \qquad C_{m_{\delta_H}} = \frac{\partial C_m}{\partial \delta_H}$$

$$C_{m_q} = \frac{\partial C_m}{\partial \frac{q \bar c}{2V}} \qquad C_{m_{\delta_e}} = \frac{\partial C_m}{\partial \delta_e}$$

$$C_{\imath_{\delta_a}} = \frac{\partial C_\imath}{\partial \delta_a} \qquad C_{n_p} = \frac{\partial C_n}{\partial \frac{pb}{2V}}$$

$$C_{\imath_{\delta_{a,s}}} = \frac{\partial C_\imath}{\partial \delta_{a,s}} \qquad C_{n_r} = \frac{\partial C_n}{\partial \frac{rb}{2V}}$$

Subscripts:

col column

com	command
i	inboard
lat	lateral
long	longitudinal
max	maximum
o	output
ol	outboard left
or	outboard right
p	pilot
s	spoiler
ss	steady state
str	stretch
td	touchdown
trim	value for trim flight condition
u	uprig

Abbreviations:

alt	altitude
c.g.	center of gravity
DOD	Department of Defense
EAS	equivalent airspeed
FCS	flight control system
fwd	forward
GS	glide slope
IFR	instrument flight rules
ILS	instrument landing system
LOC	localizer
MTC	Mach trim compensation
P.I.O.	pilot-induced oscillation
PR	pilot rating (opinion)
rms	root mean square
SAS	stability augmentation system
VFR	visual flight rule
VMS	Langley Visual/Motion Simulator
WL	work load

Categories:

A	nonterminal flight phases that require precision tracking, such as in-flight refueling
B	nonterminal flight phases normally accomplished using gradual maneuvers, such as cruising flight
C	terminal flight phases that require accurate flight path control, such as approach and landing

Description of Simulated Airplane

The baseline simulation is a full, nonlinear, six-degree-of-freedom model of a modified version of the Lockheed L-1011 airplane developed during energy-efficient transport studies at the Langley Research Center. The L-1011 is a current generation, subsonic, commercial transport airplane (fig. 1). The airplane is powered by three Rolls-Royce RB, 211-22B high-bypass-ratio turbofan engines and has a flying stabilizer with a geared elevator. Airplane geometry and weight data are presented in table I.

The simulated L-1011 uses the elevator and stabilizer for longitudinal control, the inboard and outboard ailerons and spoilers for lateral control, and the rudder for directional control. The basic longitudinal control system includes servoactuator, cable stretch, and position and rate-limiter modeling. The lateral control system also includes servoactuator and position-limiter modeling, and it should be noted that only four outboard spoiler panels (2, 4, 5, and 6) are modeled for lateral control. The directional control system determines manual and SAS contributions to the rudder position. The directional SAS consists of a yaw damper (yaw-rate gyro offset 2°) and a wheel-driven aileron/rudder interconnect for improved turn coordination. Servoactuator and rate- and position-limiter modeling were used.

Block diagrams of the longitudinal and lateral-directional control systems of the simulated airplane are presented in figure 2. Figure 2(c) indicates the position in the control loop at which the subject "additional" time delays were inserted for the present study. A partial listing of the aerodynamic data used in the modeling of the simulated airplane are presented in table II, and the dynamic stability characteristics of the simulated airplane in the landing flight condition are presented in table III. Table II presents three columns of spoiler derivatives that were computed from aileron deflection data and obtained by summing the inboard and outboard spoiler results. Plotting the spoiler contributions to C_Y, C_l, and C_n versus aileron deflection and angle of attack produced linear derivatives starting at aileron deflections of approximately 18°. (That is, for aileron deflections from 0° to 18°, there is a negligible spoiler contribution to C_Y, C_l, and C_n.) The ratio of spoiler derivative between outboard and inboard ailerons is

approximately 20 percent, and thus the appropriate spoiler calculations can be made. This is not the manner in which the computations are made within the L-1011 math model. Even though the math model does not use derivatives, the authors chose to use derivatives to minimize the amount of tabulated data presented.

The basic C_X, C_Z, and C_m data for the simulated transport (see table II) include the landing gear increments because this was the way that the simulated airplane was "flown."

Description of Simulation Equipment

The simulation study was made using the general-purpose cockpit of the Langley Visual/Motion Simulator (VMS), which is a ground-based motion simulator with six degrees of freedom. For this study, the VMS had a transport-type cockpit equipped both with conventional flight and engine-thrust controls and with a flight-instrument display representative of those found in current transport airplanes. (See fig. 3.) Instruments that indicated angle of attack, angle of sideslip, flap angle, horizontal stabilizer angle, and column force were also provided.

The control forces on the wheel, column, and rudder pedals were provided by a hydraulic system coupled with an analog computer. The system allows for the usual variable-feel characteristics of stiffness, damping, coulomb friction, breakout forces, detents, and inertia. The airport scene display used for landing was an "out-the-window" virtual image system of the beam-splitter, reflective-mirror type. (See fig. 4.) The motion performance characteristics of the VMS system possess time lags of less than 60 msec. A nonstandard washout system utilizing nonlinear coordinated adaptive motion was used to present the motion-cue commands to the motion base. (See ref. 5.) A runway "model" was programmed that had a width of 200 ft, a total length of 11 500 ft, roughness characteristics, and a slope from the center to the edge representing a runway crown. Only a dry runway was considered in this study. The only aural cue provided was engine noise.

Tests and Procedures

Approaches were flown under three types of atmospheric conditions: calm air, crosswind, or turbulent air. Those flown in turbulence were subjected to 6 ft/sec rms gust levels in all three airplane axes. The crosswind magnitude was a constant 15 knots normal to the runway and could be modeled from either direction.

Three research test pilots, with varying degrees of flying experience with large transport airplanes, flew simulated approaches and landings since this task is generally believed to be the most critical as related to handling qualities of transport-class airplanes. The approaches were initiated approximately 10 miles from the runway at an altitude of 2000 ft and were flown under IFR conditions down to a 300-ft altitude. An initial offset from the localizer and the random glide slope and localizer offsets during tight instrument tracking forced the pilot into relatively severe maneuvers. These random offset corrections, activated by the onboard engineer, were intended to bring out any handling qualities deficiencies of the configuration being tested. At an altitude of 300 ft, the airplane broke out of the simulated overcast into VFR conditions, and the pilot performed a visual landing. A raw deviation (glide slope and localizer) tracking method was used since it was believed that the use of a flight director may have a tendency to mask some handling qualities deficiencies of the airplane by "simplifying" the piloting task.

The pilots were initially asked to fly a minimum of two approaches for each configuration tested and then complete both an evaluation form (table IV) soliciting pilot comments and a Cooper-Harper handling qualities rating (table V) on each axis, as well as give an overall rating on the configuration. In addition, various airplane parameters were recorded during the simulated landing approaches in order to measure pilot performance and work load, a procedure that was very beneficial in the interpretation and analysis of the pilot ratings and comments. Statistical data, in rms form, were also gathered for three discrete altitude bands: 1500 to 400, 400 to 50, and 50 to 0 ft of altitude. These measurements allowed for quick work load and performance comparisons between the configurations tested.

A summary of the configurations evaluated is presented in table VI. The three pilots are indicated in the test matrix by number 1, 2, or 3, but note that all pilots did not evaluate all configurations. Table VI indicates the magnitude and type of "additional" control system delay, the airplane axis to which the delay was added, and the atmospheric conditions in which the configuration was flown. Note that the major emphasis was placed on the longitudinal and lateral airplane axes. (Previous studies, for example, ref. 4, had indicated that delays in the directional axis are much less critical for transport-class airplanes.) It should be mentioned, however, that the present study did not consider engine or FCS failures. Simultaneous delays in more than one axis were also briefly evaluated. However, additional work is required in the area of simultaneous delays before a more complete analysis can be performed.

The additional time delays used in the subject piloted-simulation study were incorporated into the airplane flight control system in either of two forms: as a discrete (pure) time delay ($e^{-\tau s}$) or as a first-order lag ($1/(\tau s + 1)$). (See fig. 2(c) for the location in the control loop at which the time delays were inserted.) Pure delays are the result of computational time characteristics of a digital flight control system; whereas FCS lags are normally associated with prefilters, actuator dynamics, etc. The difference in the effects of these two forms of delay on the dynamic response of the airplane is illustrated in figure 5. The response of the baseline airplane (no additional delays) is indicated by curve A and shows the normal airplane response to a pitch controller step input with its inherent lags. Curve B indicates that the addition of a pure delay moves the response along the time axis such that the response is identical but delayed τ seconds. The addition of a first-order lag to the baseline FCS, however, reduces the slope of the baseline response with increasing time constant, thereby reducing the maximum attainable response rate and delaying the steady-state response (curve C). The response occurs forthwith, even though it may not be recognized by the pilot immediately if the time constant becomes large.

The method described in reference 6 designated "effective time delay" was used to convert the different time delays. Figure 6 defines the effective time delay t_1. Time t_1 is measured from the instant of the controller force step input to the time corresponding to the intersection of the tangent to the maximum slope line with the time axis.

Results and Discussion

The present military specifications (ref. 1) state, in part, that the response of the control system surfaces in flight shall not lag the cockpit control force inputs by more than the angles shown in table VII(a) for frequencies equal to or less than the frequencies indicated. (See table VII(a).) In addition, reference 1 states that the response of the airplane motion shall not exhibit a time delay longer than that indicated in table VII(b) for a pilot-initiated step control force input. Although these reference 1 requirements are presently applicable to all airplane classes, this reference states that most of the available data used to establish these allowable time delay requirements are for class IV (fighter) airplanes; however, there are some data (e.g., ref. 7) which indicate that higher values may be acceptable for class III (transport) airplanes; but there are insufficient data to support separate requirements at this time. Therefore, it was the intent of the present study to build on the existing data base for large class III airplanes (in the area of time delays) and to utilize the results as the basis for suggested allowable response delays and allowable control surface lags for the various levels of handling qualities. The more significant results of this study are reviewed in the following sections.

Pure Time Delays

Discrete (pure) time delays are the result of computation-time characteristics of the digital control system. Figure 7 presents the pilot ratings as a function of the longitudinal and lateral control pure time delay inputs. Note that there is data scatter for each pilot and atmospheric condition and that all fairings to the data were obtained using linear least-squares curve-fitting techniques, which provide the best curve fit for minimum PR error. The analysis of these data is included in subsequent sections of this paper.

Lagged Time Delays

Normally, time lags are associated with actuator dynamics, cable stretch, inertial effects, prefilters, etc. Figure 8 presents the experimentally obtained PR's as a function of the longitudinal and lateral control lagged time delay inputs. Again, note that there is data scatter for each pilot and atmospheric condition. The difference in the effects of pure and lagged time delays on the airplane response is illustrated in figure 5. Again, the analysis of these data is included in subsequent sections of this paper.

Effective Time Delays

Digital airplane control systems are characterized by a combination of time delay in both *pure* and *lagged* form. The present military specification (ref. 1) for maximum allowable time delay in a flight control system is stated in terms of equivalent time delay. The equivalent time delay of the flight control system can be measured by matching the initial frequency response of a lower-order model, which includes a pure time delay term. The effective time delay does not require an assumed lower-order model because the value of delay calculated is a direct function of the initial airplane response. As shown in figure 6, the effective time delay t_1 as evaluated by Chalk (ref. 6) is measured from the instant of the controller force step input to the time corresponding to the intersection of the tangent to the maximum slope and the zero amplitude axis. The definition in reference 6 of effective time delay is used throughout this report.

In order to compare the experimental results of the present tests with the military specification (ref. 1), the pilot opinion data plotted as a function of

time constant were analyzed in terms of effective time delay. The baseline representation of the simulated airplane cannot be modeled without some *inherent* delay attributed to simulation system characteristics that must be added to the *input* delay to determine the *total* time delay as seen by the pilot. This inherent time delay increment is 0.047 sec and is a pure (digital) delay. The effective time delay was therefore the sum of pure delay input plus 0.09, plus 0.047 sec for the longitudinal axis and the sum of pure delay input plus 0.05, plus 0.047 sec for the lateral axis. (The 0.09- and 0.05-sec time increments represent the lags in the basic control system.) Figure 9 was derived from time history responses in q and p of the simulation model to control unit step inputs with inherent 0.047 sec pure delay and was used to convert first-order lags to effective delays in the longitudinal and lateral control axes.

Figures 10 and 11 present the combined longitudinal and lateral pure and lagged time delay data, respectively, to the effective time delay format. Again, all fairings to the data were obtained using linear least-squares curve-fitting techniques with the standard deviation of pilot rating σ_{PR} and correlation coefficient ρ noted. The standard deviation of pilot rating is a measure of dispersion around the fit of the accumulated data. The correlation coefficient indicates the "goodness of fit" between the effective time delay and pilot rating using linear least-squares curve-fitting techniques. Since a bias exists in PR's between pilots and atmospheric conditions at low levels of effective time delay, the curves in figures 10 and 11 were modified to a more consistent base. To minimize the PR bias between pilot 3 and the other two pilots, a ΔPR of 1 was subtracted from the longitudinal calm and turbulent air results of pilot 3, and a ΔPR of 1 was subtracted from the lateral calm air and crosswind results of pilot 3. (Pilot 3 was a fighter pilot with limited transport time and was consistently higher in his pilot rating when flying the large transport tasks.) The calm air and crosswind results for all pilots are averaged and presented in figure 12 and table VIII. The turbulent air results for all pilots are also averaged and used to establish allowable effective time delays and are presented in figure 13 and table VIII. Figure 14 was prepared to illustrate the effect of averaging all pilots and wind conditions, but the data are not presented in table VIII.

Most of the simulator tests were performed with a time delay incorporated into the control system of a single axis of the airplane. Table VI(b) presents the additional tests that were performed to investigate the effects of time delay in flight control systems with simultaneous delays in the pitch and roll axes. These tests were performed by pilot 2, and three examples are presented in figures 15, 16, and 17. Figure 15(a) presents the effect of simultaneous lagged time delays in pitch and roll against the lagged time delay in pitch only for pilot 2 flying in calm-air conditions. A similar result for the lateral axis is presented in figure 15(b). Both plots in figure 16 show the effects of the application of simultaneous lagged time delays about the pitch and roll axes when compared with lagged time delay in a single axis, and they clearly indicate the worsened PR's and lower allowable time delay. Figure 16 indicates the effect of simultaneous lagged time delays about the pitch and roll axes when compared with lagged time delay in the roll axis for flight in a crosswind by pilot 2. Figure 17 indicates the largest amount of control cross coupling due to simultaneous lagged time delays in pitch and roll when compared with the lagged time in either pitch or roll, respectively, for flight by pilot 2 in turbulence. It is evident that there is control cross coupling, and that additional testing with simultaneous time delays in all axes should be continued for large airplanes in all atmospheric conditions.

Figures 18 and 19 present the effects of "effective time delay" on pilot opinion, wherein pure time delay inputs were used for the longitudinal axis (fig. 18) and lagged time delay inputs were used for the lateral axis (fig. 19).

Pilot Work Load and Performance Analysis

The longitudinal and lateral work load parameters, which give an indication of how hard the pilots are working, are calculated, respectively, as follows:

$$(\mathrm{WL})_{\mathrm{long}} = \mathrm{rms}\left(\sum \frac{\delta_{\mathrm{col}}}{\delta_{c,\max}}\right)$$

and

$$(\mathrm{WL})_{\mathrm{lat}} = \mathrm{rms}\left[\sum\left(\frac{\delta_w}{\delta_{w,\max}} + \frac{\delta_p}{\delta_{p,\max}}\right)\right]$$

The parameters used in the rms calculations were sampled eight times per second. The GS error and the LOC error of the performance parameters are rms measures of deviation from the prescribed glide slope and localizer path, respectively, measured in "dots." It should be noted that a "one dot" error in the glide slope and localizer path represents an error of 0.375° and 1.250°, respectively. As the airplane approaches touchdown, this angular display of ILS information appears to the pilot as an increased sensitivity since it takes a smaller physical offset to produce the same indications.

An example of the effects of pure delay and first-order lag on pilot work load and performance (in

crosswind) is shown in figure 20. The time history plots compare pure and lagged delays of approximately equal time constants in the lateral axis in terms of wheel activity and localizer error. Note the substantial increase in wheel movement below an altitude of 500 ft with the pure delay. No appreciable difference can be seen in the localizer error traces as illustrated by the shaded areas. Figure 20 indicates that the pilot is working much harder in roll with a pure delay than with a lag to maintain the same level of performance near the ground, and this higher work load is reflected in the pilot ratings assigned. Other examples of pilot work load and performance are shown in figures 21 through 24.

Figure 21 presents pilot work load and tracking performance during an approach in turbulence as a function of control system time delay in the longitudinal axis. Note in figure 21(a) that an increase in work load does not become apparent until after 0.327 sec effective delay and does not become significant until after the effective time delay exceeds 0.727 sec. Errors above and below the glide slope during tight instrument tracking are used here as a measure of pilot performance. (See fig. 21(b).) No increase in glide slope error with increasing time delay is apparent in this case. Therefore, figure 21(a) gives an indication of how hard the pilot must work to maintain constant performance as time delay increases.

Figure 22 presents pilot work load and performance time history data for time delay in the lateral axis when flown in crosswind conditions. In this case, the plotted parameters are wheel activity and localizer error, representing work load and performance, respectively. As shown in figure 22(a), pilot work load does not increase significantly until after an effective time delay level of 0.327 sec. No increase in localizer errors with increasing time delay is apparent for this case. (See fig. 22(b).)

Figure 23 presents longitudinal work load and performance time history data for a configuration with pure time delay input in the lateral axis when flown under crosswind conditions. For this particular case, the work load in the pitch axis (fig. 23(a)) is not affected significantly when increasing the effective time delay in the roll axis. Figure 23(b) indicates that longitudinal performance (glide slope error) degrades with increasing time delays in roll, although there is no change in the longitudinal axis PR's. Figure 24 shows an example of the effect of pure time delay in the pitch axis on the lateral work load and performance for approaches and landings flown in turbulent atmospheric conditions. For this particular case, both lateral work load (fig. 24(a)) and performance (fig. 24(b)) degrade slightly with increasing time delay in pitch, although there is no change in the lateral axis PR's. Figures 23 and 24 are examples of the importance of recording work load and performance parameters rather than relying strictly on pilot rating.

Figure 25(a) presents the rate of sink at touchdown ($-\dot{h}_{td}$) for all simulated landings in turbulent atmospheric conditions. Figure 25(b) presents the angle of roll at touchdown (ϕ_{td}) for all simulated landings in crosswind. For a large class III airplane, reference 8 states that the maximum *acceptable* touchdown limits for rate of sink and bank angle are 5 ft/sec and $\pm 5°$, respectively. (The sink rate limit of 5 ft/sec is considered to be a limiting value for passenger comfort, and the bank angle limit is imposed in order to avoid having a wingtip or engine pod hit the runway during crosswind landings.) Transferring these *acceptable* limits to figure 25 results in maximum acceptable (level 2) effective time delays of 0.85 sec and 0.52 sec for rate of sink and bank angle, respectively. Note the excellent agreement of these (fig. 25) effective time delay (level 2) limits (derived from *pilot performance* considerations) with the level 2 limits presented in table VIII (derived from *pilot opinion*). Also note that both of these level 2 (maximum acceptable) limits are significantly higher than the universal 0.20 sec specified by reference 1, and that these ground-based piloted simulator data suggest the need for the specification of allowable time delay as a function of airplane axis. That is, it is indicated that higher effective time delays (on the order of 40 to 60 percent higher) are more acceptable in the longitudinal axis than in the roll axis.

In addition to these *acceptable* (level 2) implications, if the maximum *satisfactory* (level 1) limit for rate of sink at touchdown is taken to be 2.3 ft/sec (ref. 9) and this is superimposed in figure 25(a), the maximum satisfactory (level 1) limits for effective time delay in the pitch and roll axes (derived from pilot performance considerations) would be 0.18 sec and 0.52 sec, respectively. For level 1 note that the pitch axis appears to be more sensitive to time delay than the roll axis. Comparing the level 1 limits (turbulent atmospheric conditions, fig. 25) with those derived from pilot opinion (table VIII) indicates that the maximum *satisfactory* (level 1) limits for effective time delays in the pitch axis are essentially equivalent.

Allowable Control Surface Lags

The requirement of reference 1 for control system response concerns the area of phase shift between cockpit input and control surface deflection. The requirement states that the response of the control surfaces in flight shall not lag the cockpit control

force inputs by more than the angles specified in table VII(a) for frequencies equal to or less than those specified. Figure 26(a) presents a plot of control surface phase shift as a function of the lag time constant characteristic of the longitudinal control system, and figure 26(b) presents the same data for the lateral control system. Since large class III airplanes normally have characteristic frequencies less than 2.0 rad/sec, the comparison should be made at 2.0 rad/sec as specified in table VII(a). (The data shown were measured at a frequency of 1.96 rad/sec.) Maximum allowable level 1 control surface phase lags were determined by converting the effective time delay values back to equivalent first-order lag time constants. The suggested boundaries from these data for level 1 flying qualities in turbulent air are approximately 50° in the column-elevator system and approximately 40° in the wheel-aileron system for the approach and landing (category C) flight phase. (See fig. 26.) Note that the level 1 PR's from figure 14 (the average of all pilots and wind conditions) are also presented. The present criteria (table VII(a)) suggest 15° as the maximum allowable control surface phase lag for level 1 flying qualities about all axes. Levels 2 and 3 phase lag boundaries are not suggested in this report since time delay in lagged form was not tested at sufficiently high values (τ_{max} = 2.0 sec). (See fig. 9.)

Concluding Remarks

Pilot ratings, work load, and performance data have shown that current military criteria governing allowable time delay and control surface phase lag in flight control systems are somewhat restrictive for level 1 (satisfactory) handling qualities when applied to a specific transport-size airplane (an advanced Lockheed L-1011 at 330 000 lbf). A comparison of the present results with those of previous tests indicates that these limits are a function of airplane size, mission, and especially control system design and dynamics. In addition, the roll axis appears to be more critical than the pitch axis as related to time delay and phase lag. For the particular airplane configuration tested herein, the results of the tests suggest time delay limits for level 1 flying qualities of 0.15 sec in both the longitudinal and lateral axes. Also, the present results suggest a level 2 (acceptable but unsatisfactory) handling qualities limit for an effective time delay of 0.82 sec and 0.57 sec for the longitudinal and lateral axes, respectively, as opposed to the 0.20 sec of the present specifications. In the area of control surface phase lag, suggested boundaries for level 1 flying qualities in turbulent air were approximately 50° in the column-elevator system and approximately 40° in the wheel-aileron system—as opposed to 15° of the present specifications.

During an analysis of the data, major emphasis was placed on pilot ratings of flying qualities; however, time history recordings of pilot work load and tracking performance provided assistance in analyzing and understanding trends. In fact, pilot ratings appeared to relate directly with how hard the pilot had to work to track the glide slope and localizer. Data such as these indicated that pilots are better able to handle a control system time delay in lagged form than in discrete (pure) form. The work load and tracking performance data presented in this report suggest a slight degree of cross coupling between axes. That is, pilot work load and performance in a particular axis degraded as a result of time delay in the other axis. (The directional axis was not considered.) Additional testing was performed using a single pilot with pure and lagged time delays in the pitch and roll axes simultaneously, possibly providing a better representation of an actual airplane response. Significant cross coupling between axes was present and appeared dependent on ambient air conditions. However, most data were obtained with either a pure delay or first-order lag in a single airplane axis.

It is evident that for large-transport control studies, a much larger data base is required. This data base should include different airplane baselines, control systems, and flight phases with many pilots participating so that reasonable limits for control system time delay and phase lag can be established.

NASA Langley Research Center
Hampton, VA 23665-5225
December 11, 1986

References

1. Moorhouse, David J.; and Woodcock, Robert J.: *Background Information and User Guide for MIL-F-8785C, Military Specification—Flying Qualities of Piloted Airplanes.* AFWAL-TR-81-3109, U.S. Air Force, July 1982. (Available from DTIC as AD A119 421.)
2. Di Franco, Dante A.: *In-Flight Investigation of the Effects of Higher-Order Control System Dynamics on Longitudinal Handling Qualities.* AFFDL-TR-68-90, U.S. Air Force, Aug. 1968. (Available from DTIC as AD 840 752.)
3. Weingarten, Norman C.; and Chalk, Charles R.: *In-Flight Investigation of Large Airplane Flying Qualities*

for Approach and Landing. AFWAL-TR-81-3118, U.S. Air Force, Sept. 1981. (Available from DTIC as AD A120 202.)

4. Meyer, Robert T.; Knox, John R.; and Tingas, Stephen A.: *Suggested Revisions to MIL-F-8785C for Large (Class III) Aircraft.* AFWAL-TR-83-3015, U.S. Air Force, Feb. 1983. (Available from DTIC as AD A131 997.)
5. Martin, D. J., Jr.: *A Digital Program for Motion Washout on Langley's Six-Degree-of-Freedom Motion Simulator.* NASA CR-145219, 1977.
6. Chalk, C. R.: *Recommendations for SCR Flying Qualities Design Criteria.* NASA CR-159236, 1980.
7. Crother, C. A.; and Gabelman, R.: Equivalent System Modelling of the Augmented B-1. *Flying Qualities Design Criteria—Proceedings of AFFDL Flying Qualities Symposium Held at Wright-Patterson Air Force Base in October 1979,* R. B. Crombie and D. J. Moorhouse, compilers, AFWAL-TR-80-3067, U.S. Air Force, May 1980, pp. 253-277. (Available from DTIC as AD A088 629.)
8. Johnson, Walter A.; and Hoh, Roger H.: *Determination of ILS Category II Decision Height Window Requirements.* NASA CR-2024, 1972.
9. Hofmann, L. G.; Clement, W. F.; Graham, D.; Blodgett, R. E.; and Shah, K. V.: *Investigation of Measuring System Requirements for Low Visibility Landing.* AFFDL-TR-71-151, U.S. Air Force, Dec. 1971. (Available from DTIC as AD 739 932.)
10. Grantham, William D.; Person, Lee H., Jr.; Brown, Philip W.; Becker, Lawrence E.; Hunt, George E.; Rising, J. J.; Davis, W. J.; Willey, C. S.; Weaver, W. A.; and Cokeley, R.: *Handling Qualities of a Wide-Body Transport Aircraft Utilizing Pitch Active Control Systems (PACS) for Relaxed Static Stability Application.* NASA TP-2482, 1985.

Table I. Airplane Geometry and Weight Data

Wing:	
Reference area, ft^2	3456
Reference $\bar{c}$, ft	24.46
Span, ft	164.33
Aspect ratio	7.814
Sweep, deg	35
Horizontal tail:	
Area, ft^2	1282
Span, ft	71.58
Aspect ratio	4.0
Sweep, deg	35
Tail volume	0.919
Vertical tail:	
Area, ft^2	550
Span, ft	29.67
Aspect ratio	1.6
Sweep, deg	35
Tail volume	0.066
Weight:	
Maximum ramp, lbf	424 000
Maximum takeoff, lbf	422 000
Maximum landing, lbf	358 000
Nominal landing, lbf	330 000
Zero fuel, lbf	312 460
Operating empty, lbf	261 000
Simulated weight, lbf	330 000

Table II. Partial Listing of Aerodynamic Data Used in Large-Transport Simulation

[c.g. $= 0.25\bar{c}$; $\delta_f = 33°$; $\delta_H = \delta_e = 0°$]

α, deg	C_X	C_Z	C_m	$C_{L_{\dot{\alpha}}}$, rad^{-1}	C_{L_q}, rad^{-1}	$C_{m_{\dot{\alpha}}}$, rad^{-1}	C_{m_q}, rad^{-1}
−4	−0.1565	−0.0592	0.0490	2.0	8.0	−5.2	−25.4
0	−.1389	−.5270	−.0680	↓	↓	↓	↓
4	−.0865	−.9915	−.1980				
8	−.0115	−1.4458	−.3420				
12	.1158	−1.8616	−.4280				
16	.2523	−2.2111	−.5120				
20	.3929	−2.5493	−.5920				
24	.6094	−2.4817	−.6404				

α, deg	$C_{Y_{\delta_a}}$, deg^{-1}	$C_{\iota_{\delta_a}}$, deg^{-1}	$C_{n_{\delta_a}}$, deg^{-1}	$C_{Y_{\delta_{a,s}}}$, deg^{-1} (a)	$C_{\iota_{\delta_{a,s}}}$, deg^{-1} (a)	$C_{n_{\delta_{a,s}}}$, deg^{-1} (a)
−4	0	0.00118	0.00013	−0.00093	0.00166	0.00029
0	↓	.00117	.00018	−.00114	.00192	.00046
4		.00116	.00020	−.00137	.00216	.00063
8		.00115	.00022	−.00179	.00230	.00077
12		.00113	.00019	−.00223	.00243	.00089
16		.00085	.00017	−.00223	.00240	.00096
20		.00039	−.00004	−.00123	.00131	.00064
24		.00014	−.00014	−.00039	.00057	.00031

α, deg	C_{Y_β}, deg^{-1}	C_{ι_β}, deg^{-1}	C_{n_β}, deg^{-1}	$C_{Y_{\delta_r}}$, deg^{-1}	$C_{\iota_{\delta_r}}$, deg^{-1}	$C_{n_{\delta_r}}$, deg^{-1}
−4	−0.0222	−0.00298	0.01024	0.00402	0.00056	−0.00191
0	−.0221	−.00360	.00972	↓	.00033	−.00188
4	−.0220	−.00416	.00884		.00035	−.00186
8	−.0225	−.00462	.00776		.00038	−.00184
12	−.0235	−.00490	.00664		.00028	−.00154
16	−.0248	−.00502	.00544		.00038	−.00141
20	−.0265	−.00476	.00284		.00026	−.00128
24	−.0280	−.00396	−.00596		.00022	−.00119

[a]Spoiler contribution based on aileron deflection. $C_{Y_{\delta_{a,s}}}$, $C_{\iota_{\delta_{a,s}}}$, and $C_{n_{\delta_{a,s}}} = 0$ for $\delta_a \leq 18°$.

Table II. Concluded

α, deg	$C_{X_{\delta_H}}$, deg^{-1}	$C_{Z_{\delta_H}}$, deg^{-1}	$C_{m_{\delta_H}}$, deg^{-1}	$C_{X_{\delta_e}}$, deg^{-1}	$C_{Z_{\delta_e}}$, deg^{-1}	$C_{m_{\delta_e}}$, deg^{-1}
−4	−0.00011	−0.01607	−0.0398	−0.00054	−0.00853	−0.0210
0	−.00035	−.01610	↓	−.00052	−.00851	↓
4	−.00030	−.01616	↓	−.00047	−.00855	↓
8	−.00028	−.01629	↓	−.00033	−.00862	↓
12	−.00030	−.01647	↓	−.00014	−.00873	↓
16	−.00110	−.01670	↓	.00012	−.00882	↓
20	−.00332	−.01815	↓	.00058	−.00885	↓
24	−.00560	−.02012	↓	.00104	−.00885	↓

α, deg	C_{Y_p}, rad^{-1}	C_{l_p}, rad^{-1}	C_{n_p}, rad^{-1}	C_{Y_r}, rad^{-1}	C_{l_r}, rad^{-1}	C_{n_r}, rad^{-1}
−4	0.0595	−0.7170	0.0171	0.3814	0.1816	−0.3127
0	.2669	−.7067	−.0744	.3800	.2430	−.2989
4	.4526	−.7150	−.1436	.4126	.2988	−.2872
8	.5713	−.6794	−.1827	.4640	.3454	−.2718
12	.5870	−.6608	−.2180	.4974	.3616	−.2540
16	.4196	−.6456	−.2366	.4510	.3216	−2439
20	.0717	−.6555	−.2102	.2818	.2727	−.2229
24	−.3277	−.6453	−.1507	−.0017	.1811	−.2195

Table III. Dynamic Stability Characteristics of Simulated Airplane in Landing Flight Condition

[V = 139 knots; c.g. = $0.25\bar{c}$; $\delta_f = 33°$; gear down; altitude, 2000 ft]

Short-period mode:	
ω_{sp}, rad/sec	0.940
P_{sp}, sec	8.55
ζ_{sp}	0.623
L_α/ω_{sp}	0.594
n/α, g units/rad	4.22
Phugoid mode:	
ω_{ph}, rad/sec	0.163
P_{ph}, sec	38.6
ζ_{ph}	0.057
Roll mode:	
τ_R, sec	0.47
Spiral mode:	
t_{s_2}, sec	25
Dutch roll mode:	
ω_d, rad/sec	1.532
P_d, sec	9.31
ζ_d	0.898
ϕ/β	1.51
ω_ϕ/ω_d	0.94

Table IV. Pilot Evaluation Form

PILOT:_____ DATE:_____ RUN NO.:_____

	Longitudinal	Lateral	Directional
AIRCRAFT RESPONSE RATE			
Excessive Control Power			
Sufficient Control Power			
Marginal Control Power			
Inadequate Control Power			
Comments			
AIRCRAFT RESPONSE LAG			
Not noticeable			
Noticeable—not objectionable			
Objectionable			
Comments			
AIRCRAFT DYNAMICS			
Oscillatory			
Aperiodic			
Fast			
Slow			
Damped			
Coupled			
Comments			
ABILITY TO ESTABLISH NEW PATH/ATTITUDE			
Comments			
P.I.O. TENDENCIES			
Comments			
TURBULENCE EFFECTS			
Comments			
COOPER-HARPER RATING			Overall
MAIN FACTOR INFLUENCING RATING			
Comments			

Table V. Pilot Rating System

<table>
<tr><td rowspan="10">CONTROLLABLE
Capable of being controlled or managed in context of mission, with available pilot attention.</td><td rowspan="5">ACCEPTABLE
May have deficiencies which warrant improvement, but adequate for mission.
Pilot compensation, if required to achieve acceptable performance, is feasible.</td><td rowspan="2">SATISFACTORY
Meets all requirements and expectations; good enough without improvement.
Clearly adequate for mission.</td><td>Excellent, highly desirable.</td><td>1</td></tr>
<tr><td>Good, pleasant, well-behaved.</td><td>2</td></tr>
<tr><td>Fair. Some mildly unpleasant characteristics. Good enough for mission without improvement.</td><td>3</td></tr>
<tr><td rowspan="3">UNSATISFACTORY
Reluctantly acceptable. Deficiencies which warrant improvement. Performance adequate for mission with feasible pilot compensation.</td><td>Some minor but annoying deficiencies. Improvement is requested. Effect on performance is easily compensated for by pilot.</td><td>4</td></tr>
<tr><td>Moderately objectionable deficiencies. Improvement is needed. Reasonable performance requires considerable pilot compensation.</td><td>5</td></tr>
<tr><td>Very objectionable deficiencies. Major improvements are needed. Requires best available pilot compensation to achieve acceptable performance.</td><td>6</td></tr>
<tr><td colspan="2" rowspan="4">UNACCEPTABLE
Deficiencies which require improvement. Inadequate performance for mission even with maximum feasible pilot compensation.</td><td>Major deficiencies which require improvement for acceptance. Controllable. Performance inadequate for mission, or pilot compensation required for minimum acceptable performance in mission is too high.</td><td>7</td></tr>
<tr><td>Controllable with difficulty. Requires substantial pilot skill and attention to retain control and continue mission.</td><td>8</td></tr>
<tr><td>Marginally controllable in mission. Requires maximum available pilot skill and attention to retain control.</td><td>9</td></tr>
<tr><td colspan="3">UNCONTROLLABLE
Control will be lost during some portion of mission.</td><td>Uncontrollable in mission.</td><td>10</td></tr>
</table>

Table VI. Summary of Configurations and Flight Conditions Evaluated

(a) Single-axis time delays evaluated by pilots 1, 2, and 3

Delay, sec	Longitudinal			Lateral			Directional		
	Calm air	Turbulence	Cross-wind	Calm air	Turbulence	Cross-wind	Calm air	Turbulence	Cross-wind
0	1, 2, 3	1, 2, 3	1, 2, 3	1, 2, 3	1, 2, 3	1, 2, 3	1, 3	1, 3	1, 3
.090	3	2, 3	1, 2, 3		1, 2, 3	2			
.190	1, 2, 3	1, 2	2, 3	1, 2, 3	1, 2, 3	1, 2, 3	1		
.310	2, 3	2, 3	1, 2, 3	1, 2, 3	1, 2	1, 2			1, 3
.410	1, 2, 3	1, 2	1, 2	1, 2, 3	1, 2, 3	1, 2, 3			
.590	2	2, 3	1, 3	1, 2, 3	1, 2	1, 2			1
.810	1, 2, 3	1, 2, 3	1, 2, 3	1, 2, 3	3	1, 3			3
1.000	1, 2	1, 2, 3	2	1, 2	1				1
1.250	1	1	1						1, 3
1.500	1	1					3		

Lag, τ, sec	Longitudinal			Lateral			Directional		
	Calm air	Turbulence	Cross-wind	Calm air	Turbulence	Cross-wind	Calm air	Turbulence	Cross-wind
0.100	2, 3		2	3		2, 3			
.200	2, 3	2, 3	1, 2	1, 2, 3	1, 2	1, 2, 3			
.300	2, 3	2		3	2	2			
.400	2, 3	2, 3	1, 2	1, 2, 3	1, 2	2, 3			
.500		2		2, 3	2				
.600	2, 3	2, 3	2	1, 2, 3	1, 2	1, 2, 3			
.800	2, 3	2, 3	1, 2	1, 2, 3	1, 2	1, 2, 3			
1.000	1, 2, 3	2, 3	1, 2	1, 2, 3	1, 2	1, 2			
1.250		2		1	1	1			
1.500	2, 3	2, 3	1, 2	2, 3	1, 2	1, 2			
2.000	2, 3	2	1, 2			2			

(b) Simultaneous time delays in pitch and roll axes evaluated by pilot 2; $\tau_{pitch} = \tau_{roll}$

Calm air	Crosswind	Turbulence
Pure time delay, sec		
0	0	0.094
.094	.094	.188
.188	.188	.313
.313	.313	.406
.406	.406	.500
.500	.500	
.594	.594	
.813	.813	
Lagged time delay, sec		
0.100	0.100	0.100
.200	.200	.200
.400	.400	.300
.600	.600	.400
.800	.800	.500
1.000	1.000	.600
1.500	1.500	.700
2.000	2.000	.800
		1.000
		1.500

Table VII. MIL-F-8785C Control Surface Lag and Airplane Response Delay

[Data taken from ref. 1]

(a) Allowable control surface lags (phase shift)

Flight quality level	Allowable lag, deg, for flight phases for—	
	Categories A and C	Category B
1	15	30
2	30	45
3	60	60

Control	Upper frequency, rad/sec
Pitch	Larger value of ω_{sp} or 2.0
Roll and yaw	Largest value of $\dot{\omega}_d$, $1/\tau_R$, or 2.0

(b) Allowable airplane response delay

Flying quality level	Description	Allowable delay, sec
1	Satisfactory	0.10
2	Acceptable but unsatisfactory	.20
3	Unacceptable	.25

Table VIII. Summary of Time Delays From Several Test Programs

Flying quality level	Effective time delay, sec, for—						
				Present results based on adjusted PR's			
				Average of calm air and crosswinds		Average of turbulent air	
	MIL-F-8785C (ref. 1)	Large-airplane flight simulation (ref. 3)	Lockheed C-5A ground-based simulation (ref. 4)	Pitch	Roll	Pitch	Roll
1	0.10	0.20	0.40	0.33	0.25	0.15	0.15
2	.20	.27	.60	.69	.68	.82	.57
3	.25	.40	.70	1.45	1.12	1.49	.99

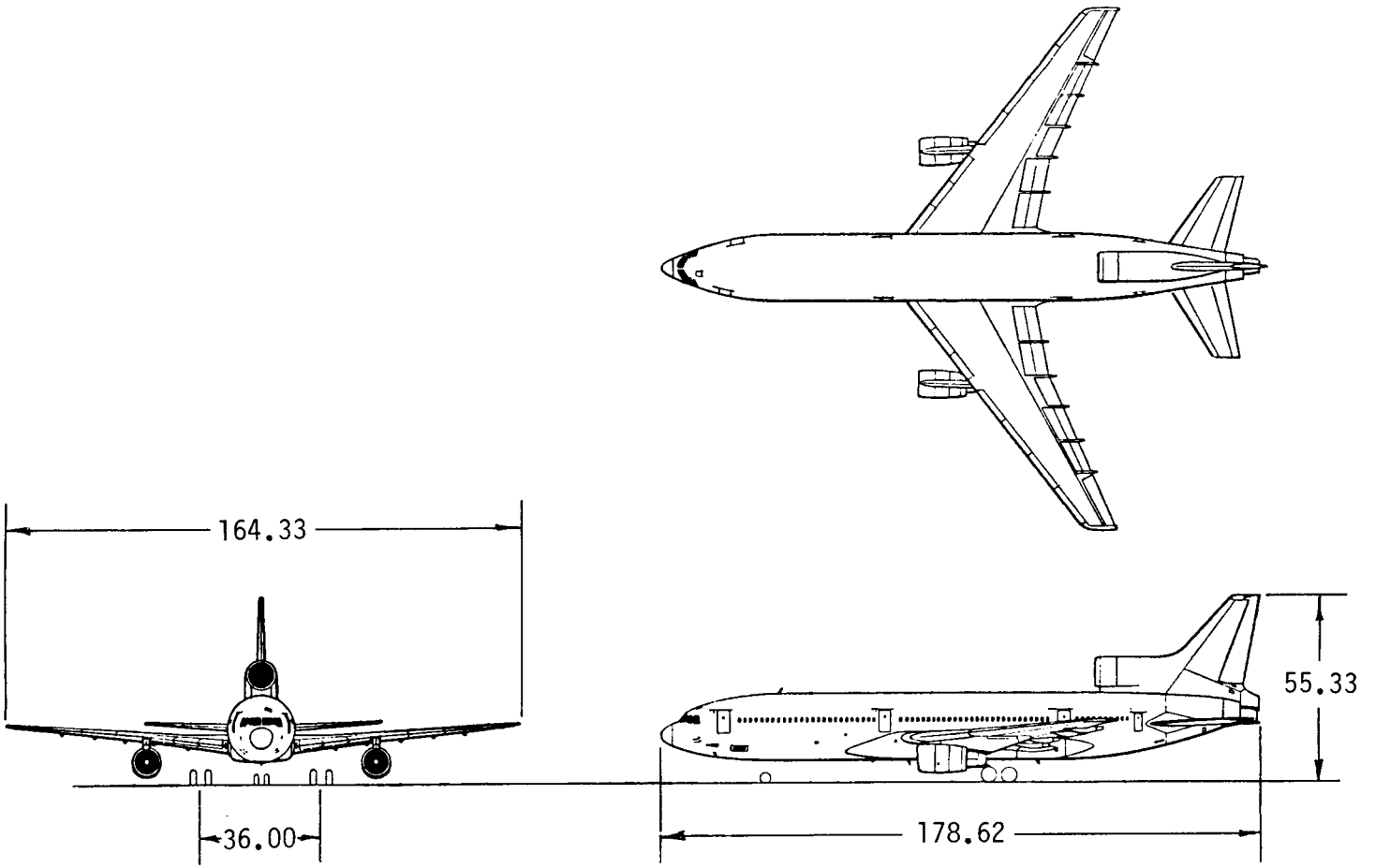

Figure 1. Three-view sketch of simulated Lockheed L-1011 airplane. All dimensions indicated are in feet.

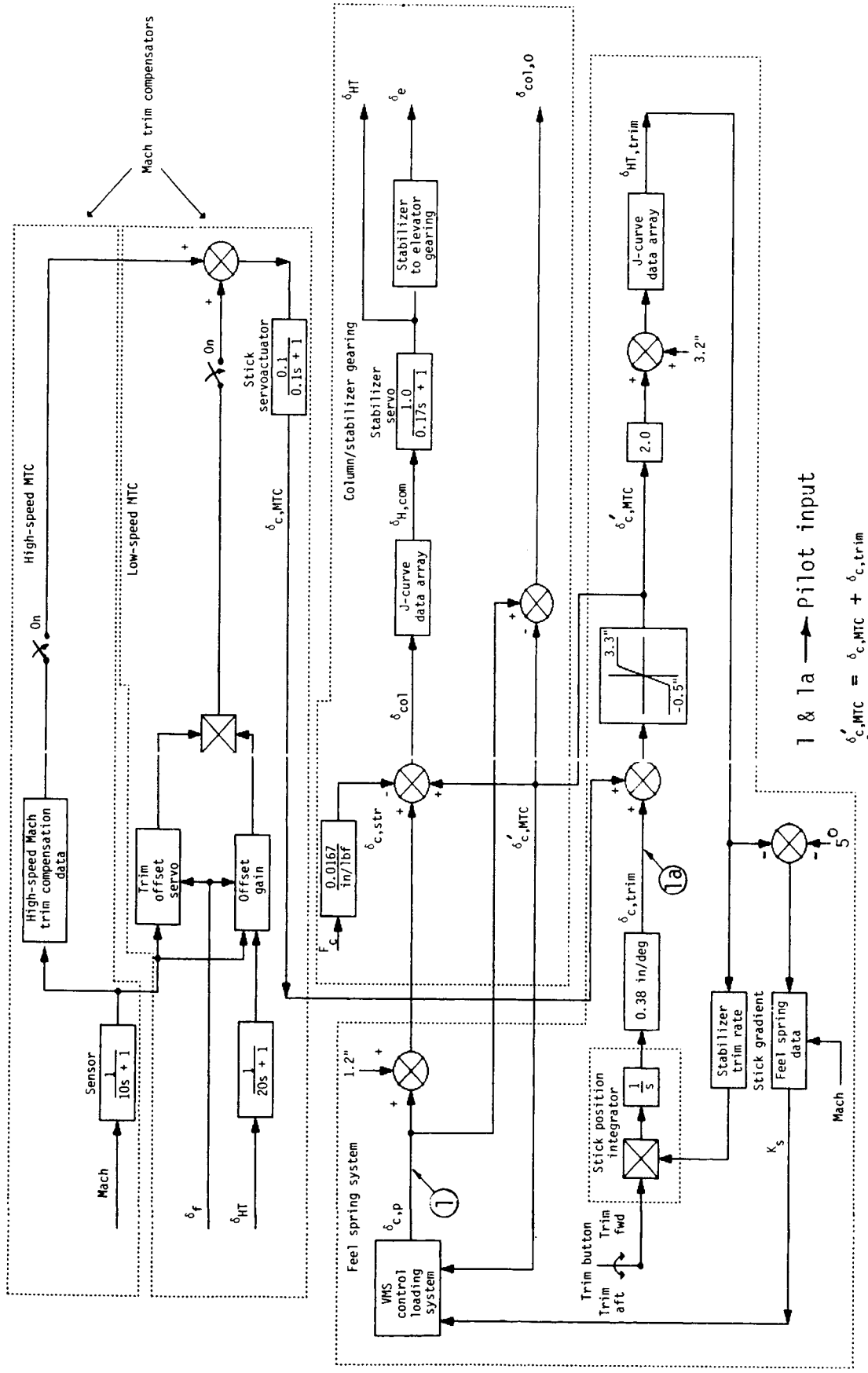

(a) Longitudinal control. Illustration of J-curve data array is found in reference 10.

Figure 2. Ccntrol system block diagrams.

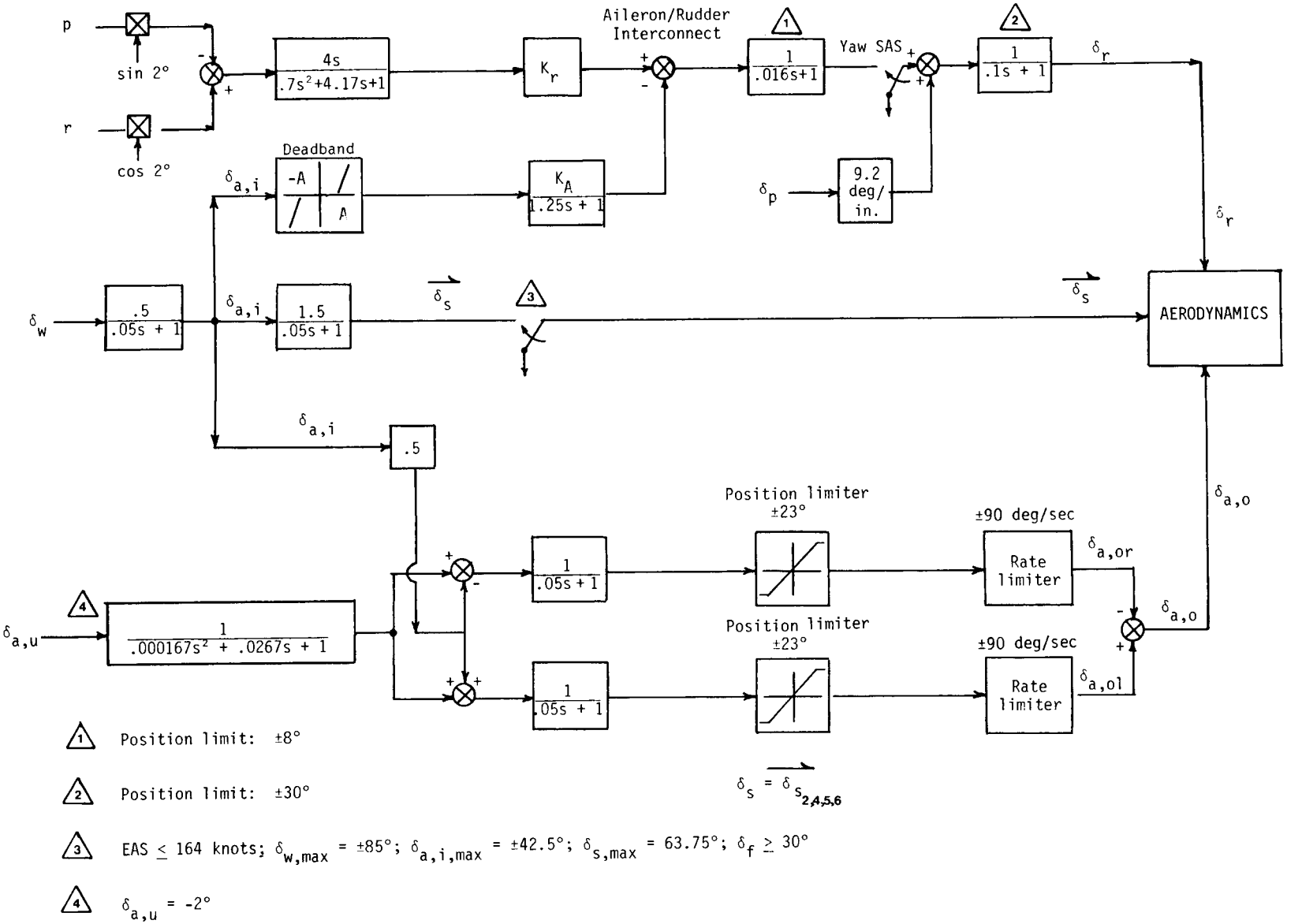

(b) Lateral-directional control. $K_r = 6$; $K_A = 2$; $A = 2$.

Figure 2. Continued.

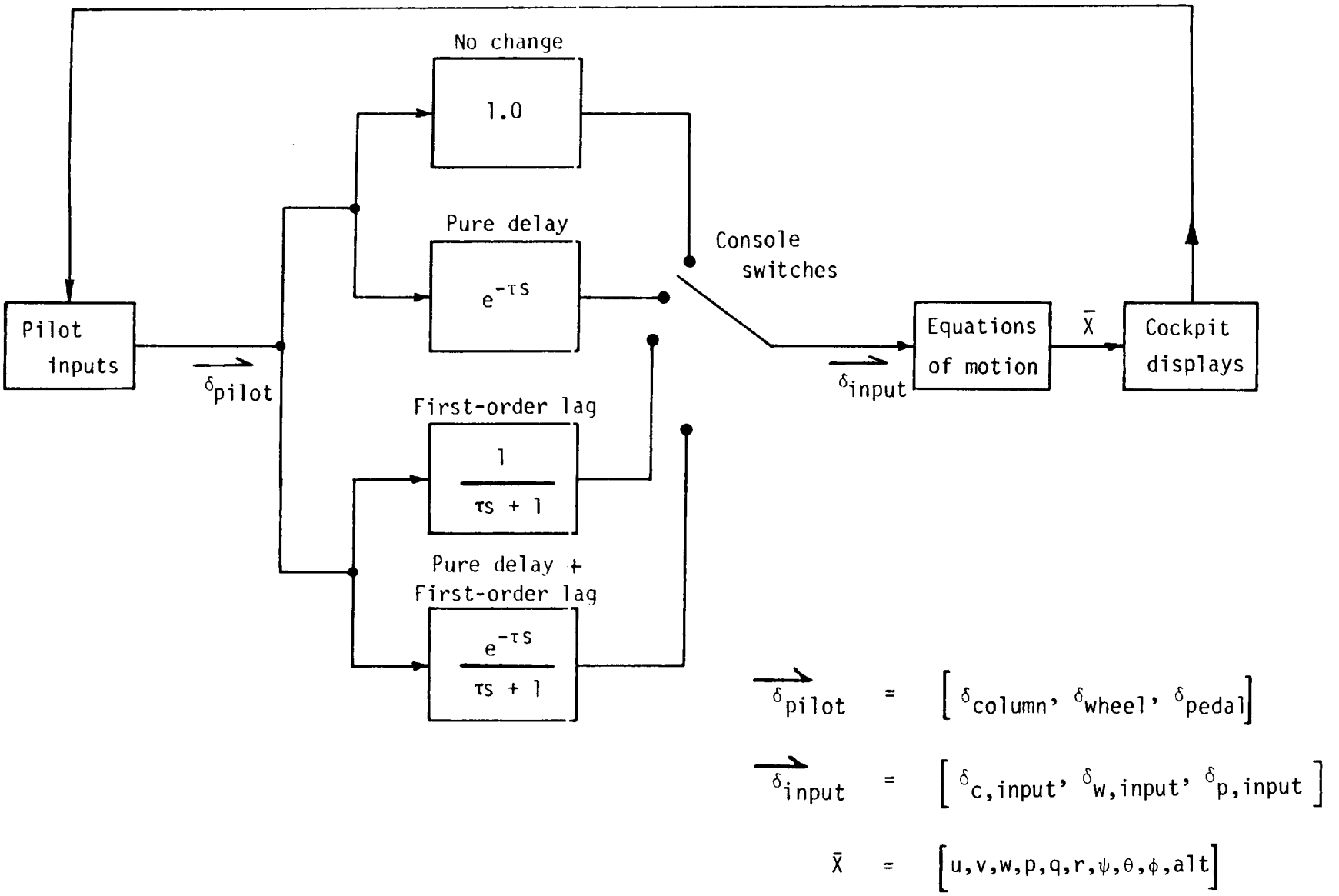

(c) Time delay of control inputs from simulator.

Figure 2. Concluded.

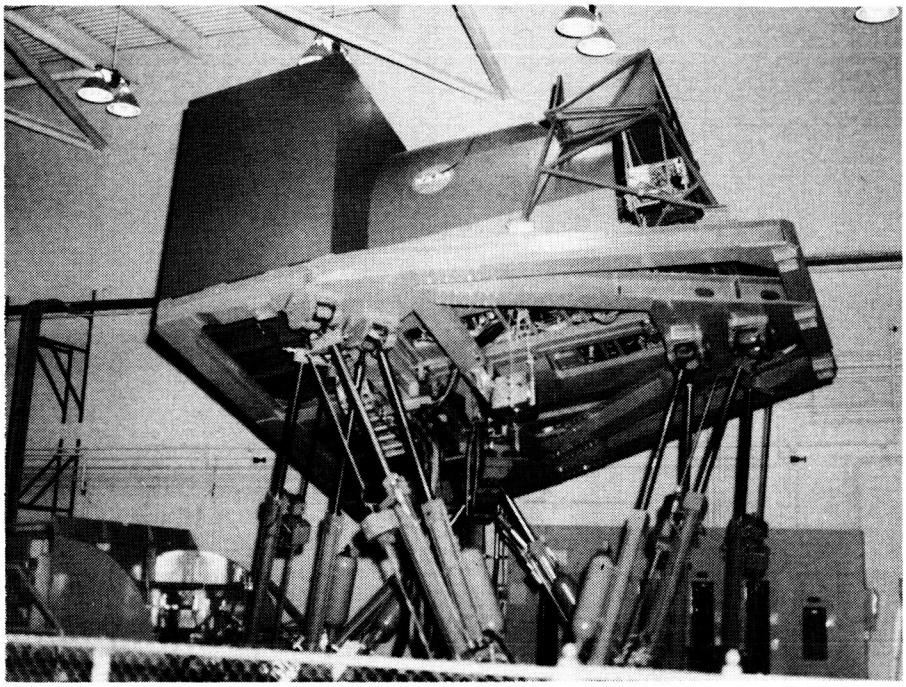

L-75-7570

(a) Langley Visual/Motion Simulator.

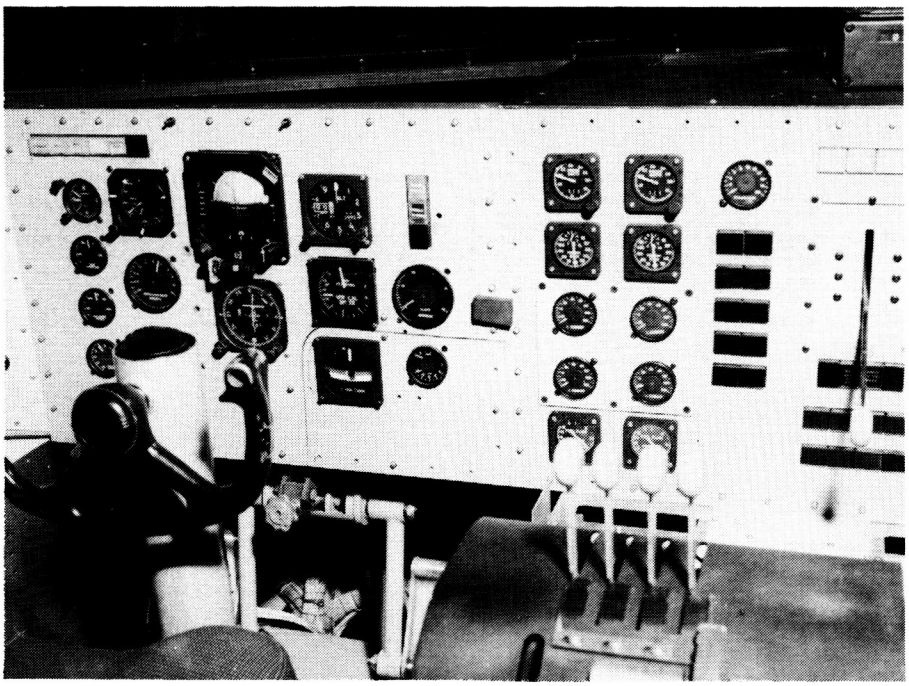

L-78-7794

(b) Instrument panel.

Figure 3. Langley Visual/Motion Simulator and instrument panel display.

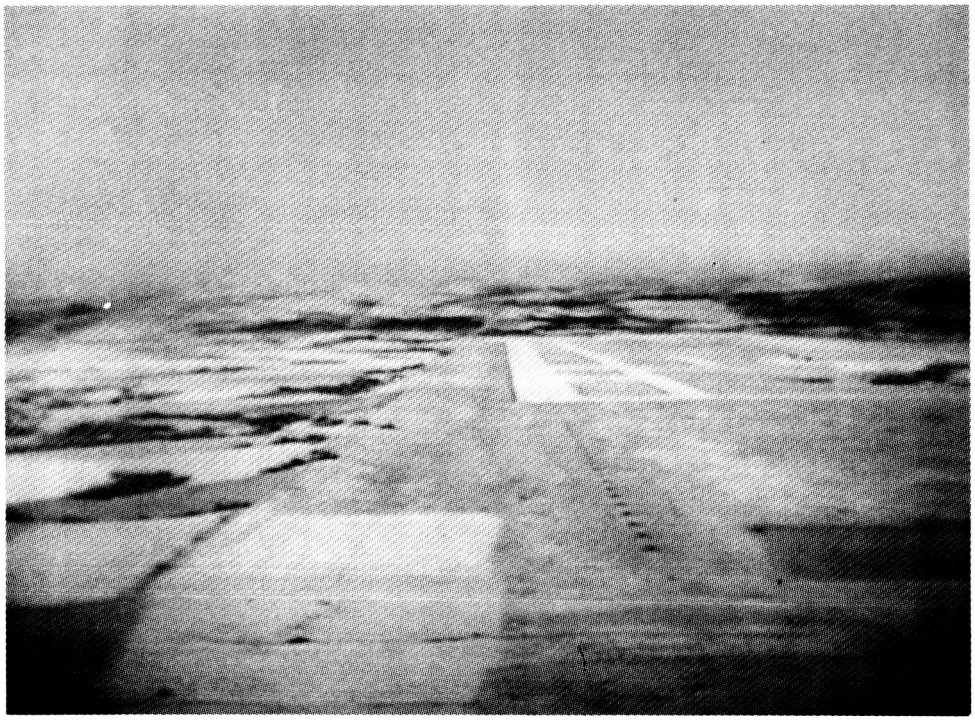

L-82-1255

(a) Approach scene.

L-82-1249

(b) Landing scene.

Figure 4. View of airport scene as observed by pilot.

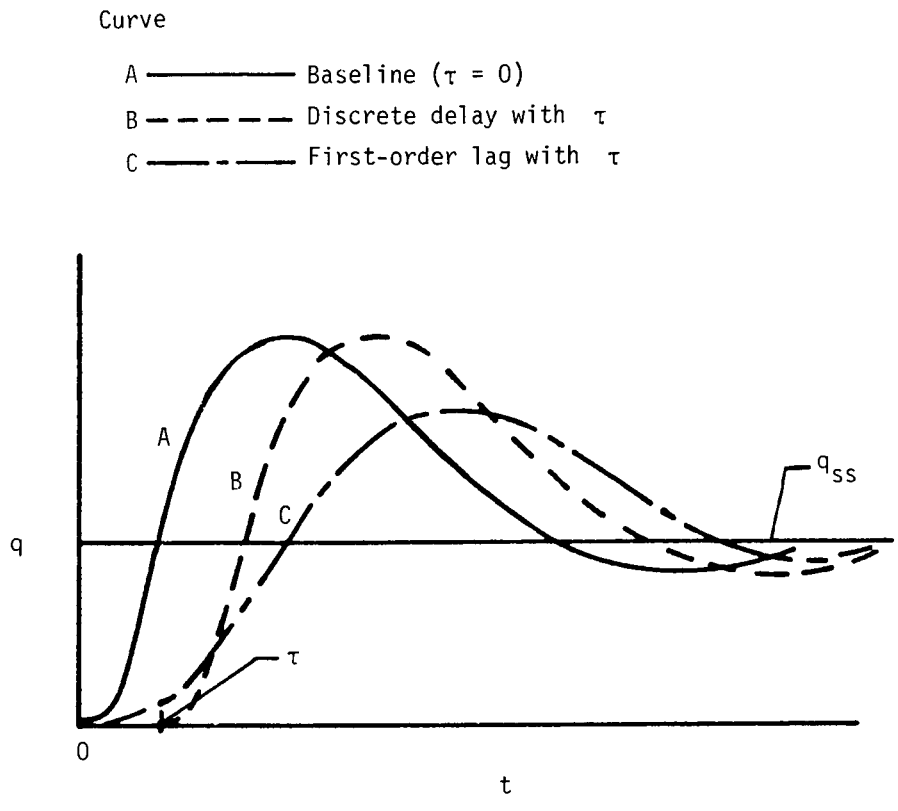

Figure 5. Illustration of effects of FCS pure delay and first-order lag on airplane response. Pitch controller step input at $t = 0$.

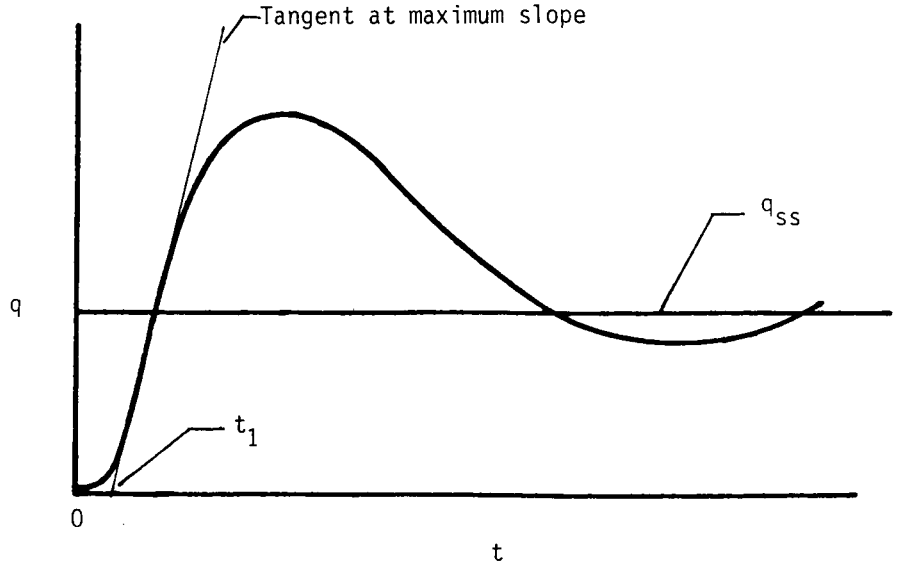

Figure 6. Indication of effective time delay t_1. Response to controller step input at $t = 0$.

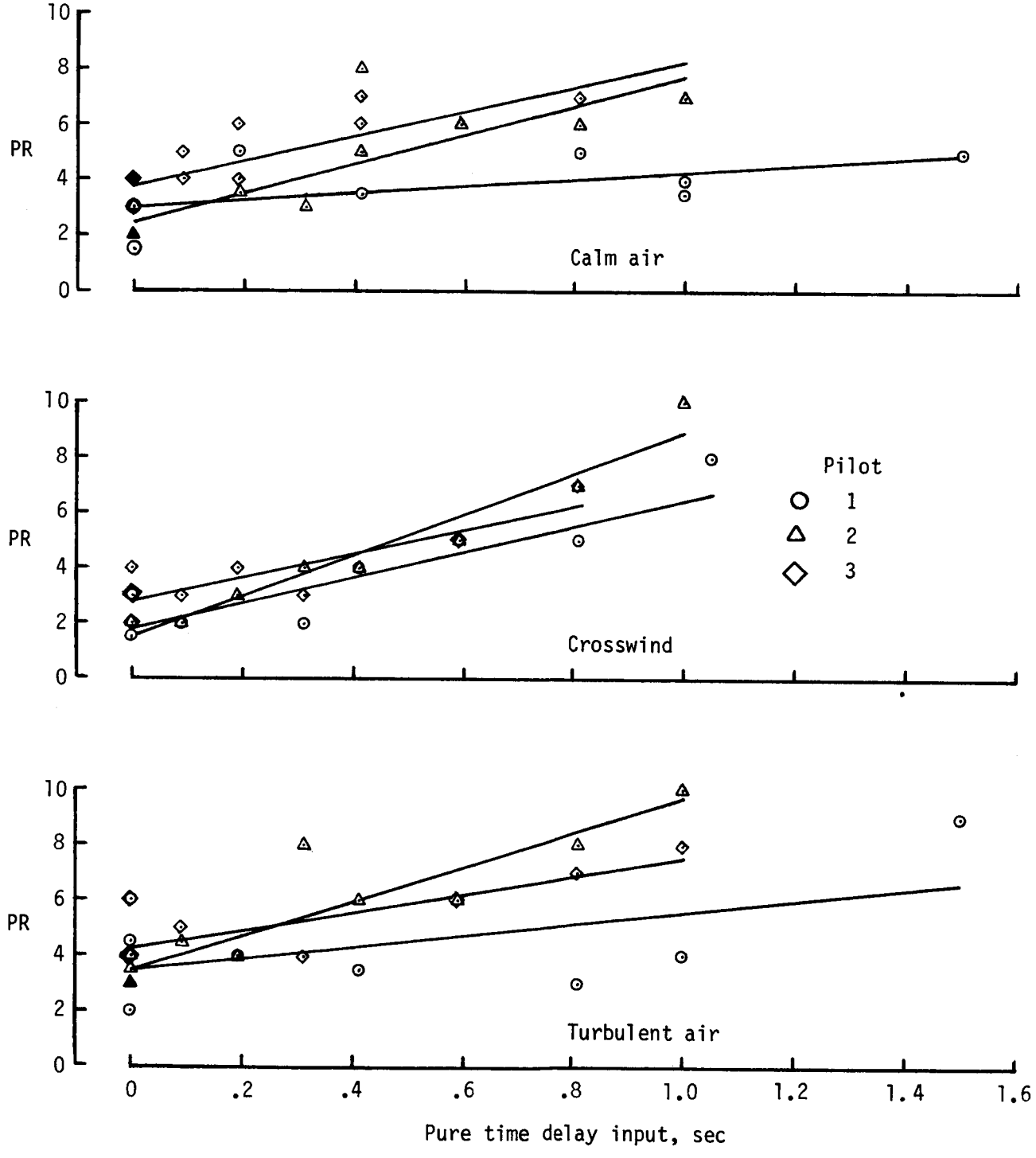

(a) Longitudinal control.

Figure 7. Pilot rating (PR) as a function of pure time delay input of longitudinal and lateral control. Solid symbols equate to two or more data points.

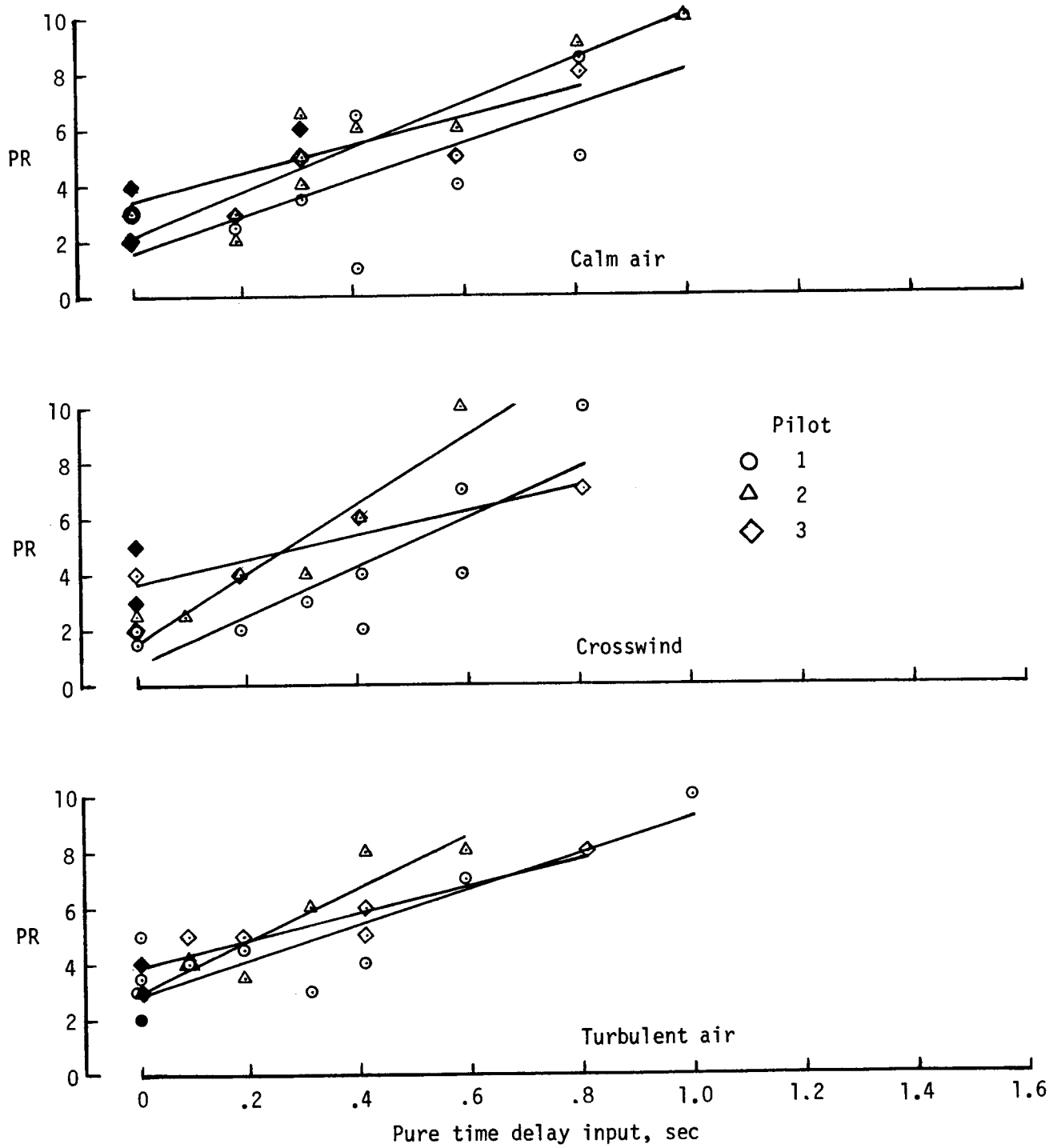

(b) Lateral control.

Figure 7. Concluded.

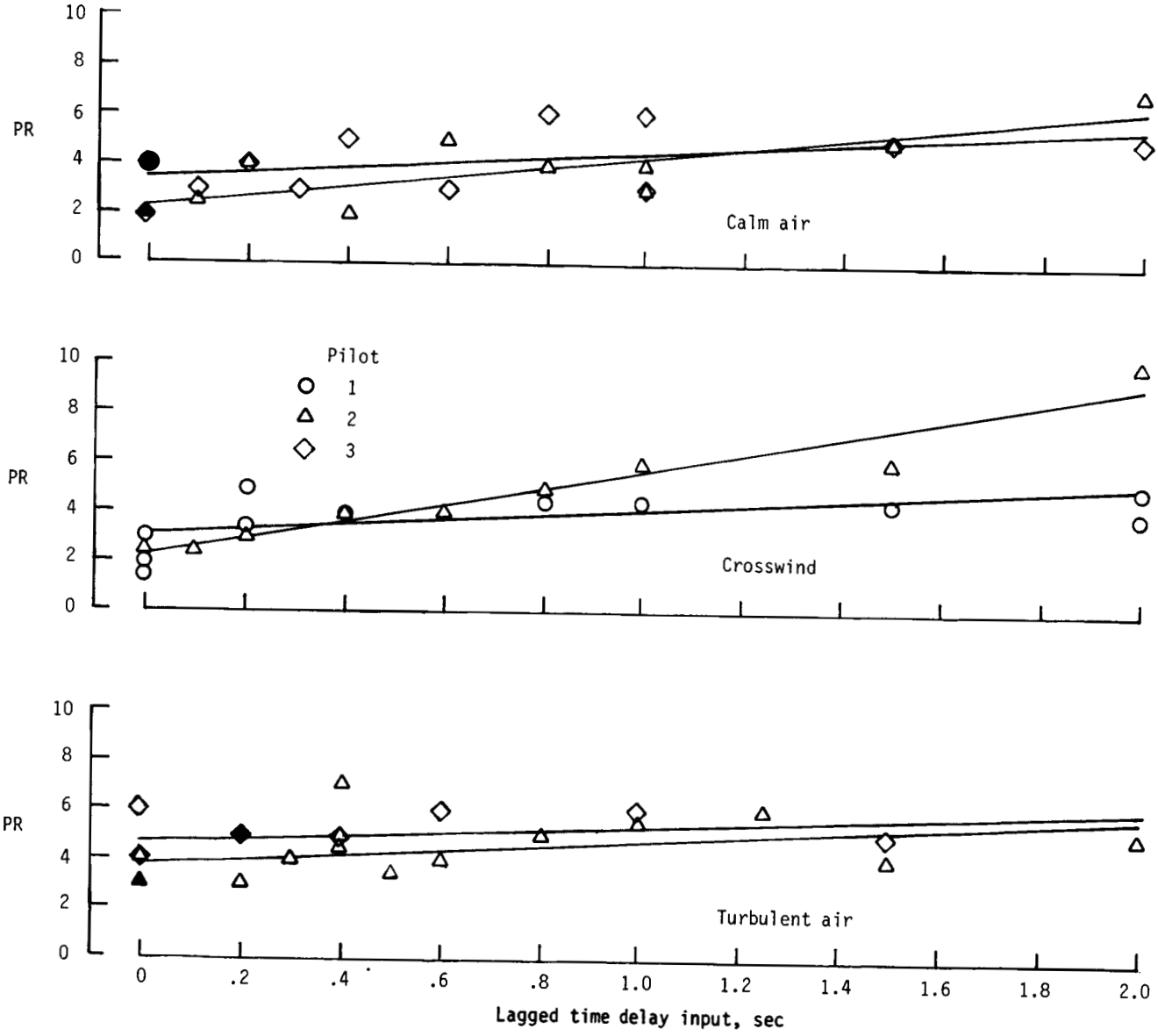

(a) Longitudinal control.

Figure 8. Pilot rating (PR) as a function of lagged time delay input of longitudinal and lateral control. Solid symbols equate to two or more data points.

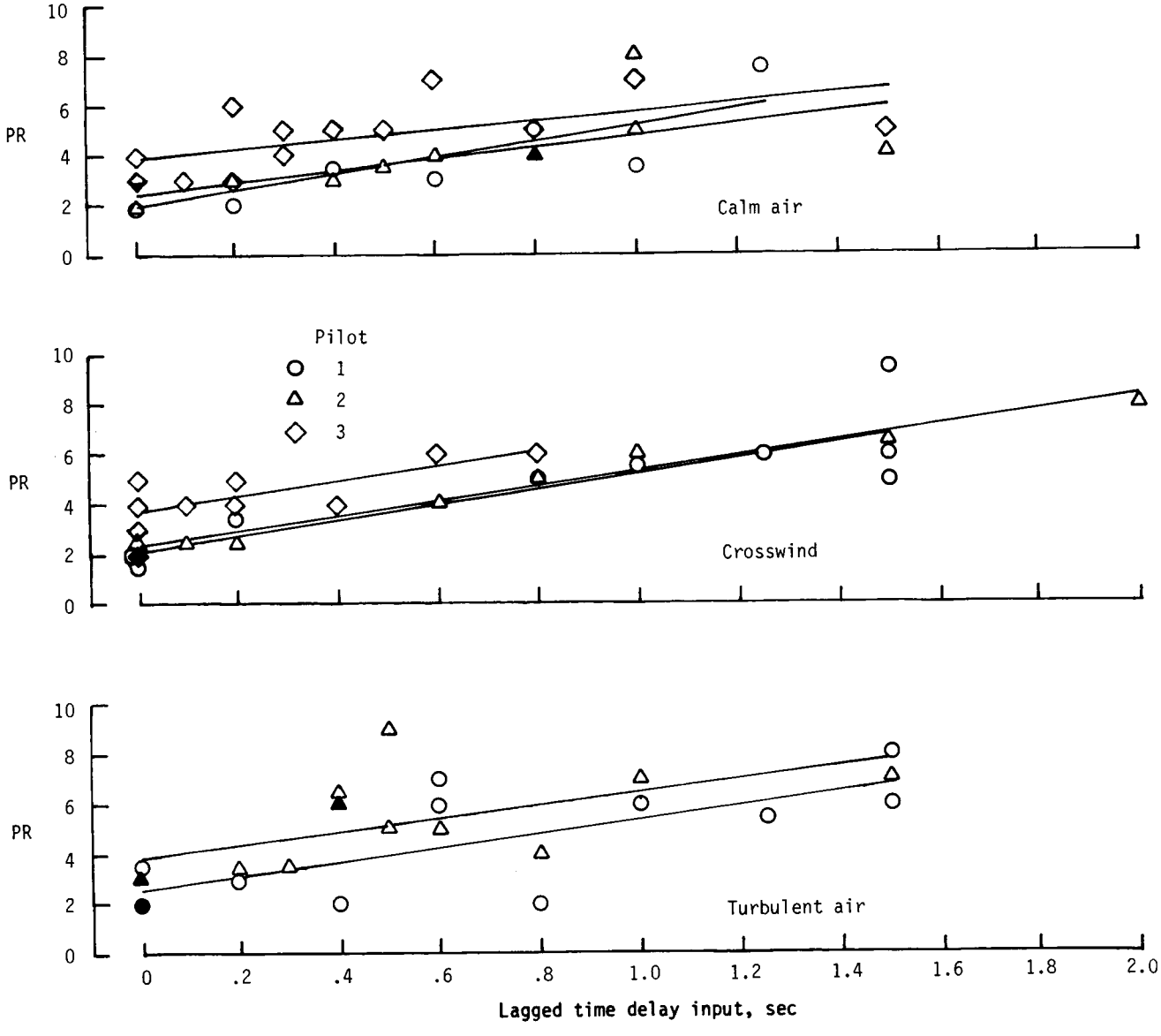

(b) Lateral control.

Figure 8. Concluded.

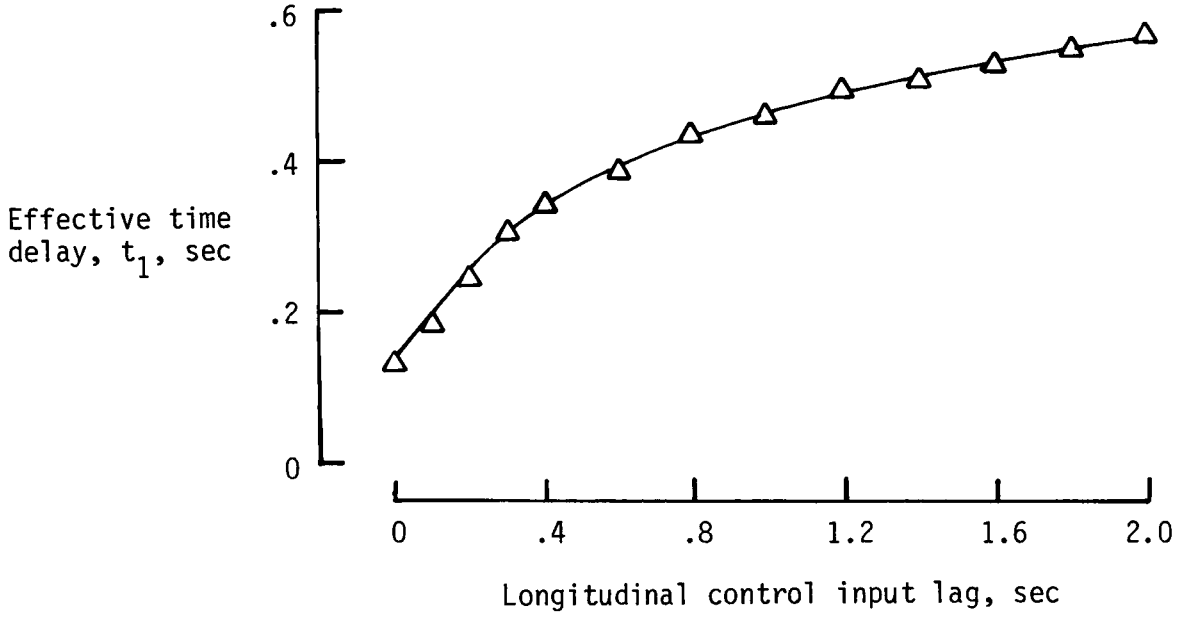

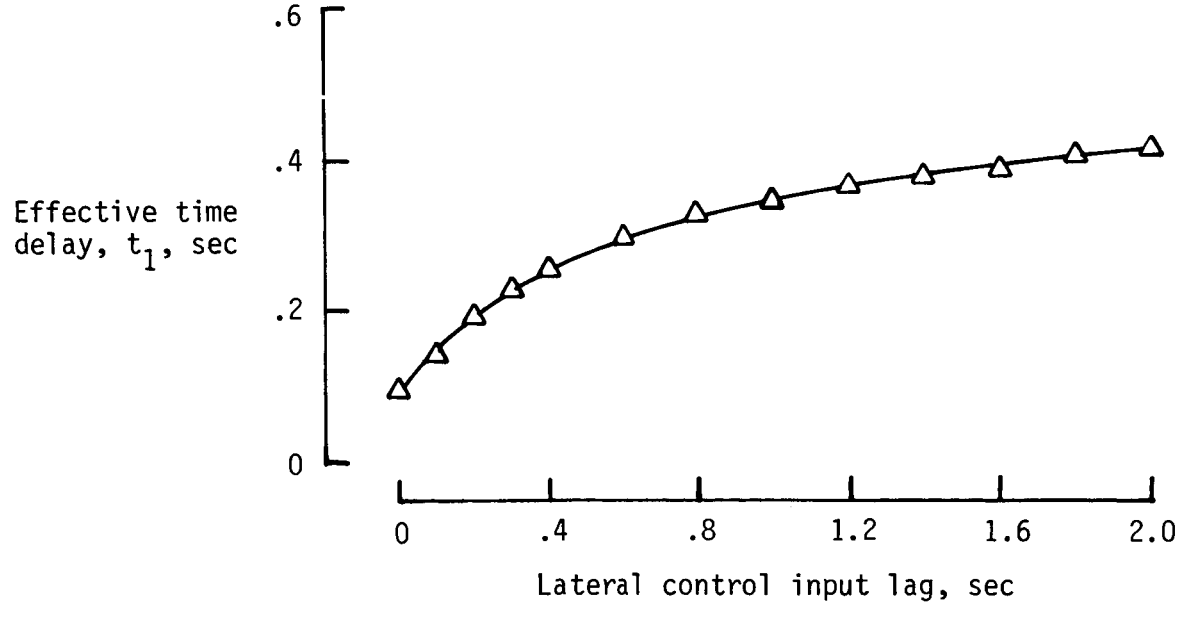

Figure 9. Conversion from longitudinal and lateral control input lags to effective time delay.

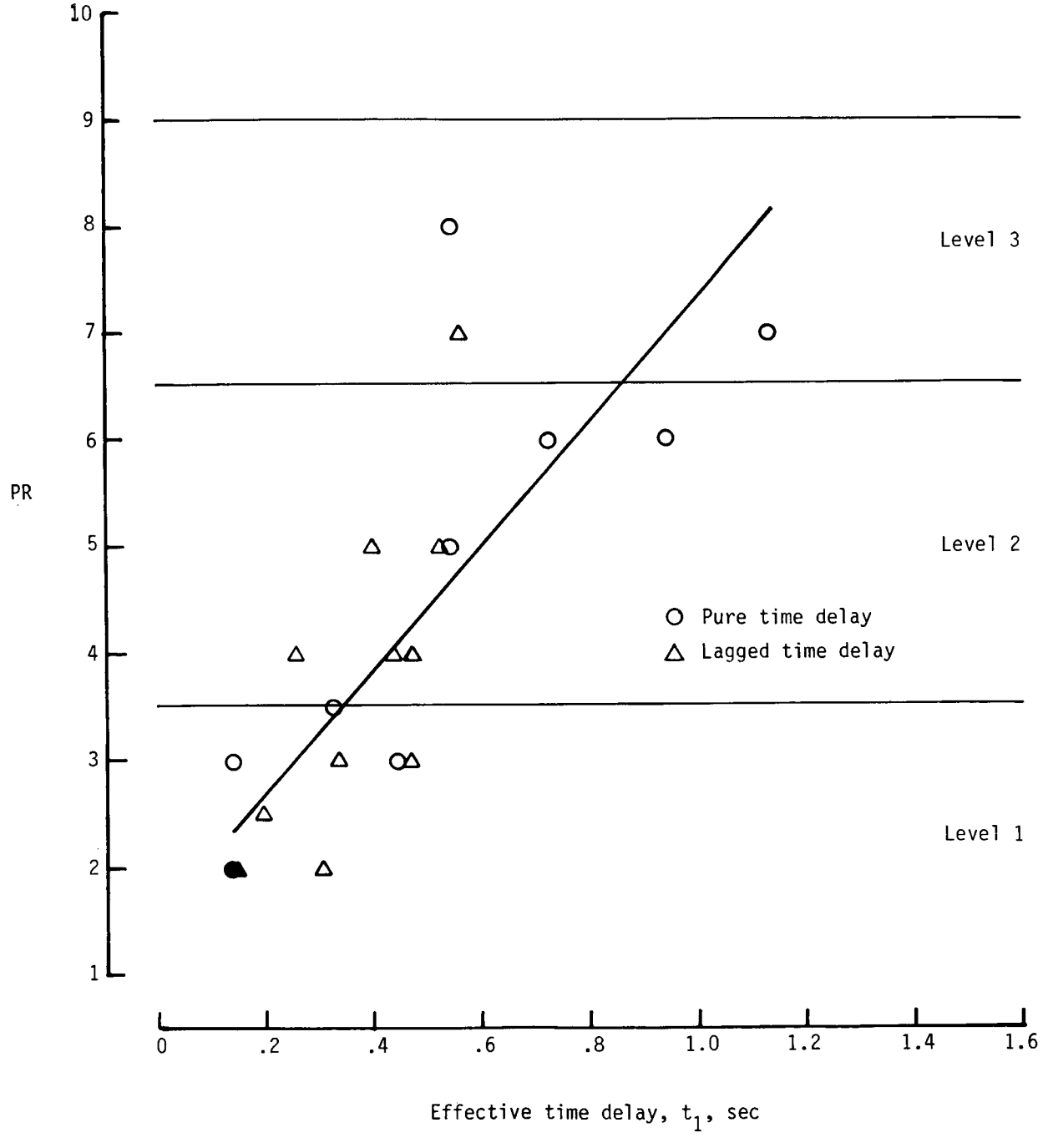

(a) Calm air; pilot 2; $\sigma_{PR} = 1.06$; $\rho = 0.829$.

Figure 10. Pilot rating as a function of effective time delay of longitudinal control. Solid symbols equate to two or more data points.

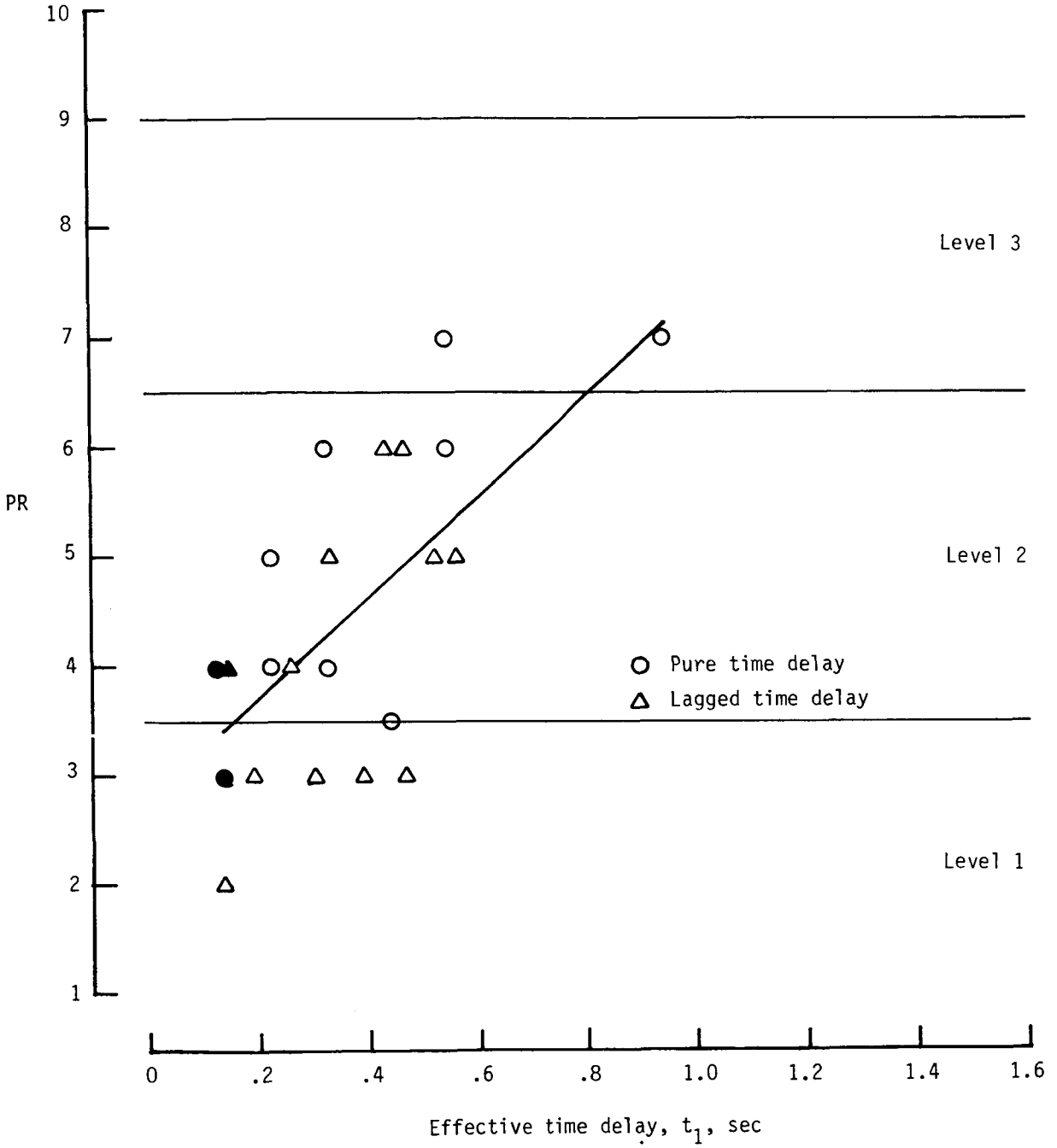

(b) Calm air; pilot 3; $\sigma_{PR} = 1.02$; $\rho = 0.663$.

Figure 10. Continued.

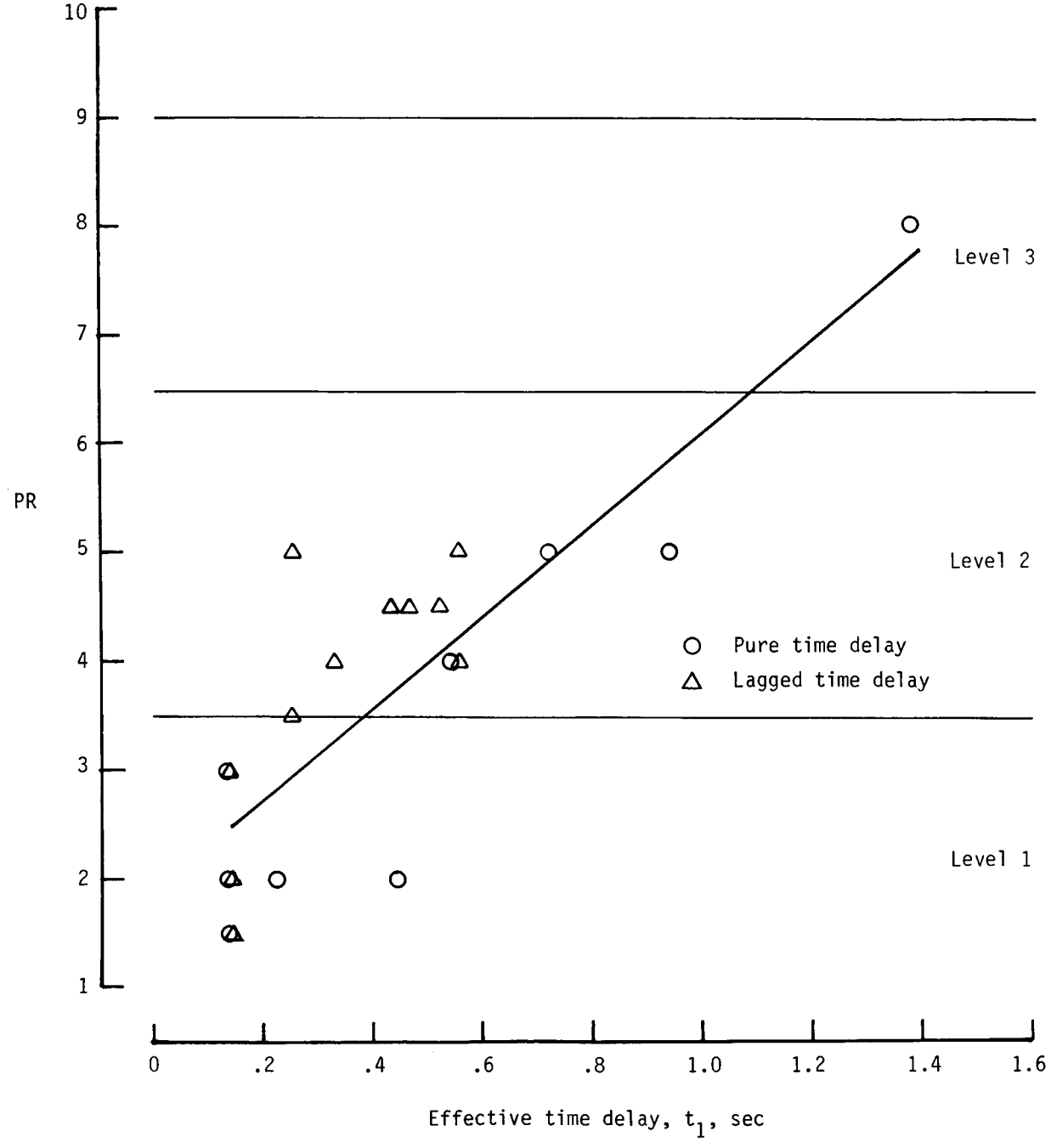

(c) Crosswind; pilot 1; $\sigma_{PR} = 0.89$; $\rho = 0.835$.

Figure 10. Continued.

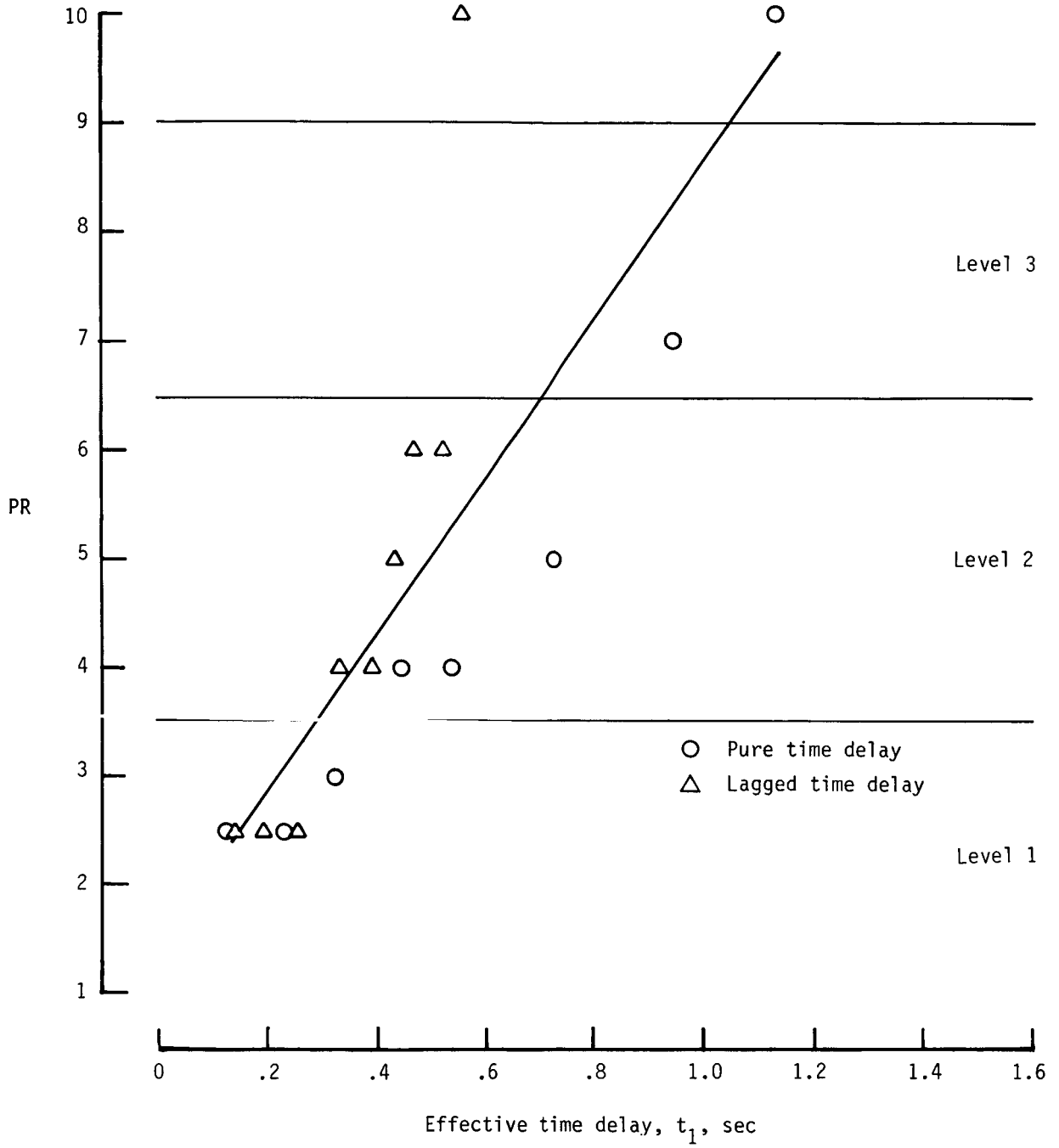

(d) Crosswind; pilot 2; $\sigma_{PR} = 1.44$; $\rho = 0.817$.

Figure 10. Continued.

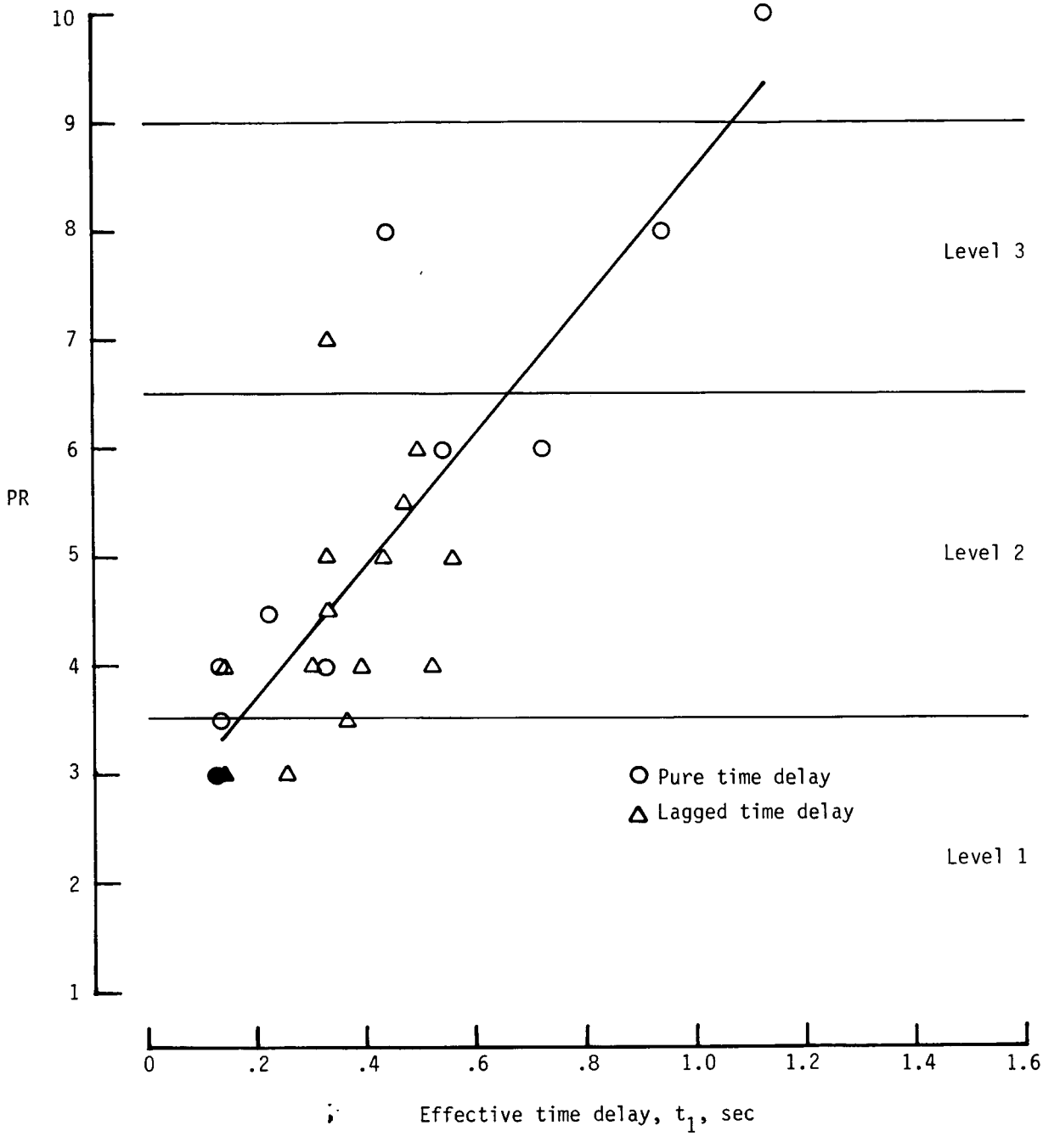

(e) Turbulence; pilot 2; $\sigma_{PR} = 0.92$; $\rho = 0.844$.

Figure 10. Continued.

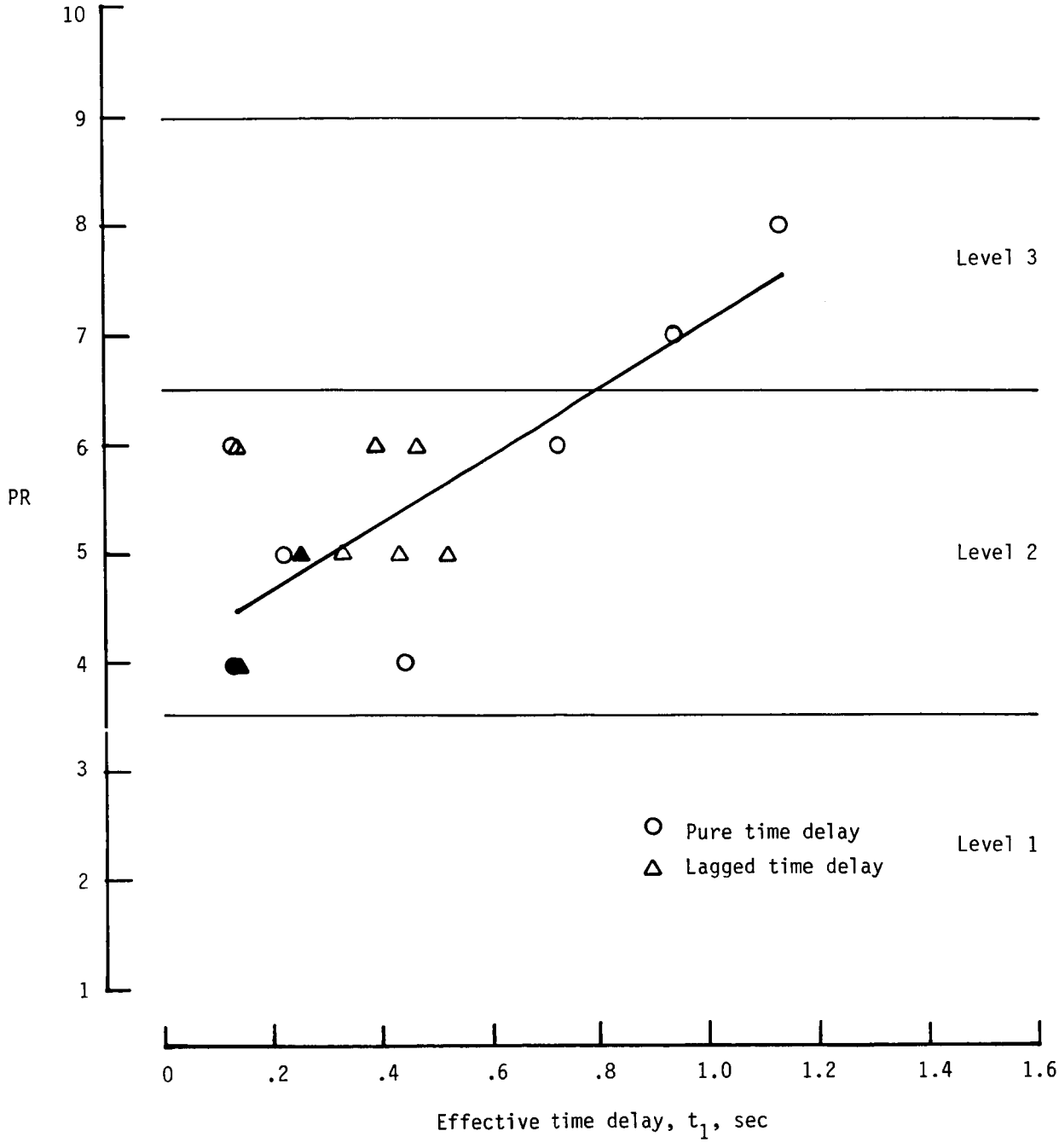

(f) Turbulence; pilot 3; $\sigma_{PR} = 0.74$; $\rho = 0.774$.

Figure 10. Concluded.

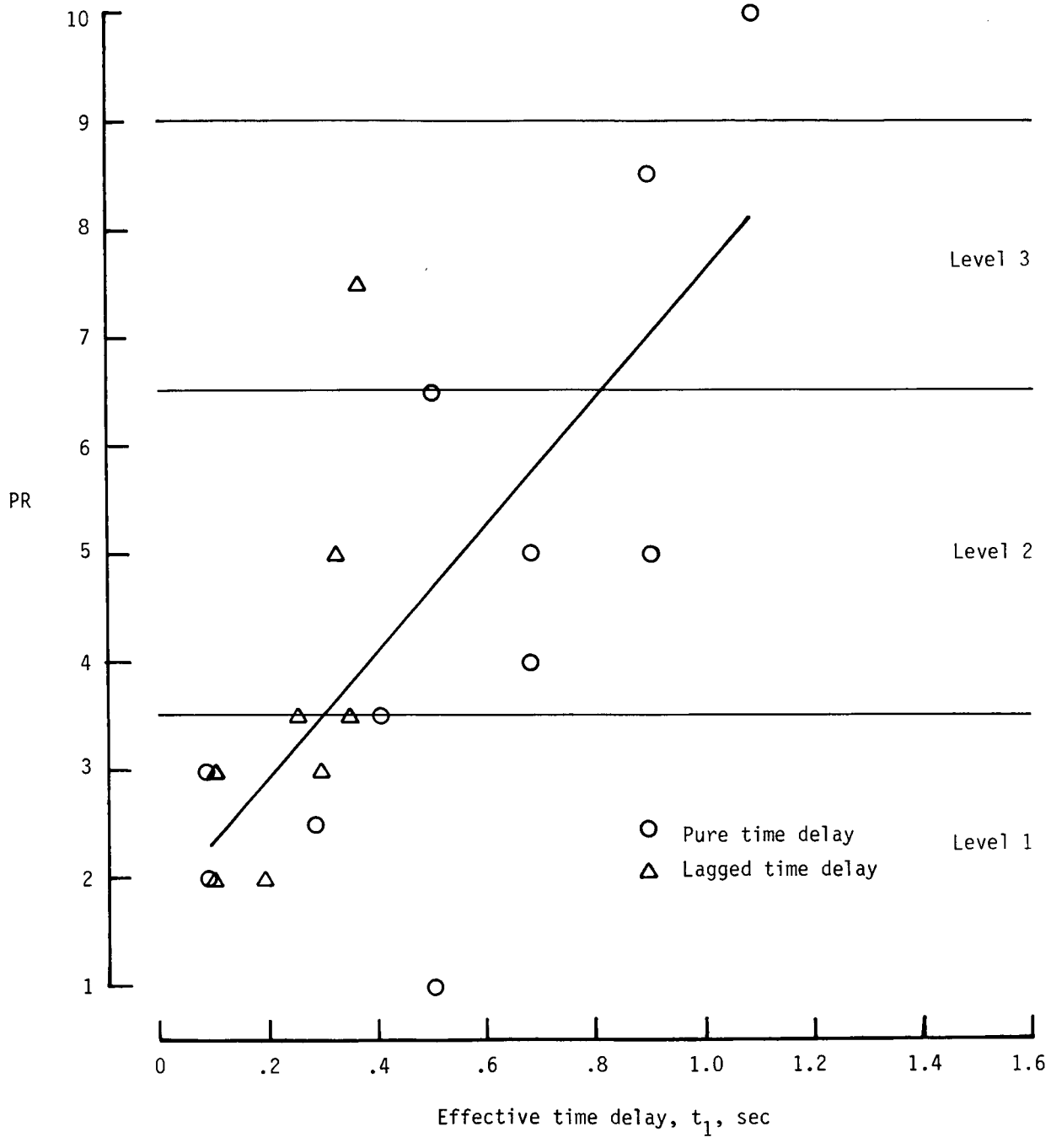

(a) Calm air; pilot 1; $\sigma_{PR} = 1.69$; $\rho = 0.730$.

Figure 11. Pilot rating as a function of effective time delay of lateral control. Solid symbols equate to two or more data points.

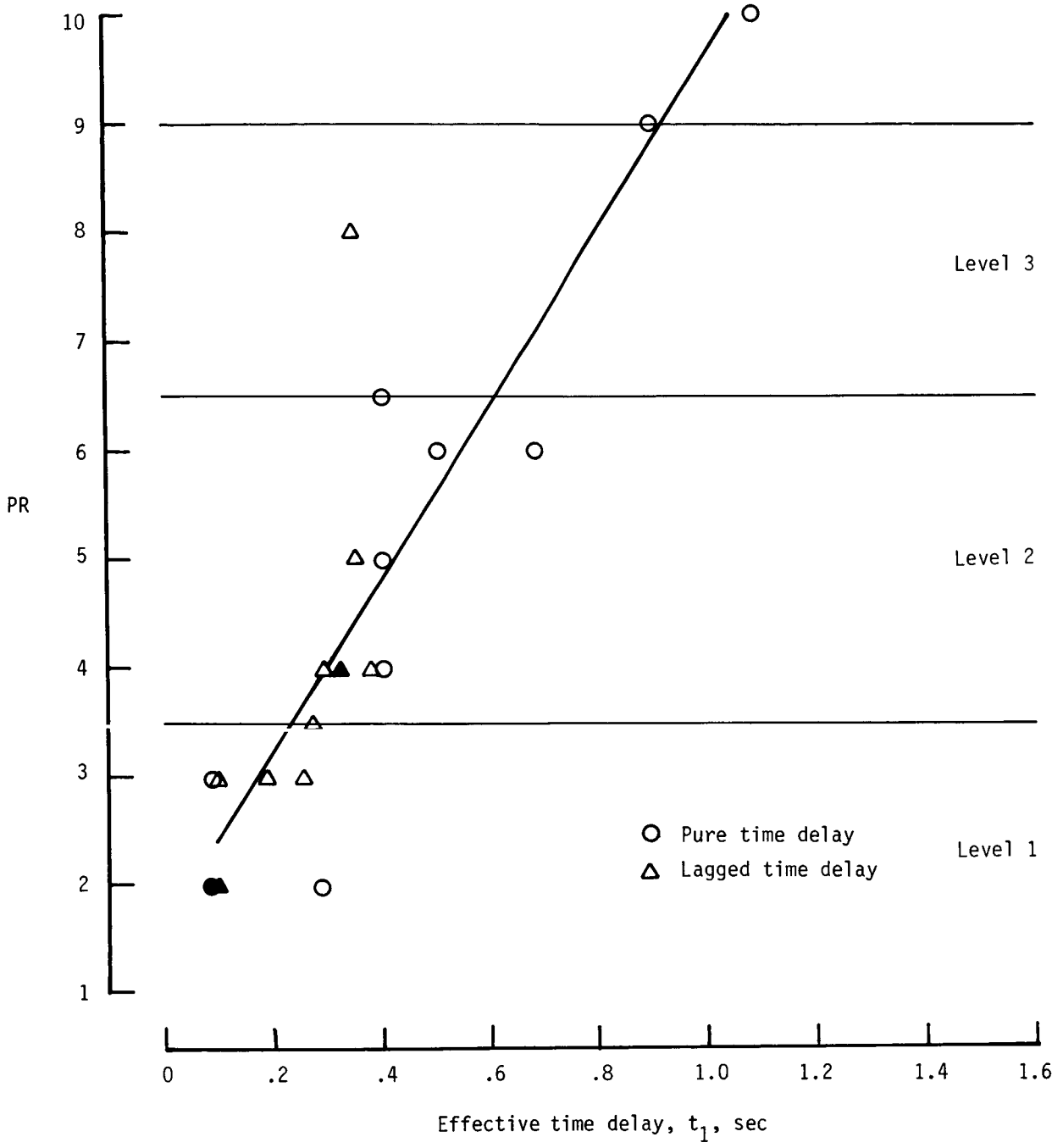

(b) Calm air; pilot 2; $\sigma_{PR} = 1.03$; $\rho = 0.897$.

Figure 11. Continued.

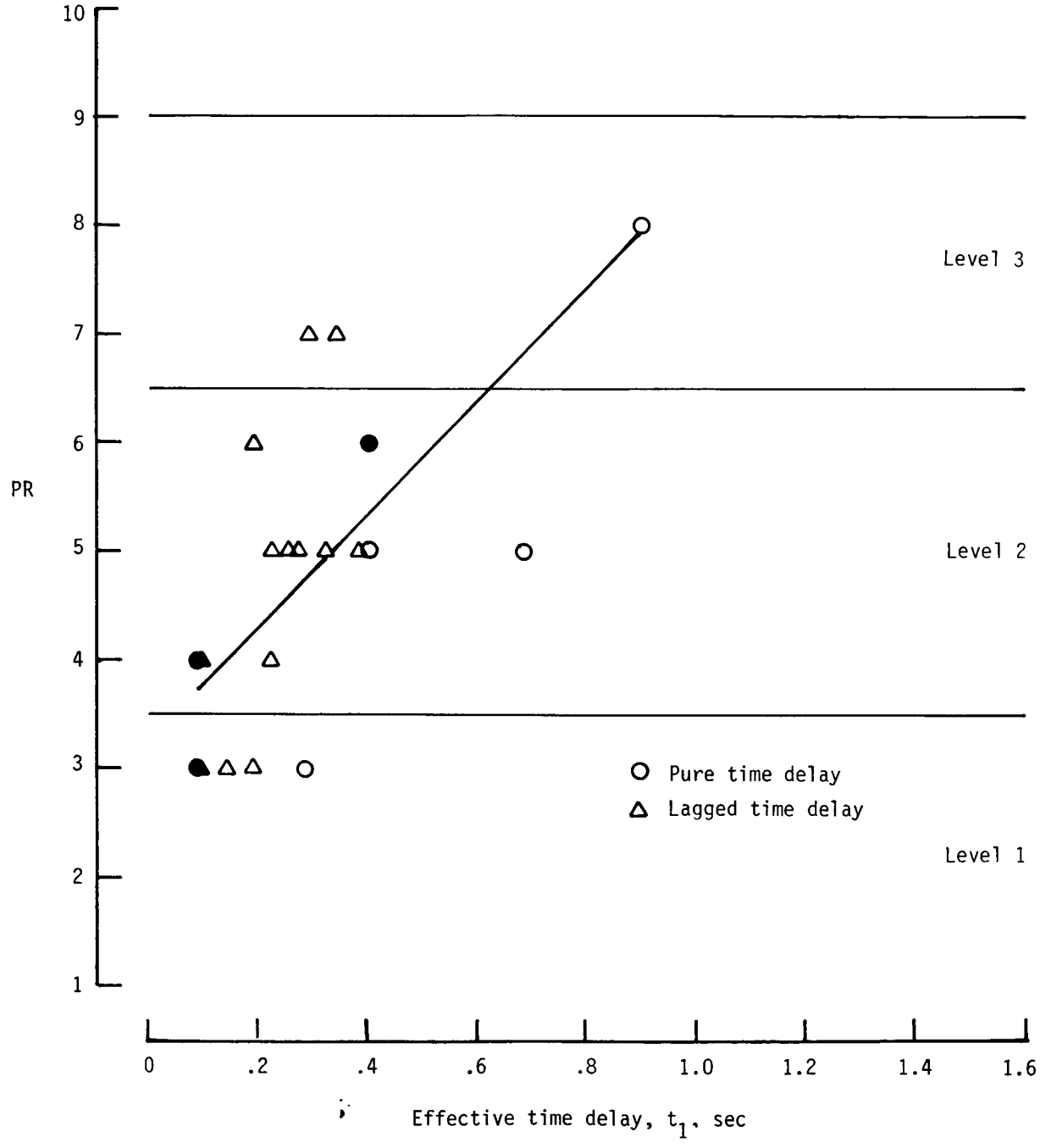

(c) Calm air; pilot 3; $\sigma_{PR} = 1.04$; $\rho = 0.707$.

Figure 11. Continued.

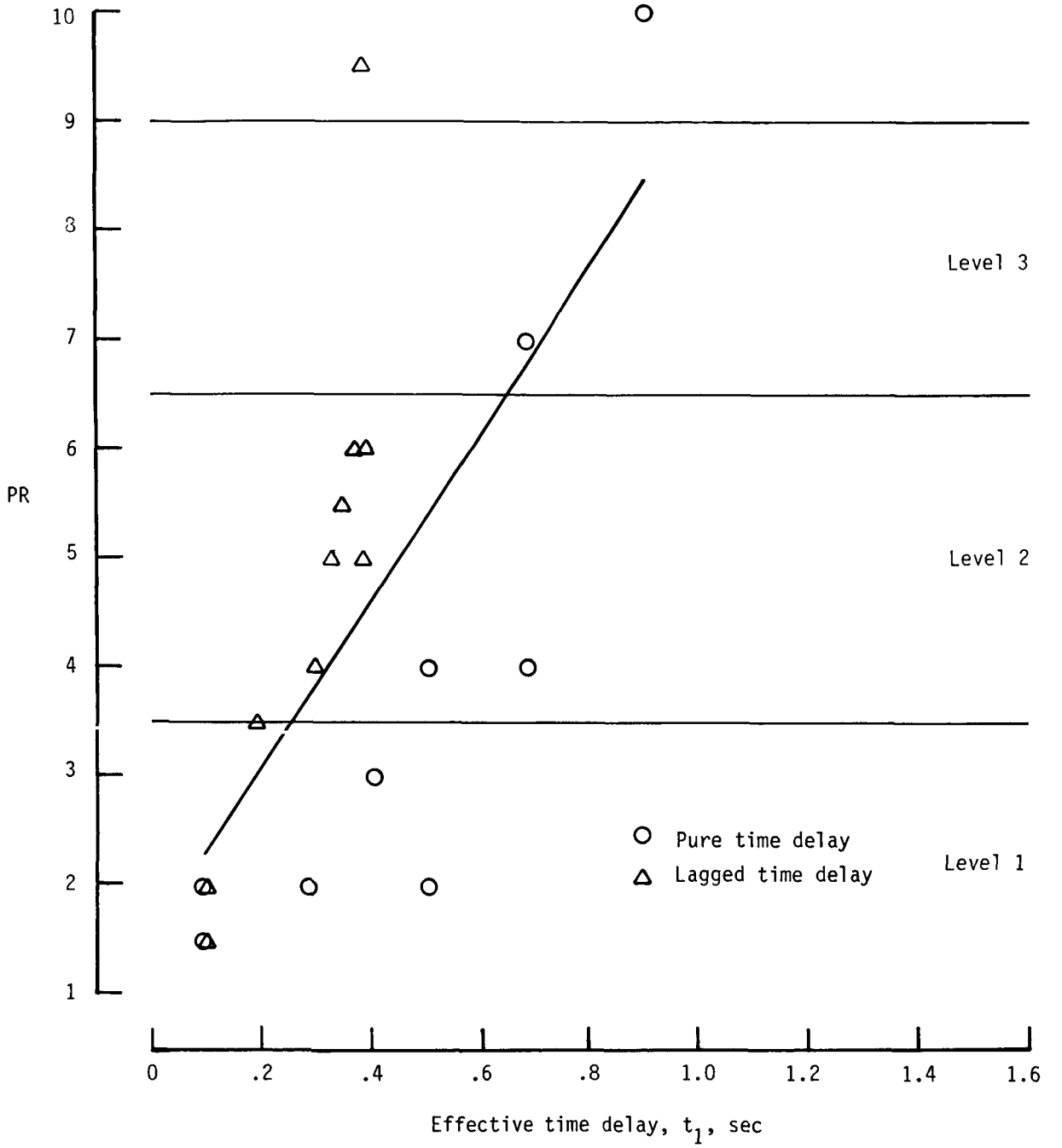

(d) Crosswind; pilot 1; $\sigma_{PR} = 1.94$; $\rho = 0.665$.

Figure 11. Continued.

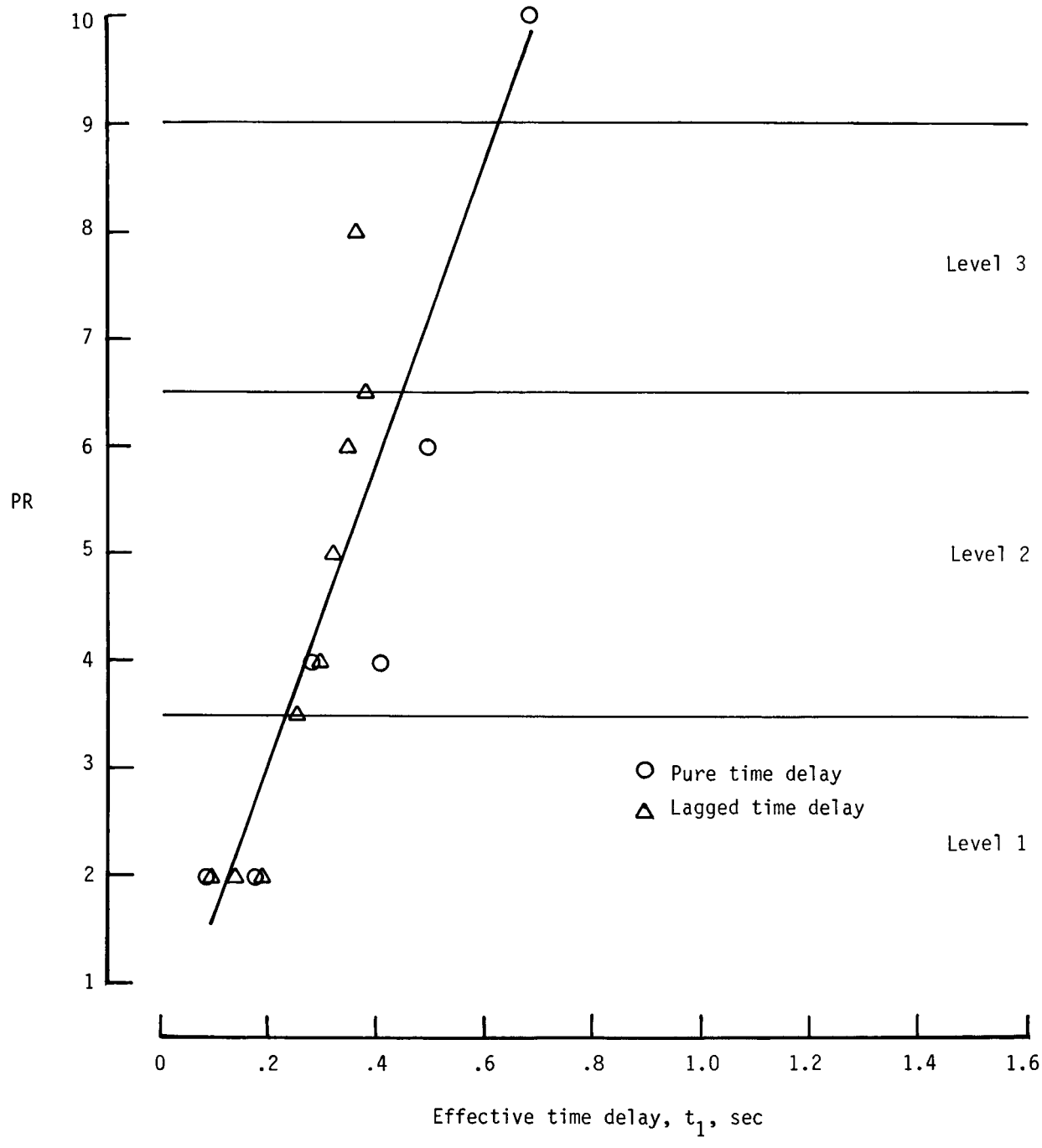

(e) Crosswind; pilot 2; $\sigma_{PR} = 1.11$; $\rho = 0.900$.

Figure 11. Continued.

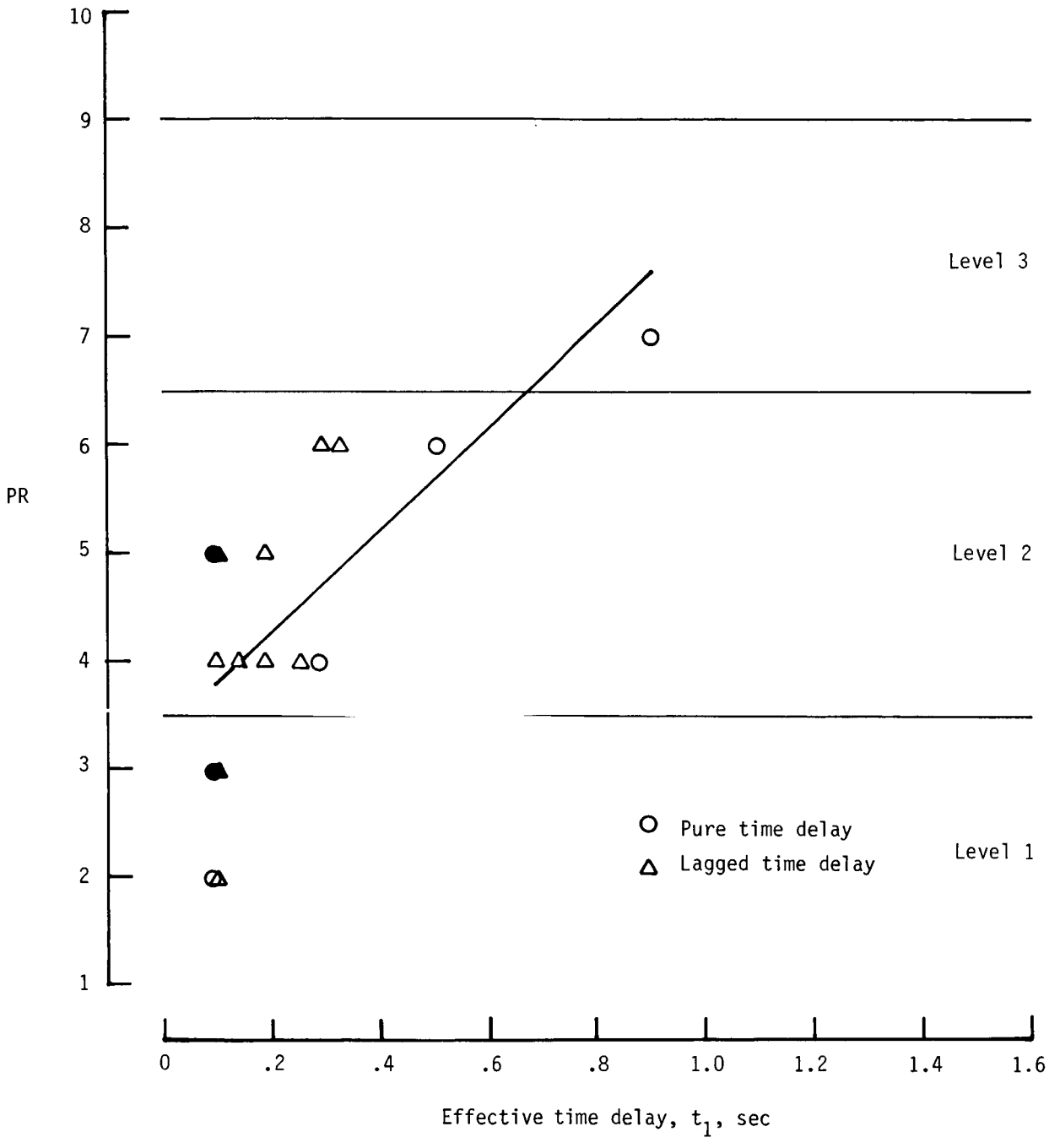

(f) Crosswind; pilot 3; $\sigma_{PR} = 1.02$; $\rho = 0.678$.

Figure 11. Continued.

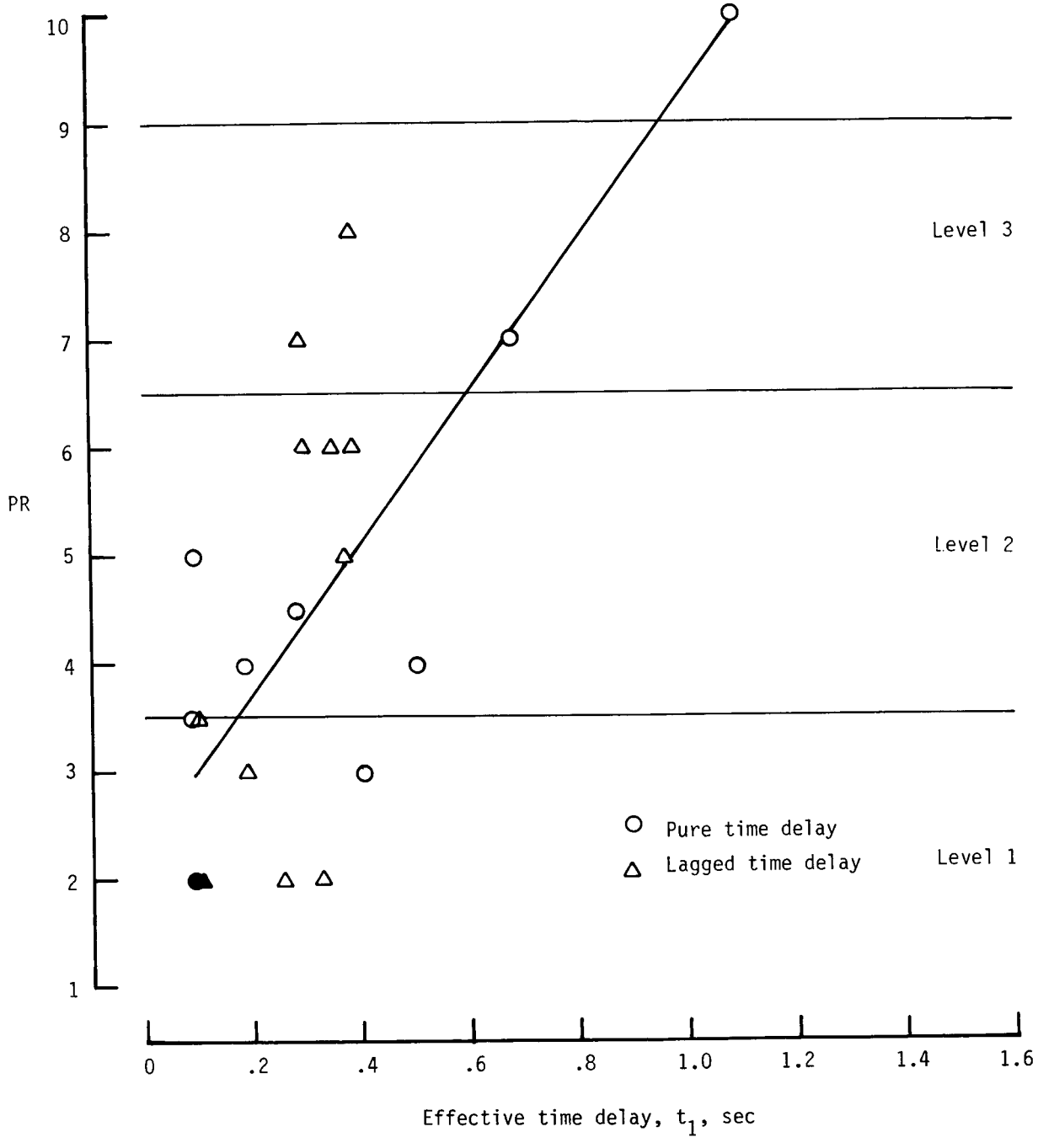

(g) Turbulence; pilot 1; $\sigma_{PR} = 1.56$; $\rho = 0.736$.

Figure 11. Continued.

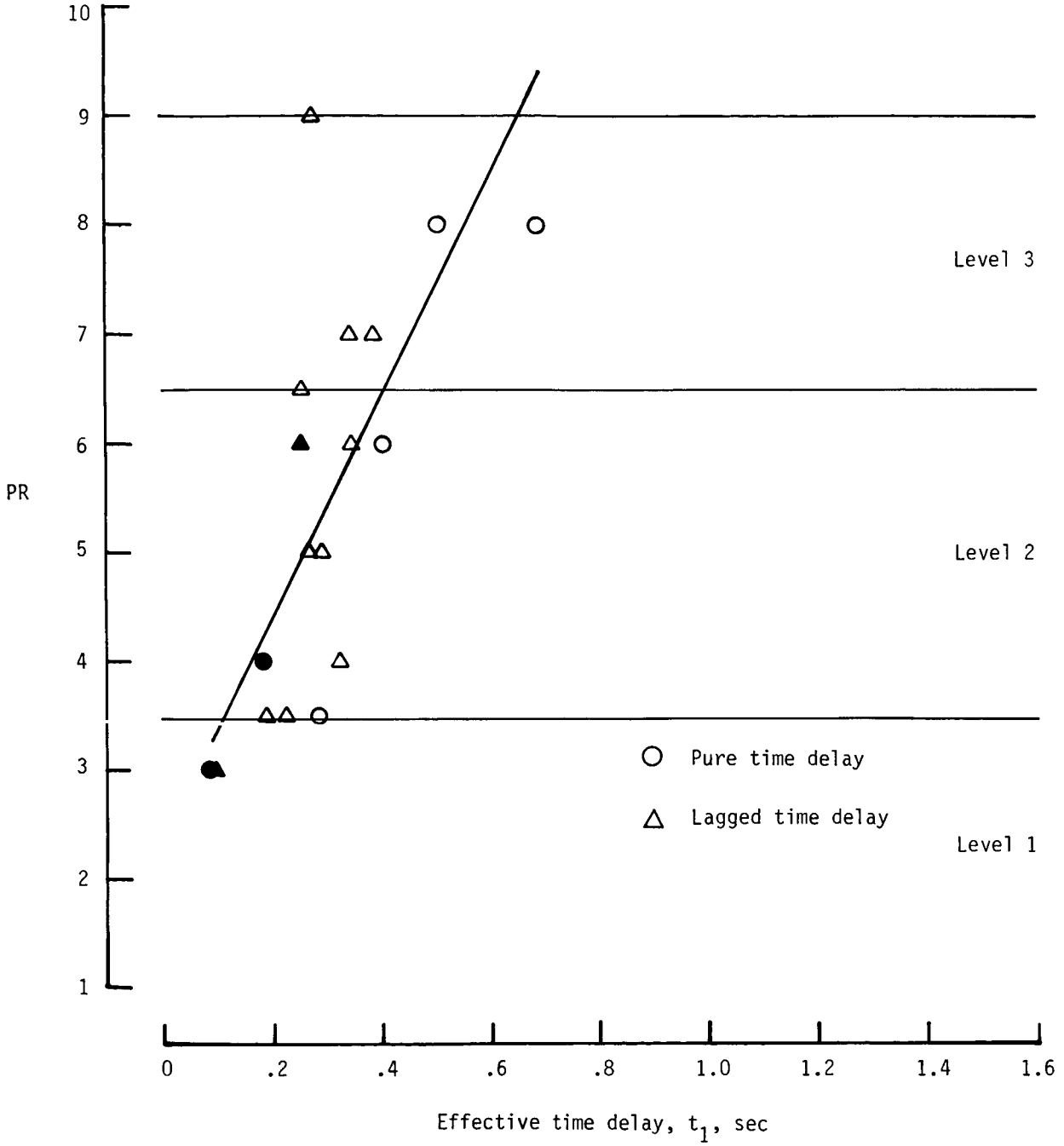

(h) Turbulence; pilot 2; $\sigma_{PR} = 1.23$; $\rho = 0.778$.

Figure 11. Concluded.

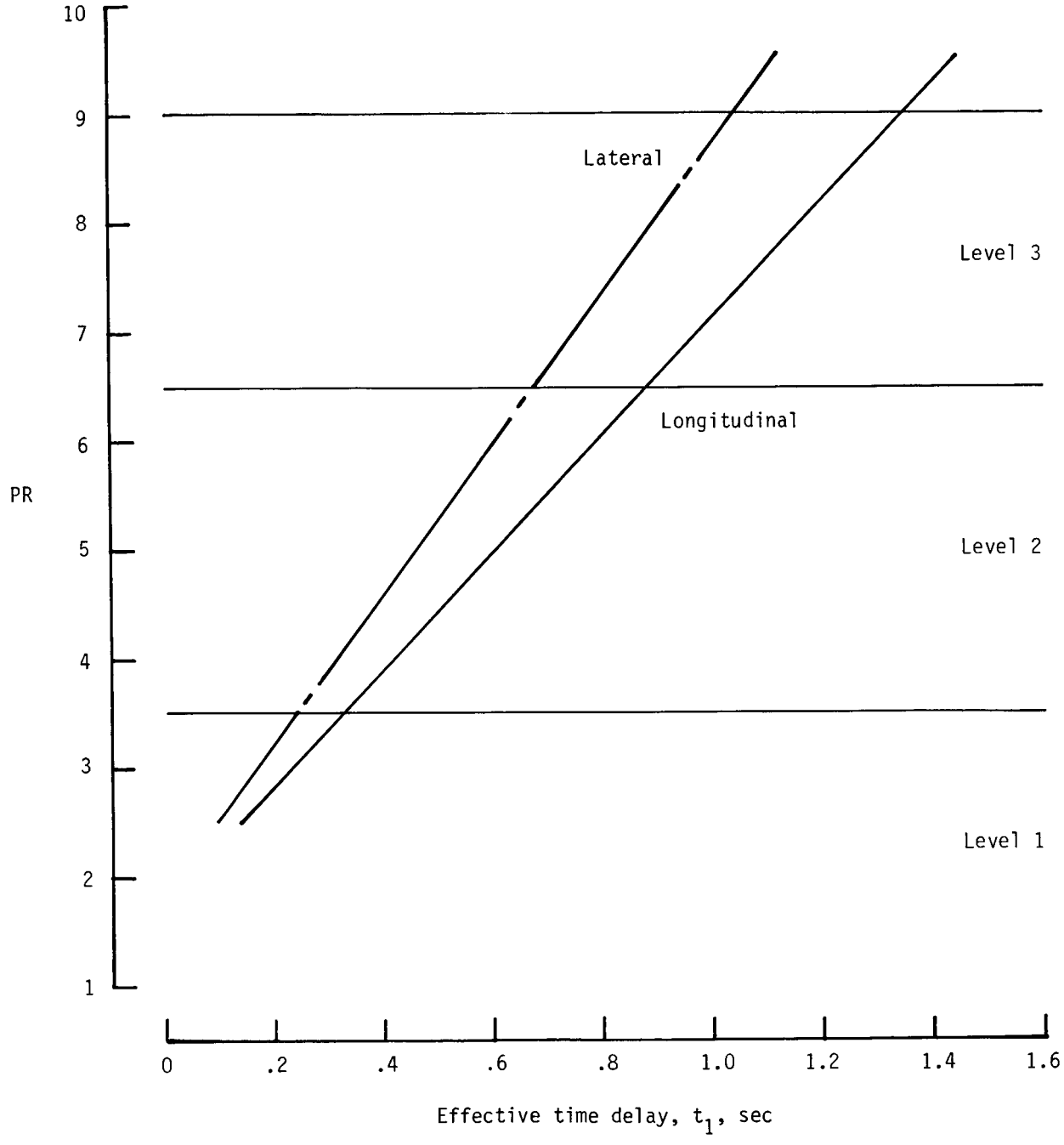

Figure 12. Averaged and adjusted calm air and crosswind results of pilot rating plotted against effective time delay. Ratings for pilot 3 were adjusted by −1 for calm air (longitudinal) and calm air and crosswind (lateral).

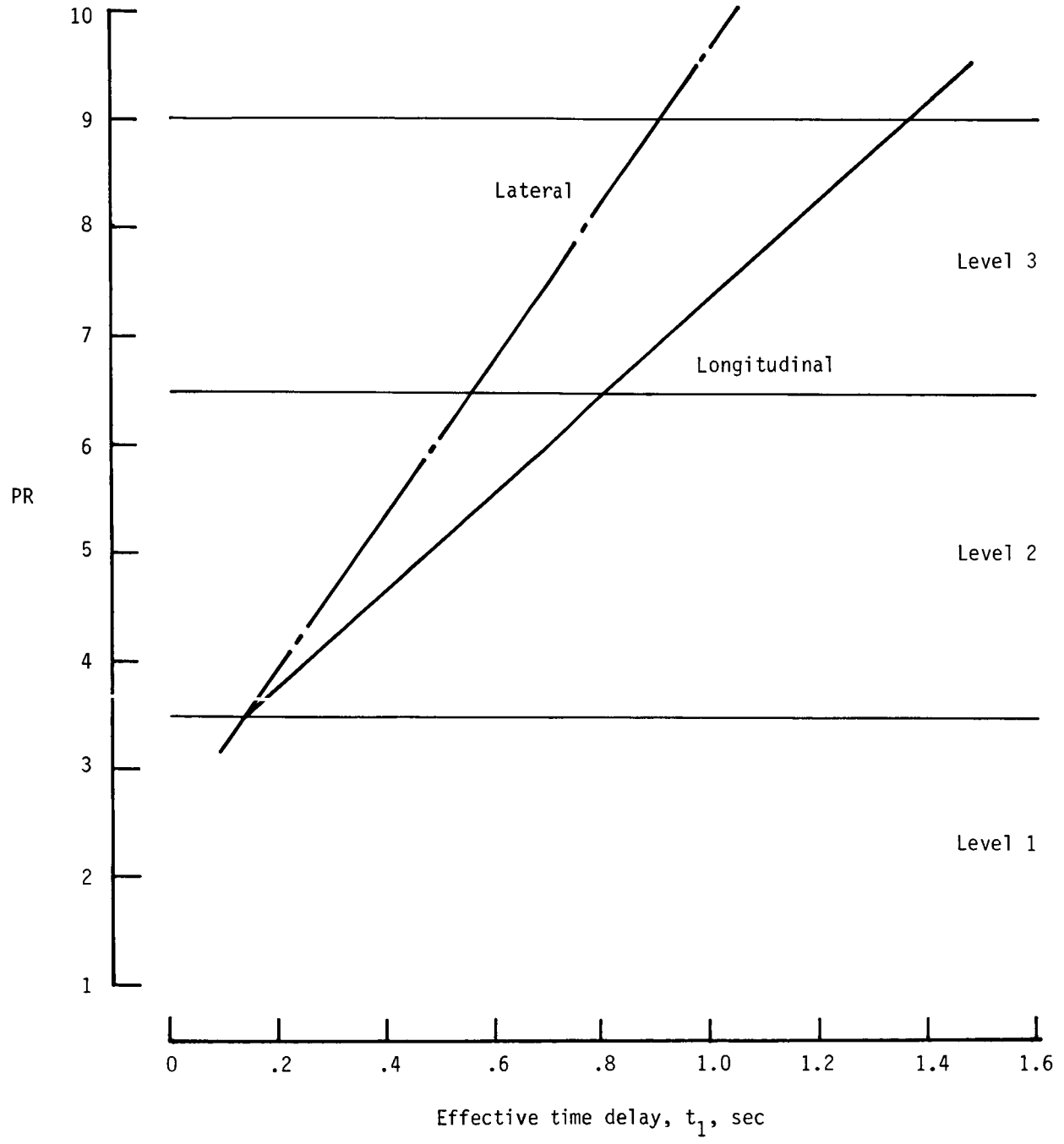

Figure 13. Averaged and adjusted turbulent air results of pilot rating plotted against effective time delay. Ratings for pilot 3 were adjusted by −1 for turbulence (longitudinal).

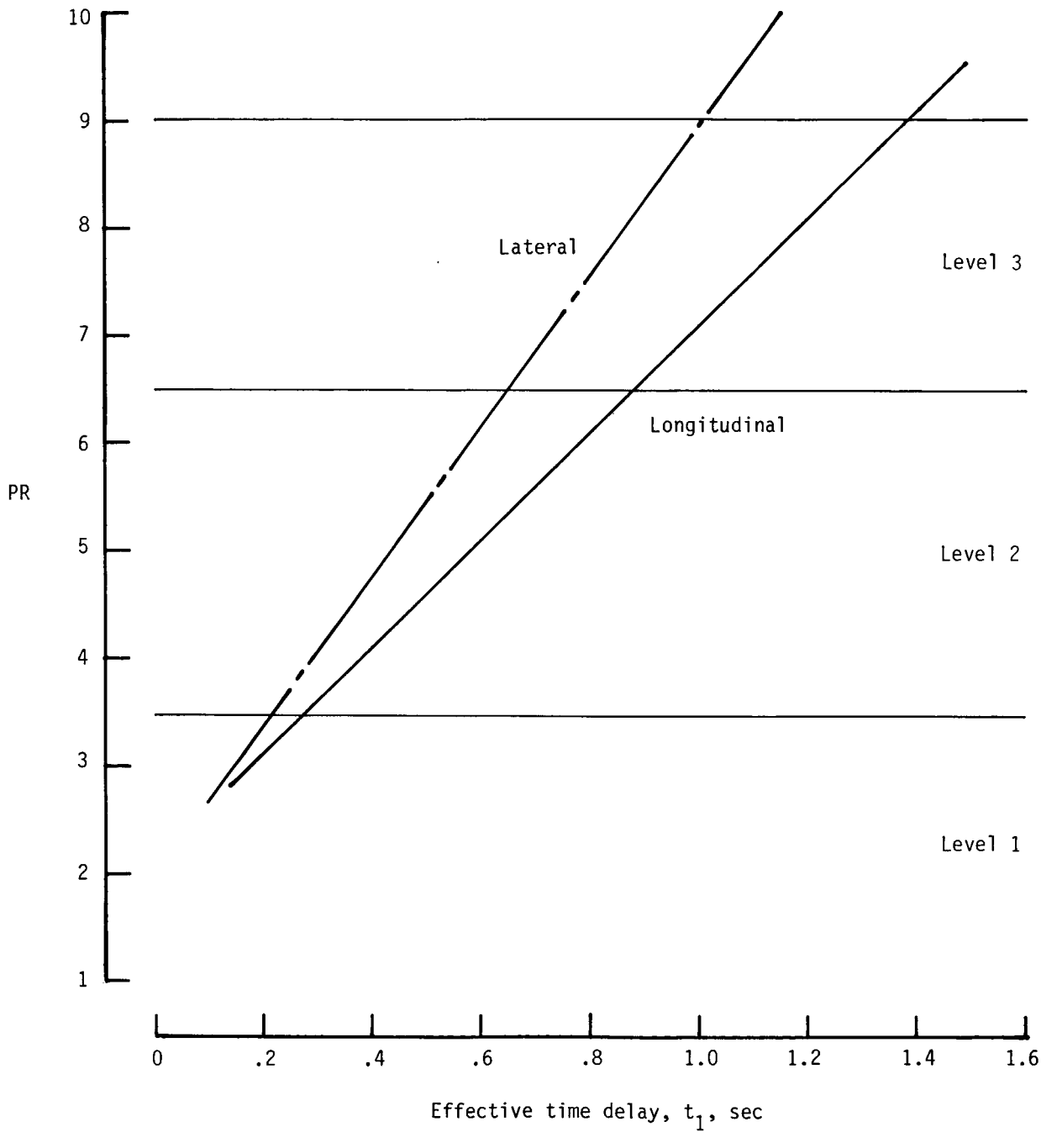

Figure 14. Averaged and adjusted calm air, crosswind, and turbulence results of pilot rating plotted against effective time delay. Ratings for pilot 3 were adjusted by −1 for calm air and turbulence (longitudinal) and calm air and crosswind (lateral).

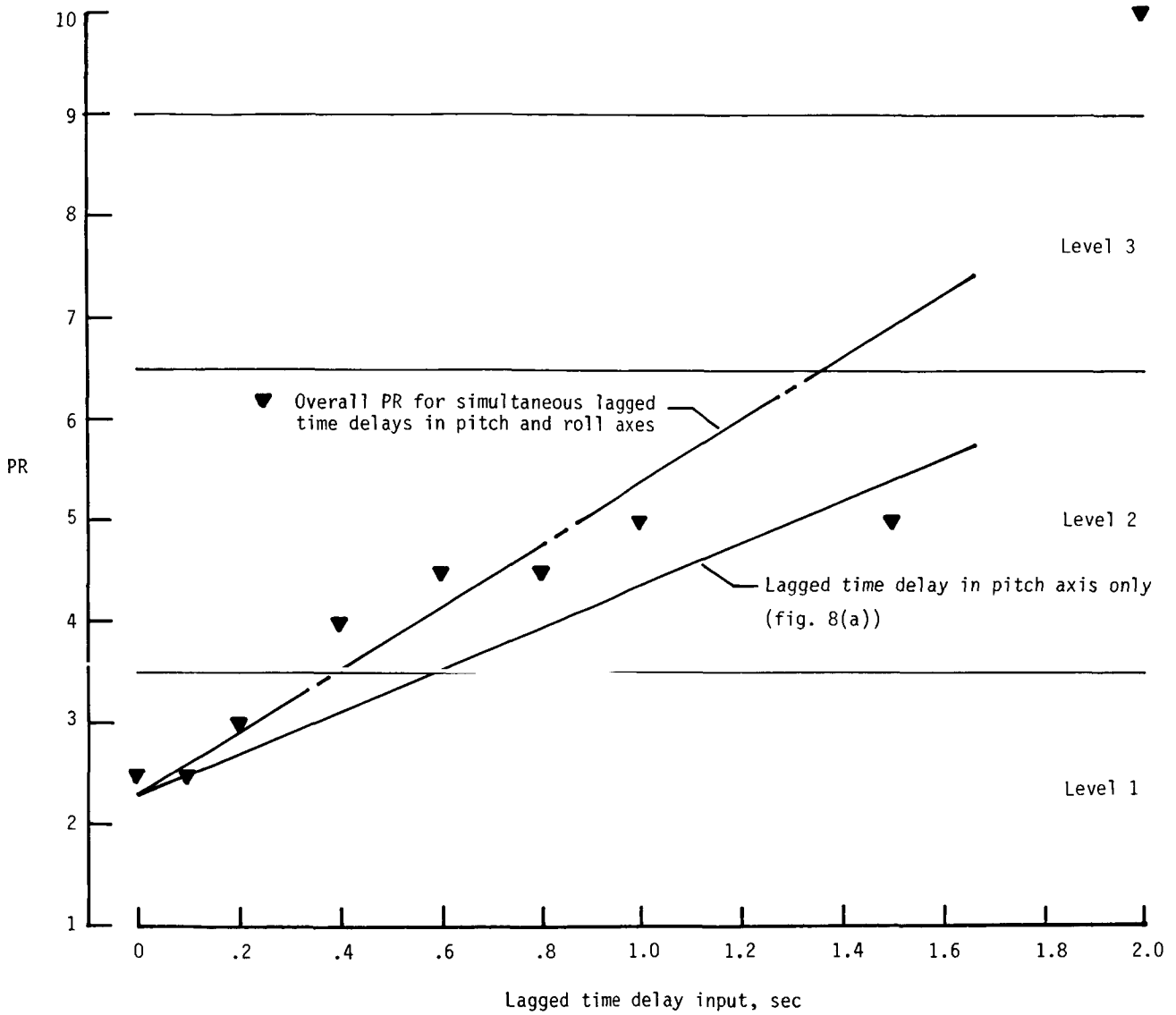

(a) Comparison with pitch axis.

Figure 15. Effect of simultaneous lagged time delays about two axes compared with a single axis. Flight in calm air; pilot 2.

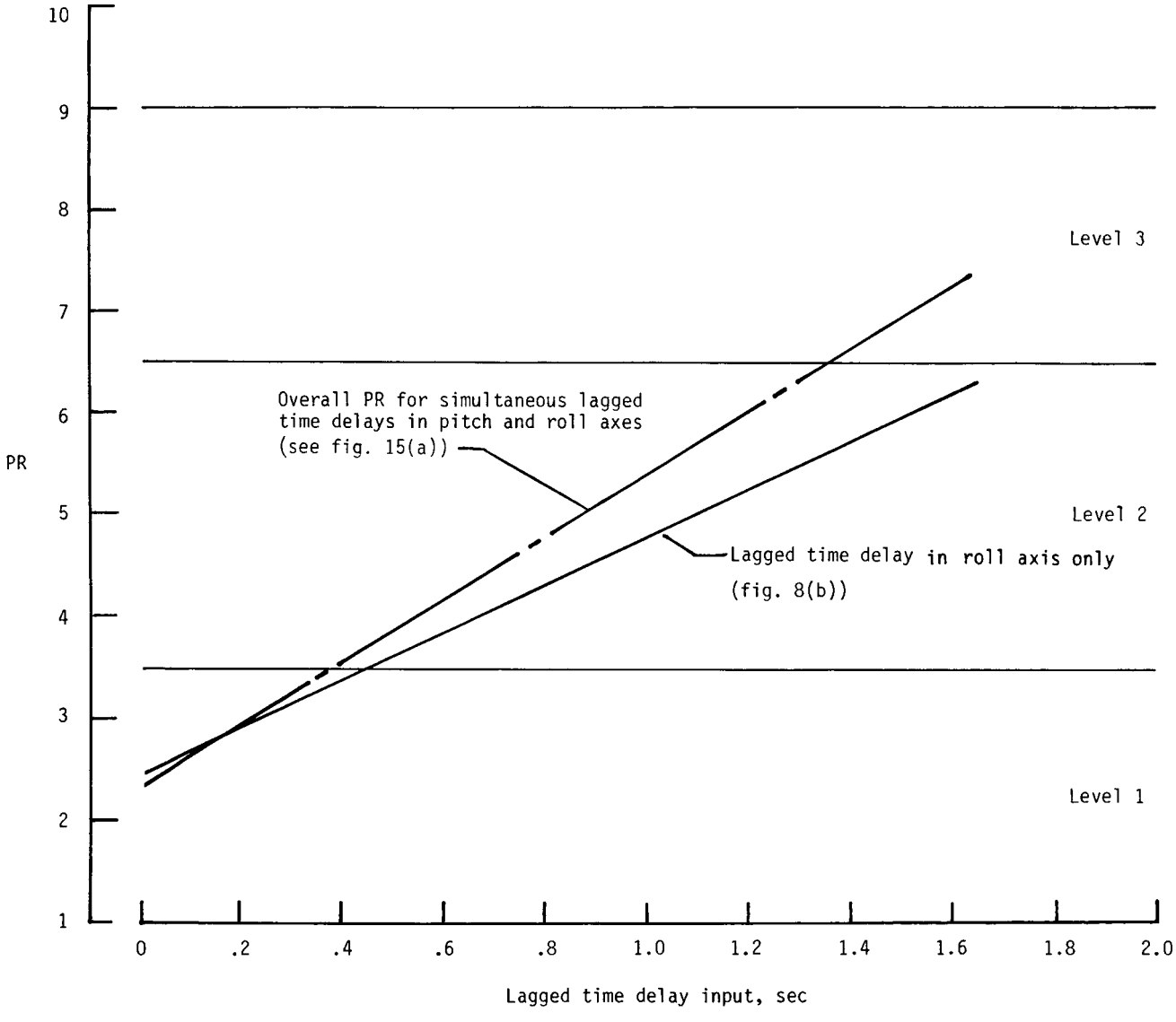

(b) Comparison with roll axis.

Figure 15. Concluded.

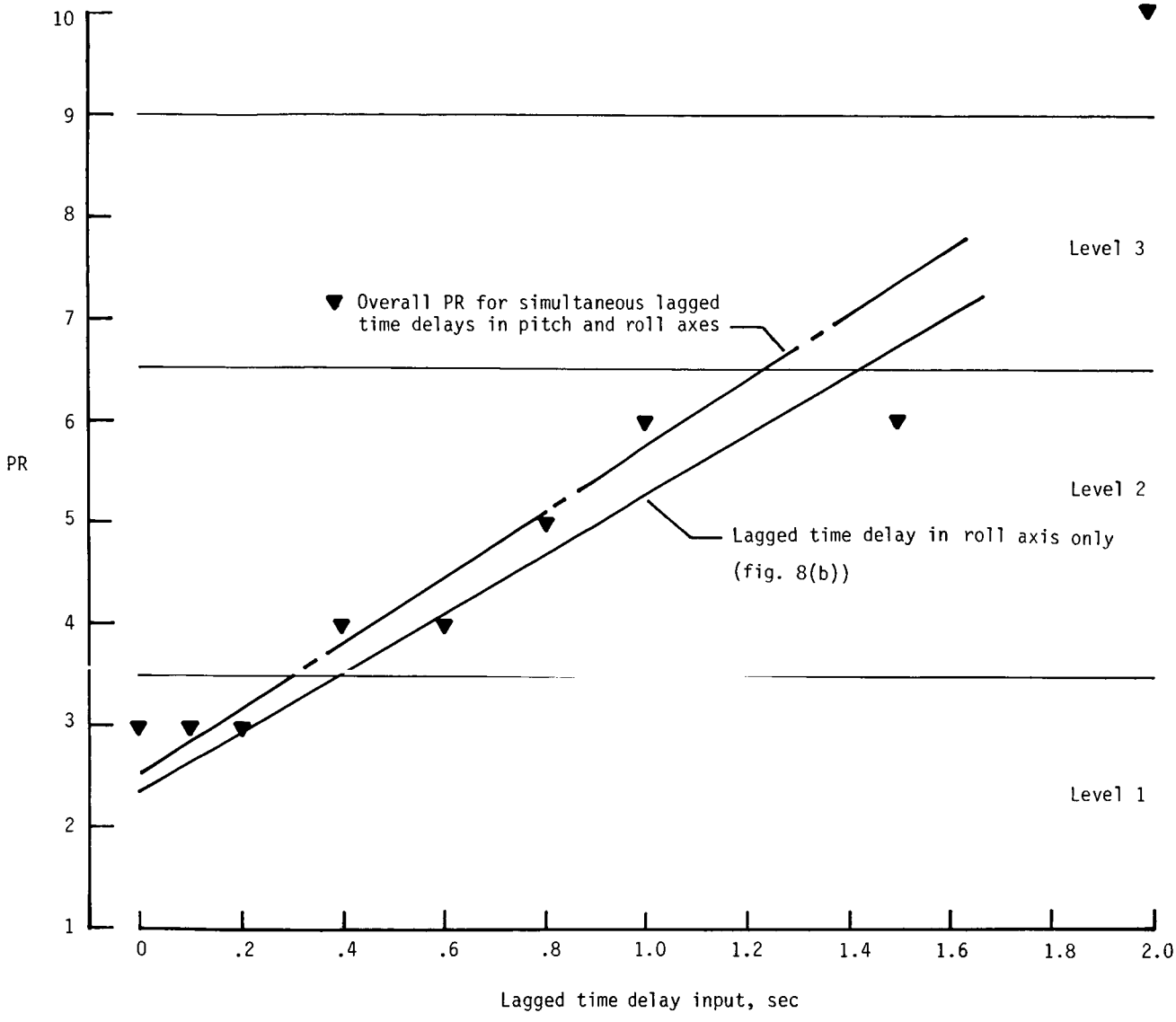

Figure 16. Effect of simultaneous lagged time delays about two axes compared with a single roll axis. Flight in crosswind; pilot 2.

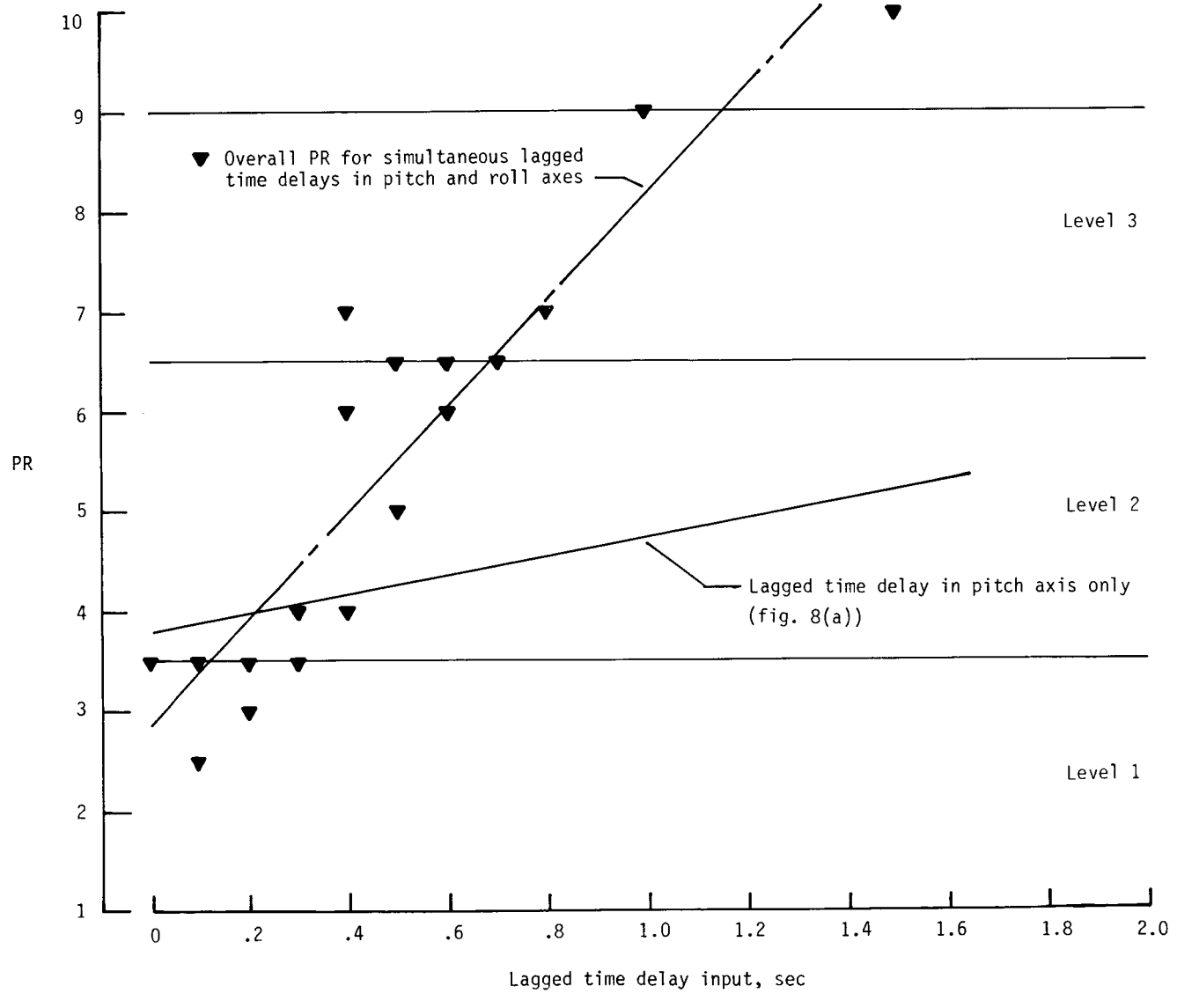

(a) Comparison with pitch axis.

Figure 17. Effect of simultaneous lagged time delays about two axes compared with a single axis. Flight in turbulence; pilot 2.

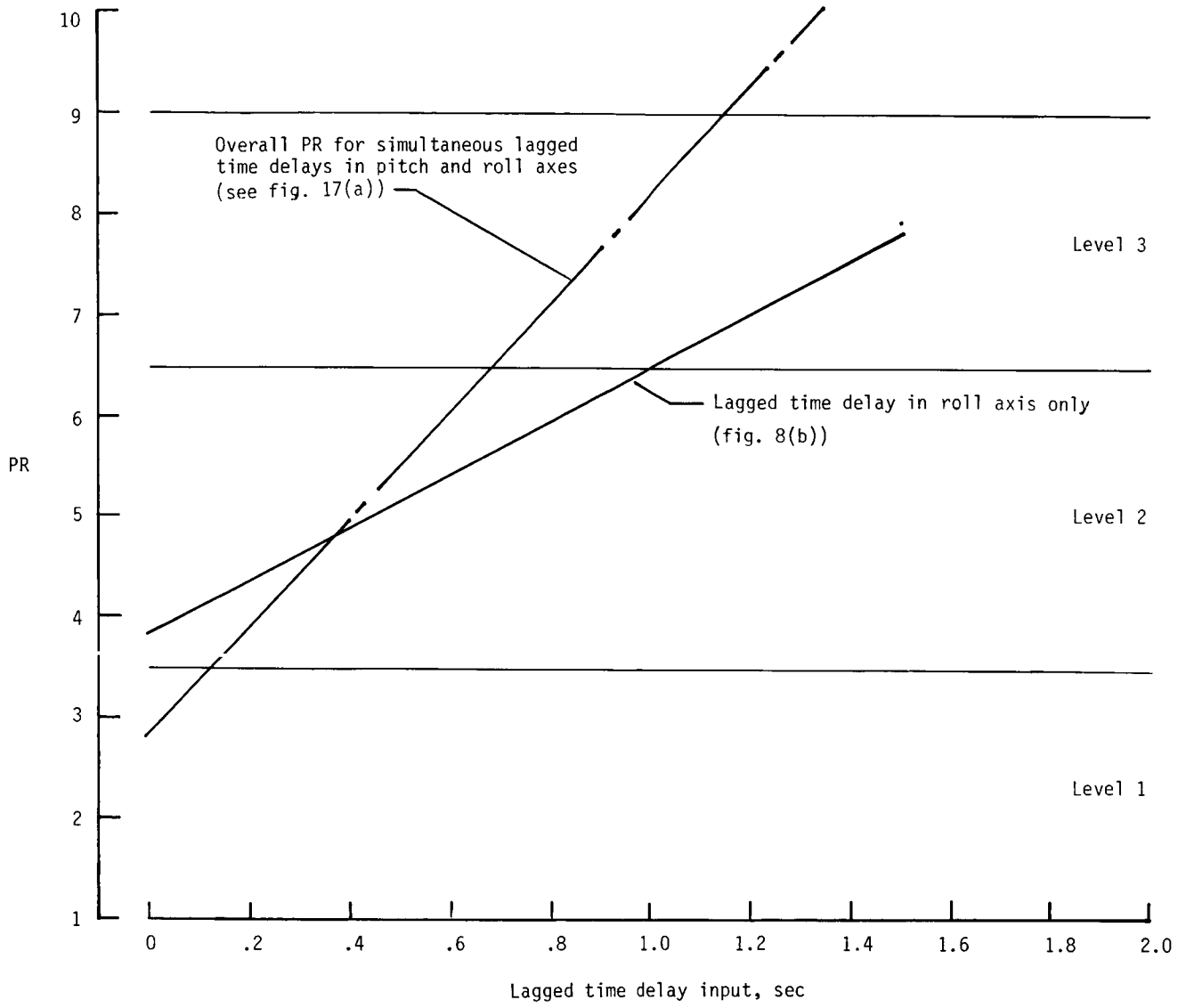

(b) Comparison with roll axis.

Figure 17. Concluded.

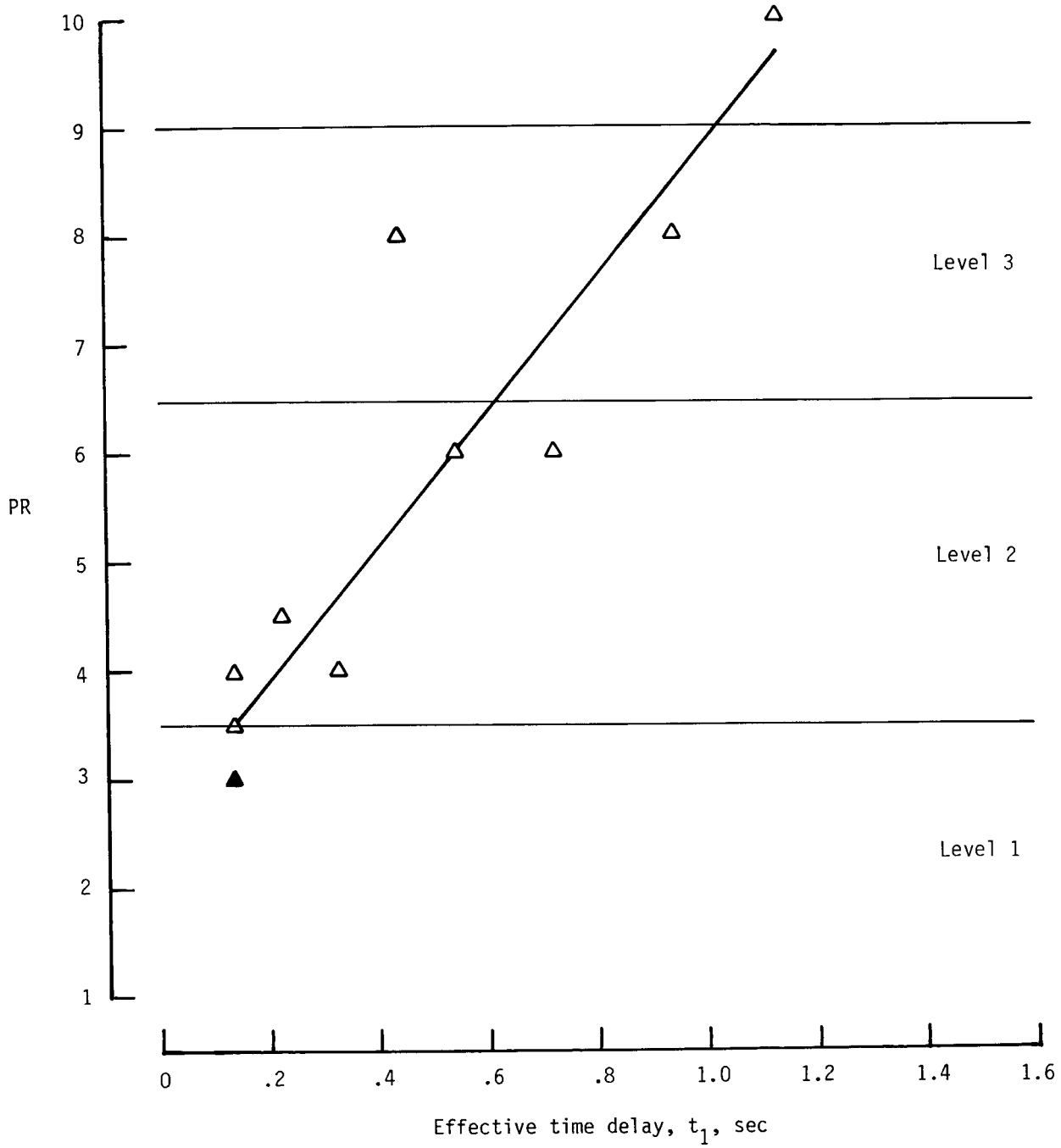

Figure 18. Effect of longitudinal effective time delay on pilot rating. Pilot 2; pure time delay; turbulent conditions; solid symbol equates to two or more data points.

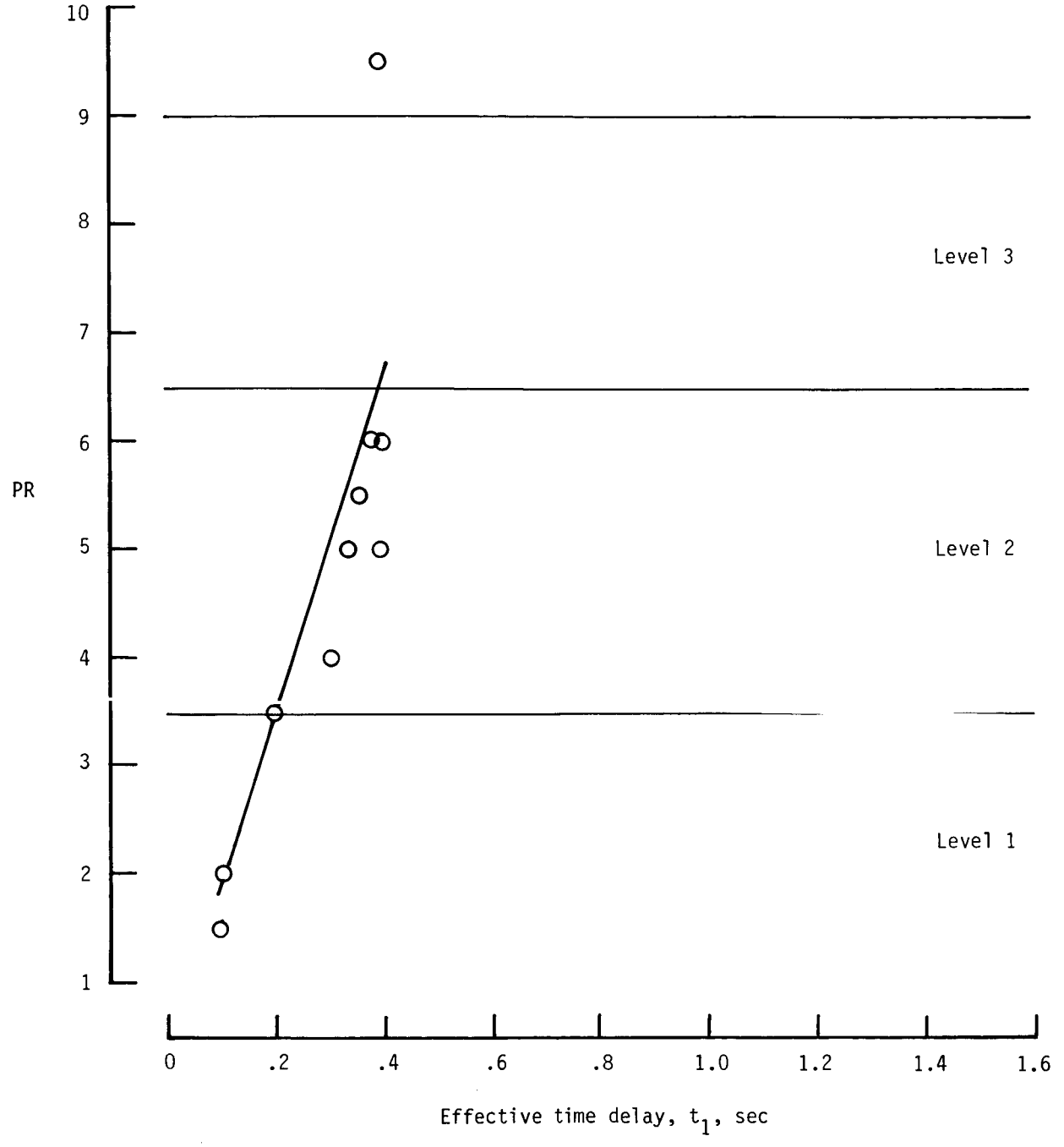

Figure 19. Effect of lateral effective time delay on pilot rating. Pilot 1; lagged time delay; crosswind conditions.

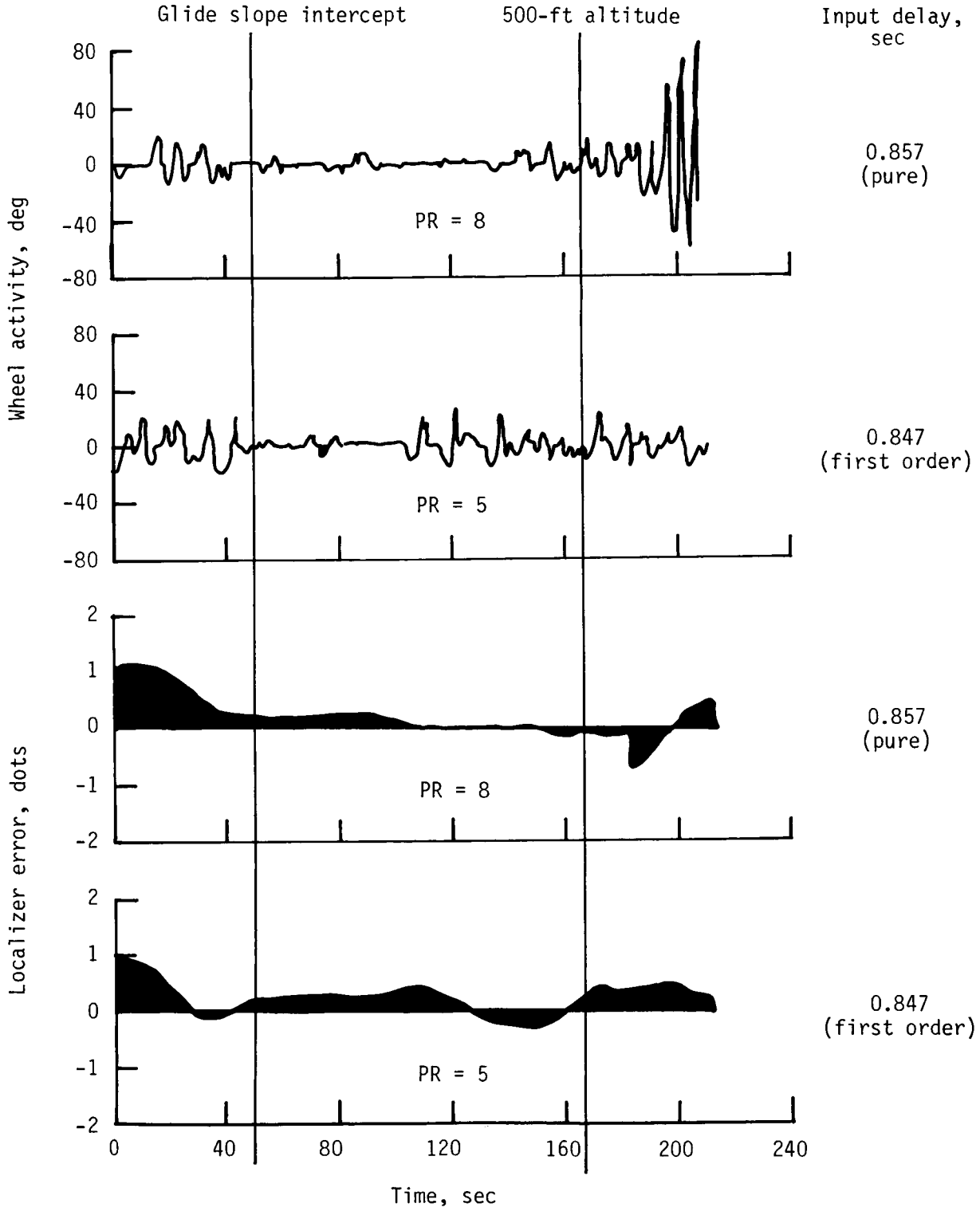

Figure 20. Comparison of effects of pure and lagged input delays on pilot work load (wheel activity) and tracking performance (localizer error). Pilot 1; crosswind conditions; one dot in localizer path represents error of 1.250°.

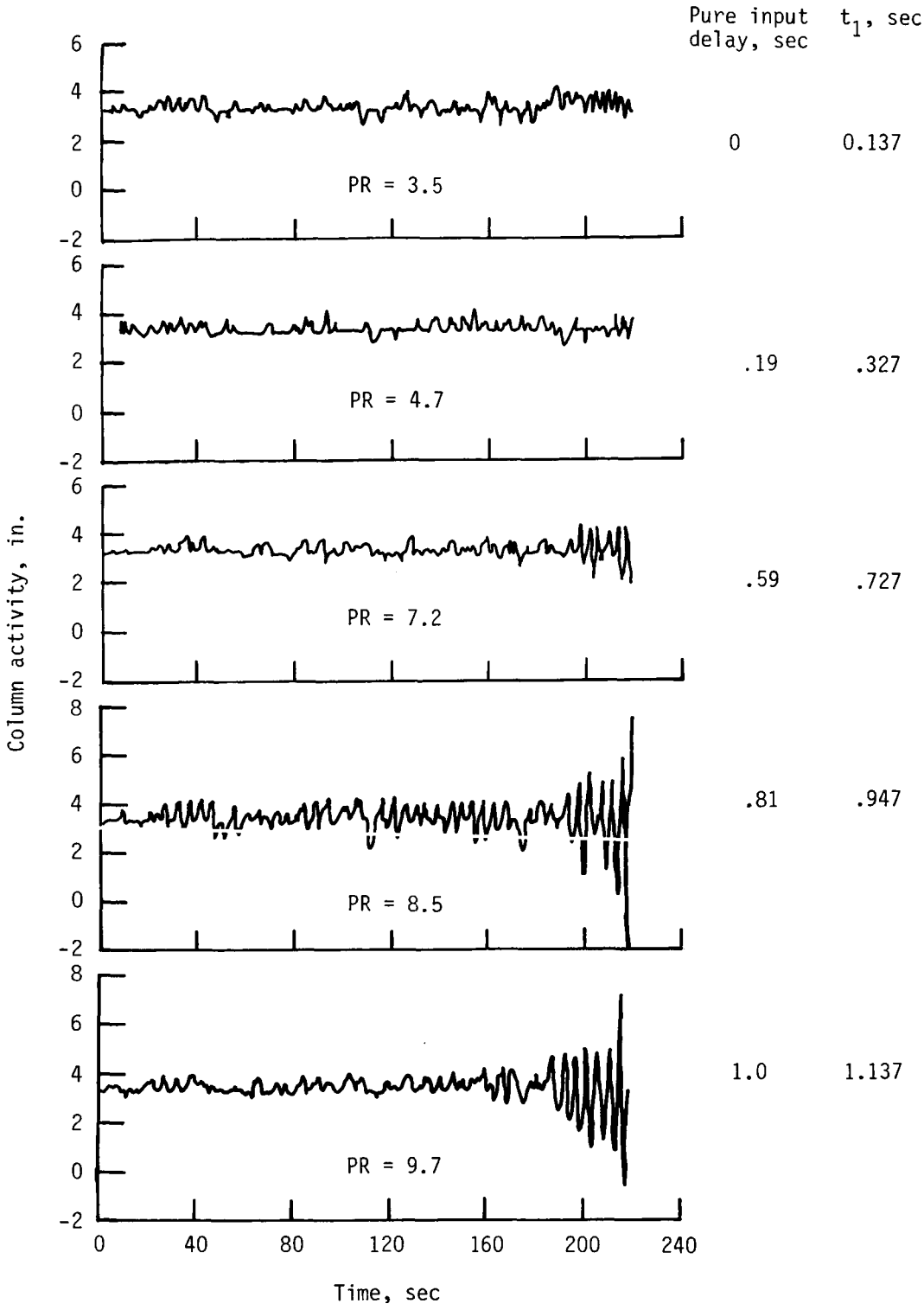

(a) Pilot work load (column activity).

Figure 21. Effect of column pure delay on longitudinal axis activity. Pilot 2; turbulent conditions; PR taken from fairing in figure 18.

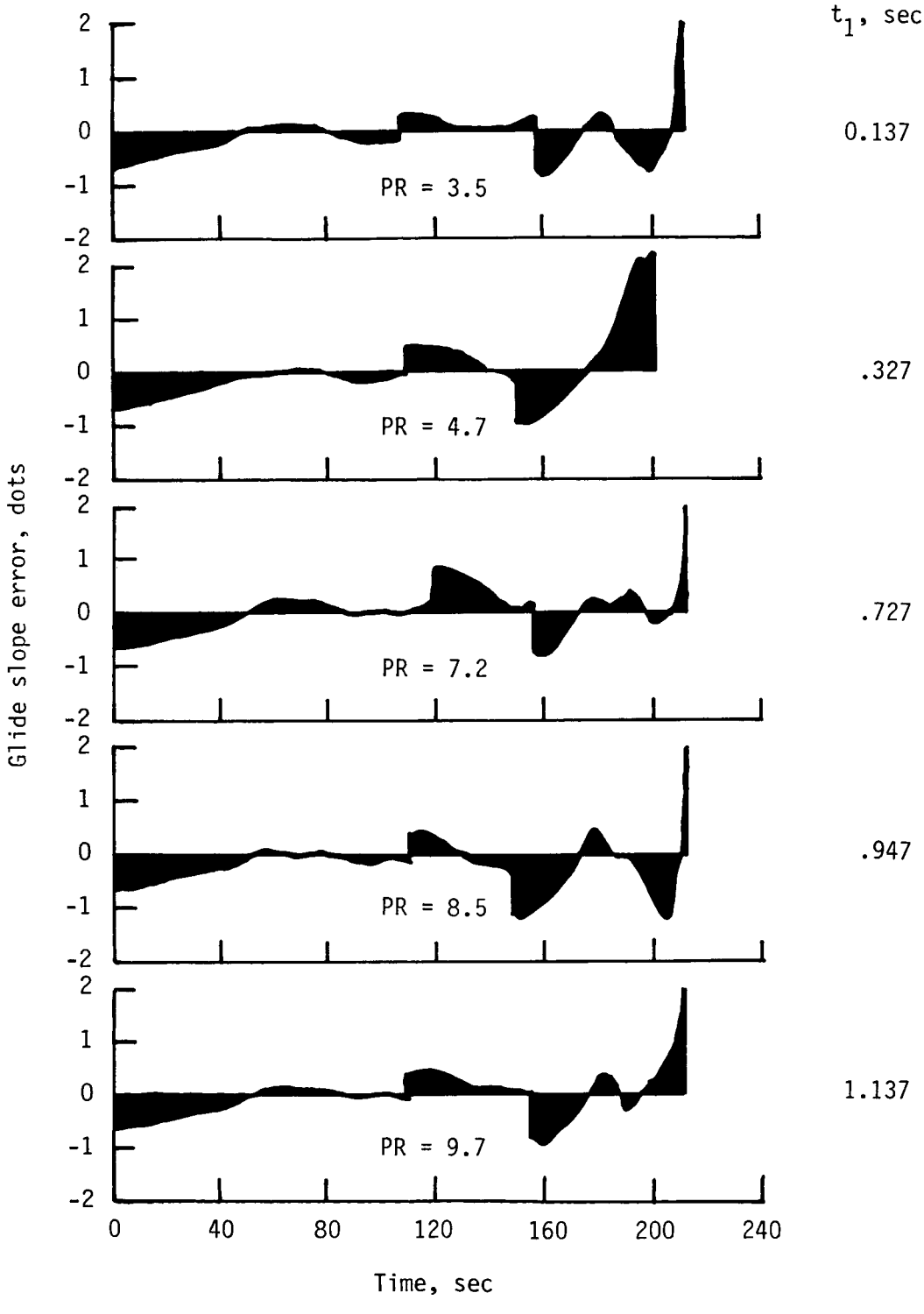

(b) Tracking performance (glide slope error). One dot in glide slope path represents error of 0.375°.

Figure 21. Concluded.

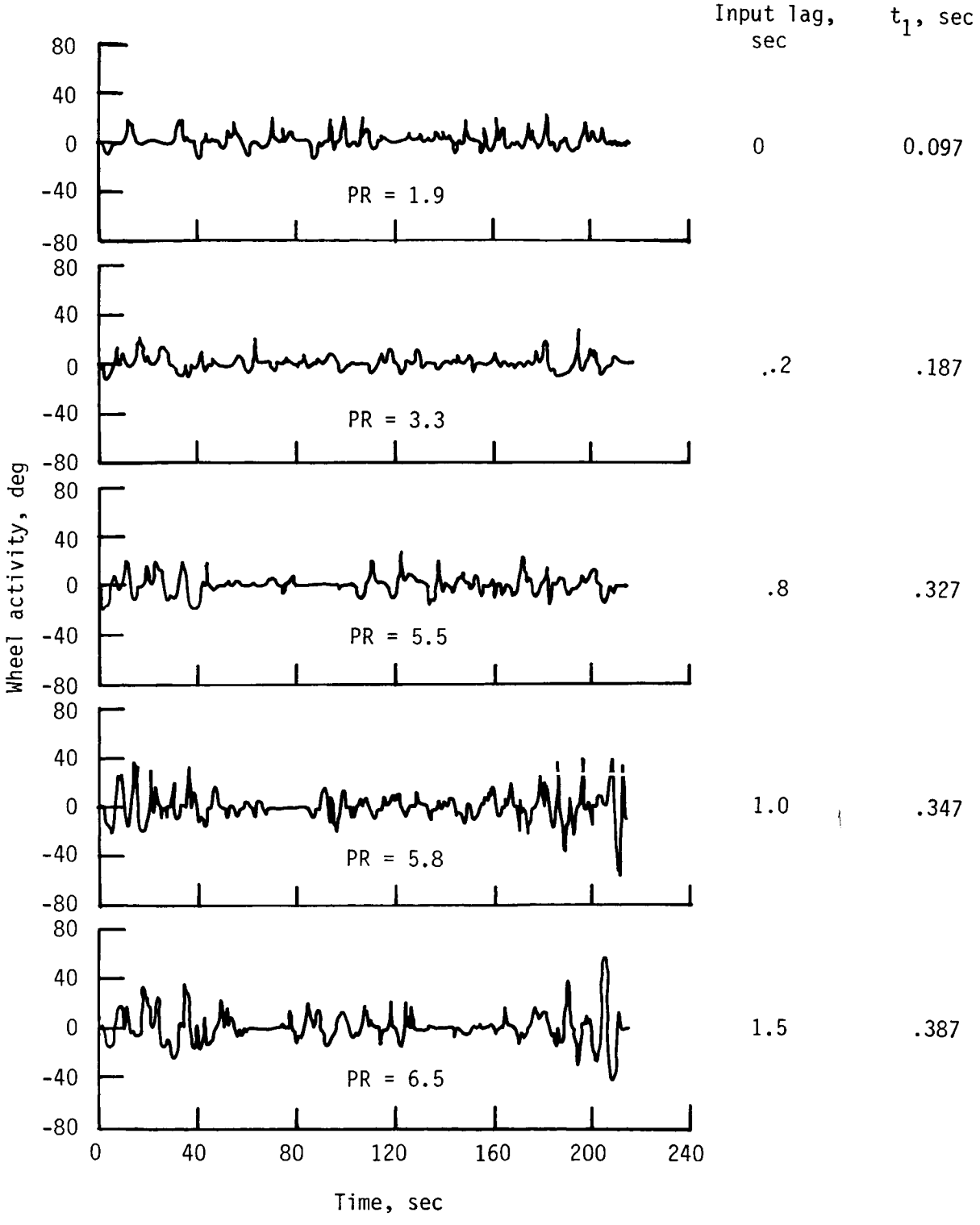

(a) Pilot work load (wheel activity).

Figure 22. Effect of wheel first-order lag on lateral axis activity. Pilot 1; crosswind conditions; PR taken from fairing in figure 19.

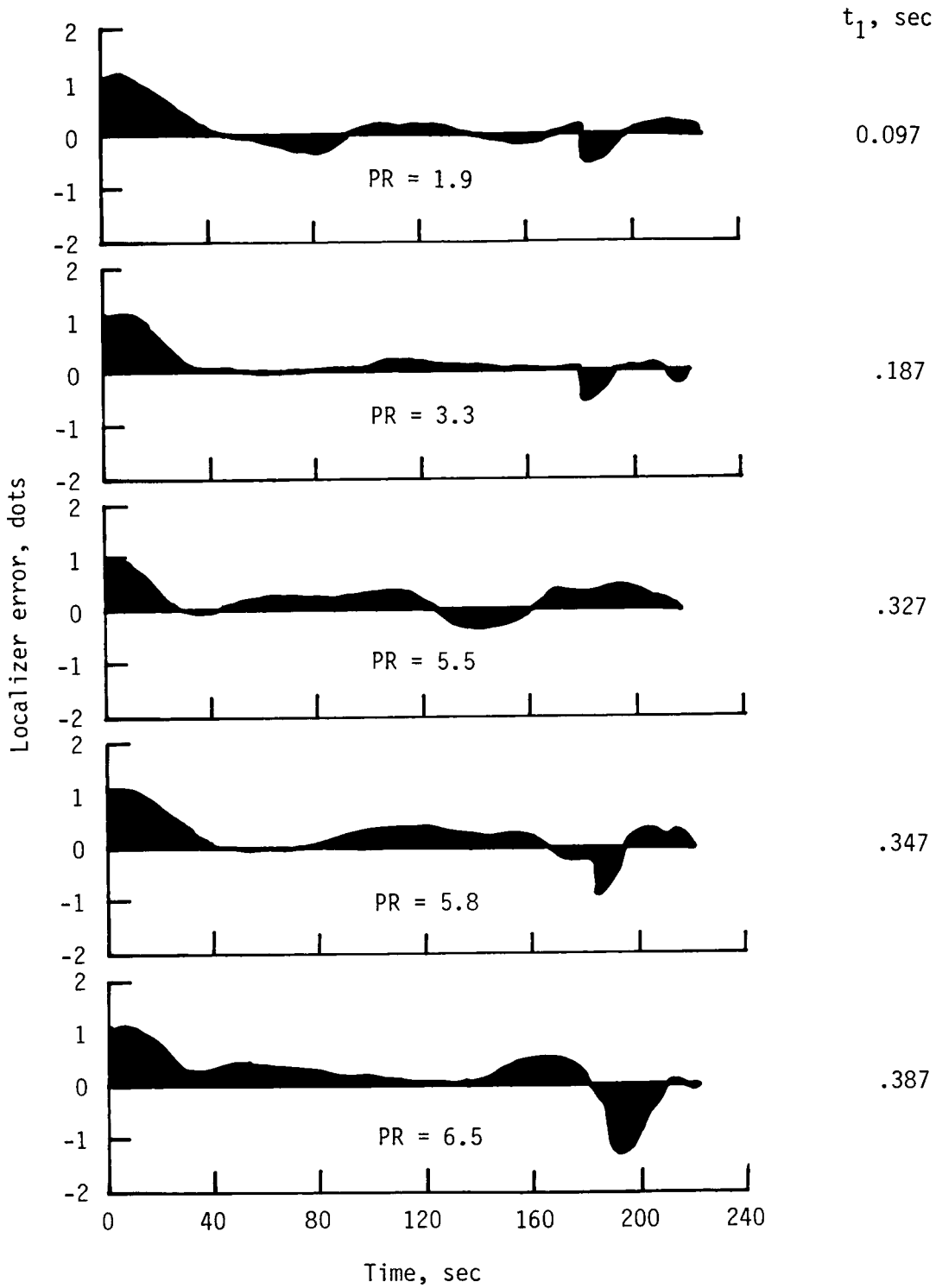

(b) Tracking performance (localizer error). One dot in localizer path represents error of 1.250°.

Figure 22. Concluded.

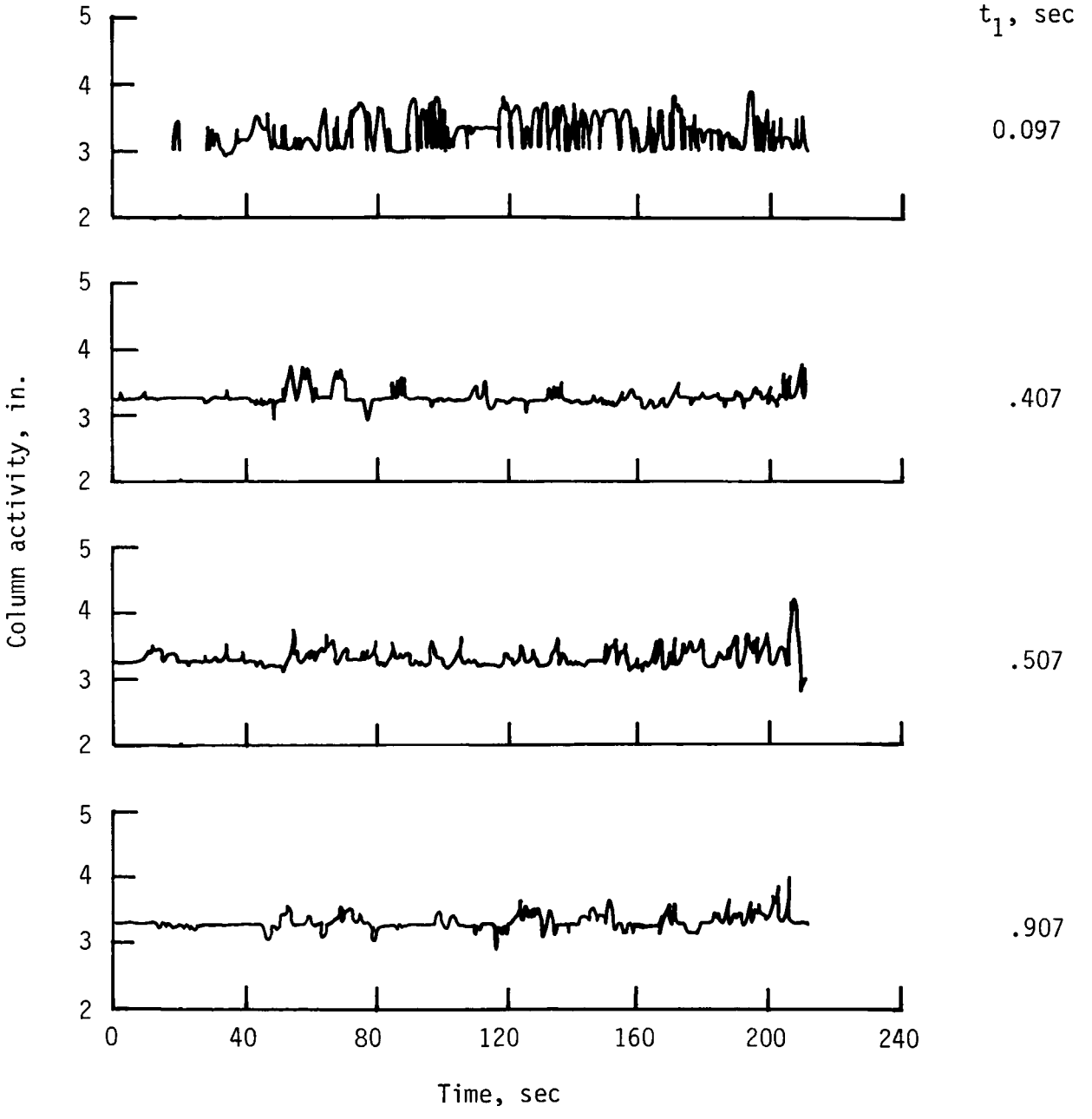

(a) Pilot work load (column activity).

Figure 23. Effect of wheel pure delay on longitudinal axis activity. Pilot 1; crosswind conditions; PR = 2.

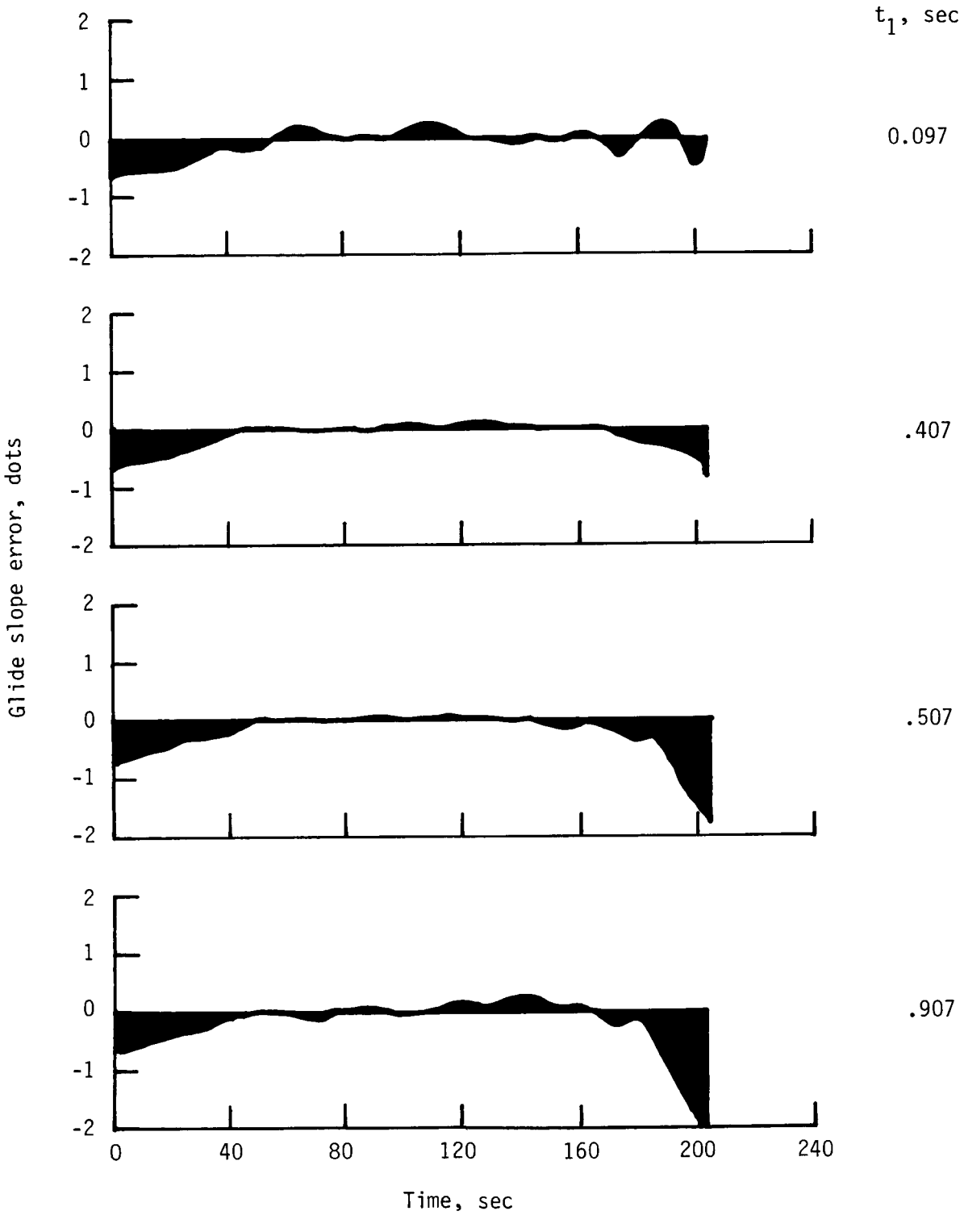

(b) Tracking performance (glide slope error). One dot in glide slope path represents error of 0.375°.

Figure 23. Concluded.

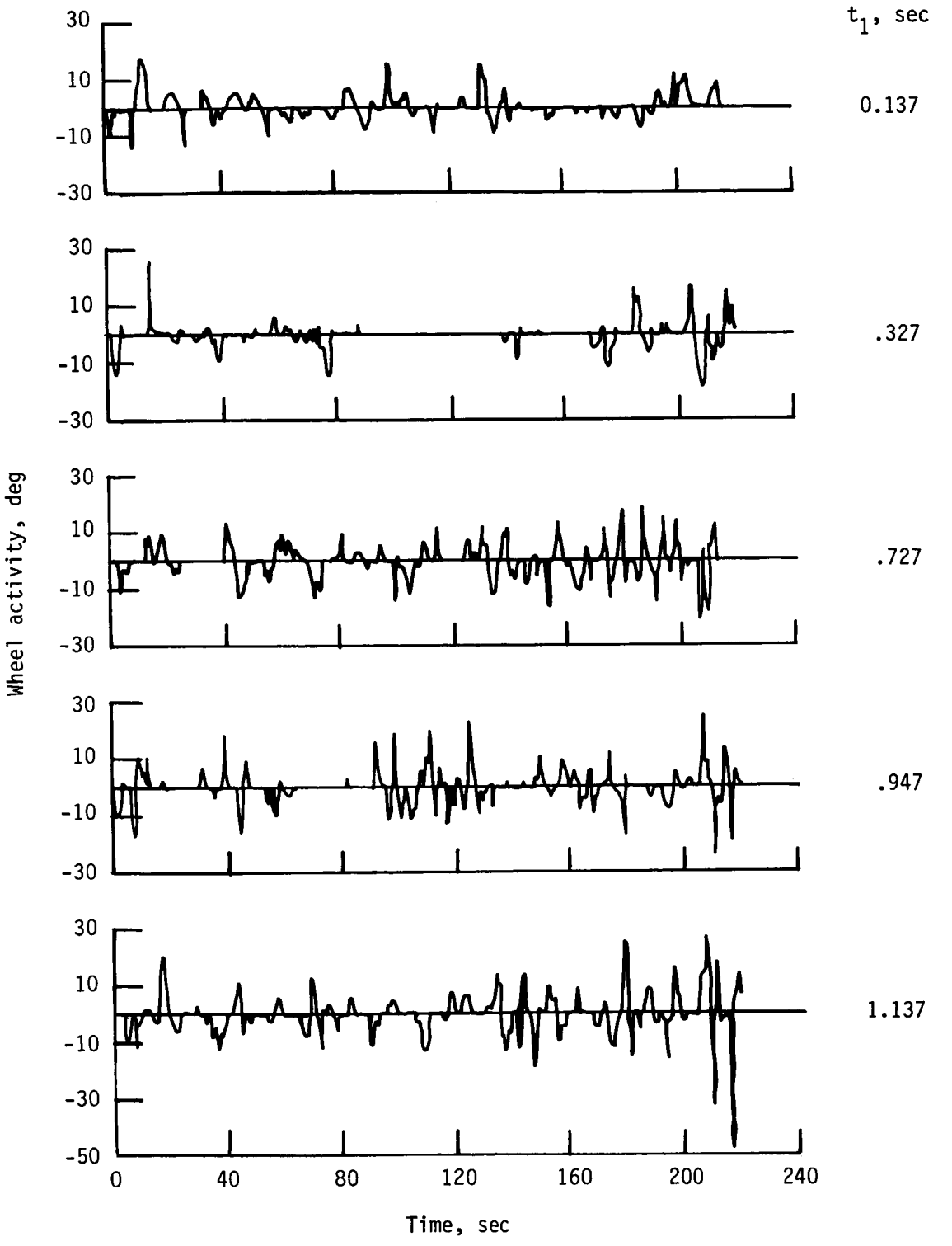

(a) Pilot work load (wheel activity).

Figure 24. Effect of column pure delay on lateral axis activity. Pilot 2; turbulent conditions; PR = 2.

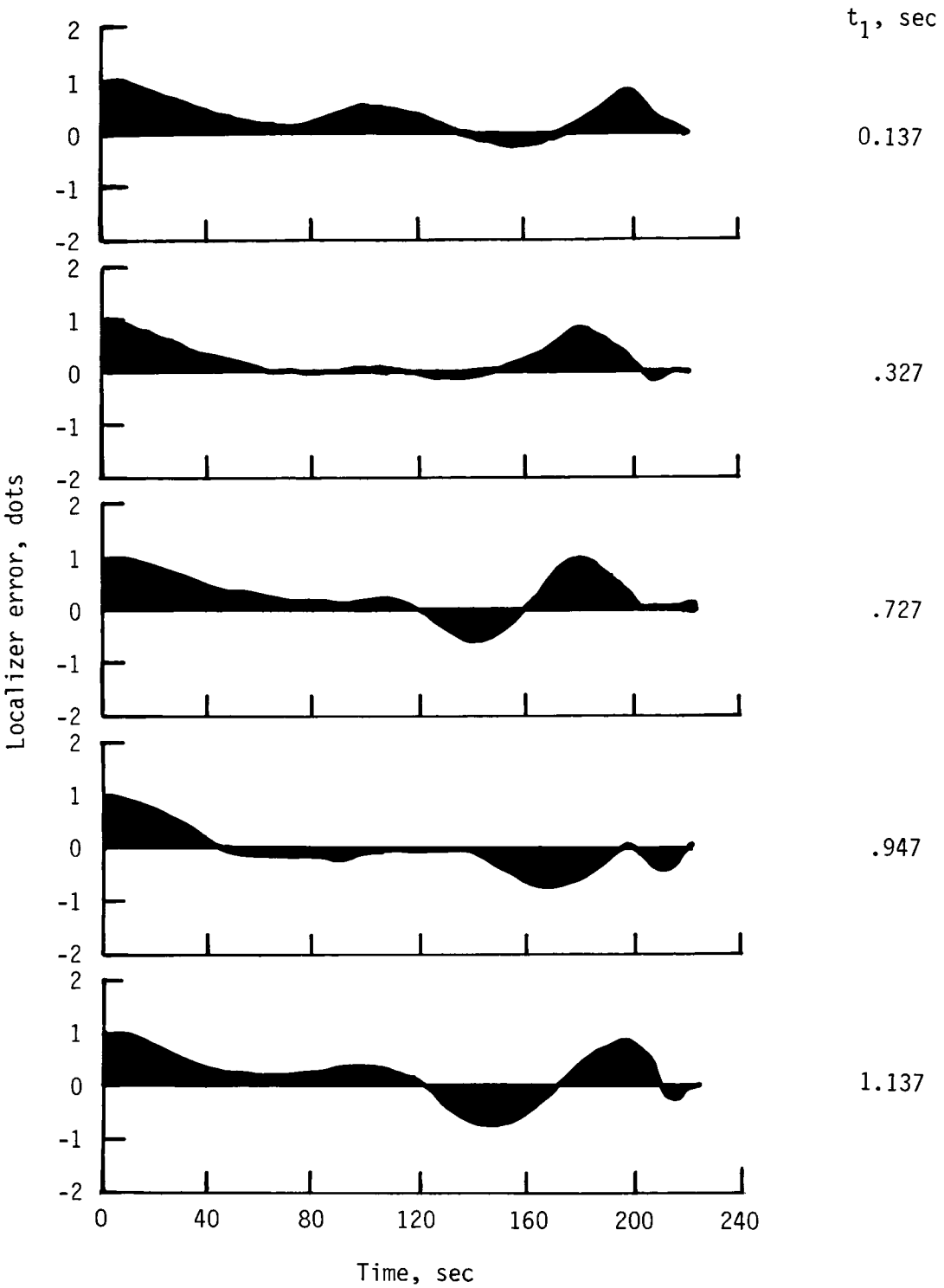

(b) Tracking performance (localizer error). One dot in localizer path represents error of 1.250°.

Figure 24. Concluded.

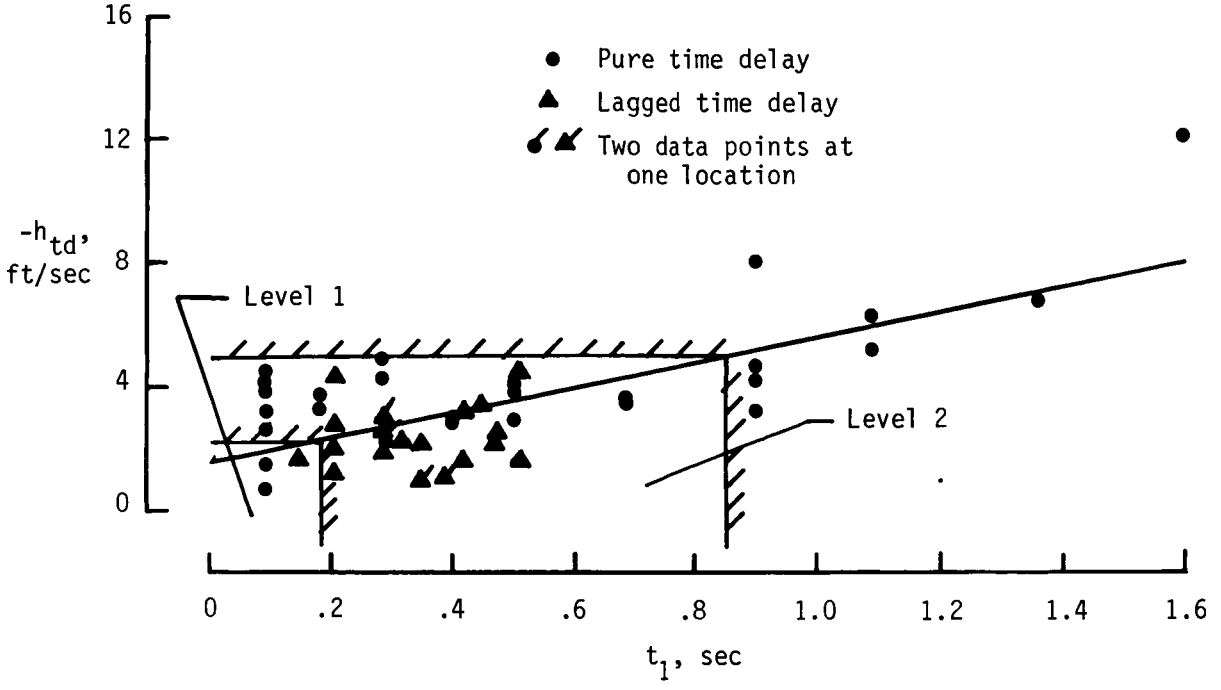

(a) Rate of sink at touchdown. Pilots 1, 2, and 3; turbulent conditions.

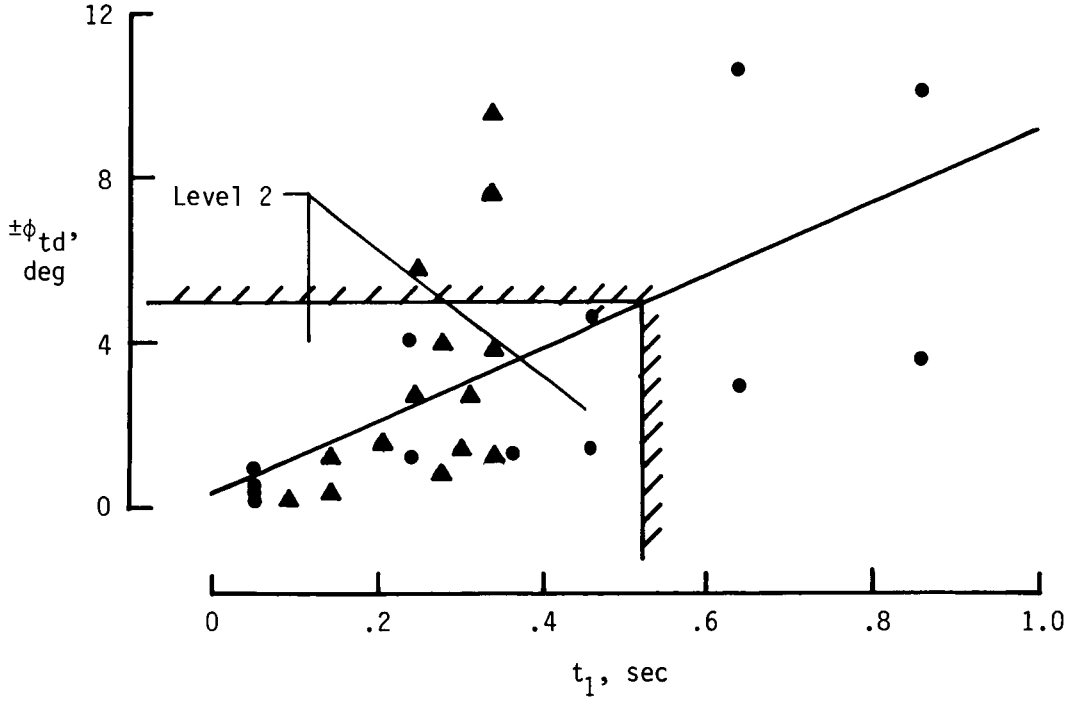

(b) Angle of roll at touchdown. Pilots 1 and 3; crosswind conditions.

Figure 25. Measured rate of sink and angle of roll at touchdown.

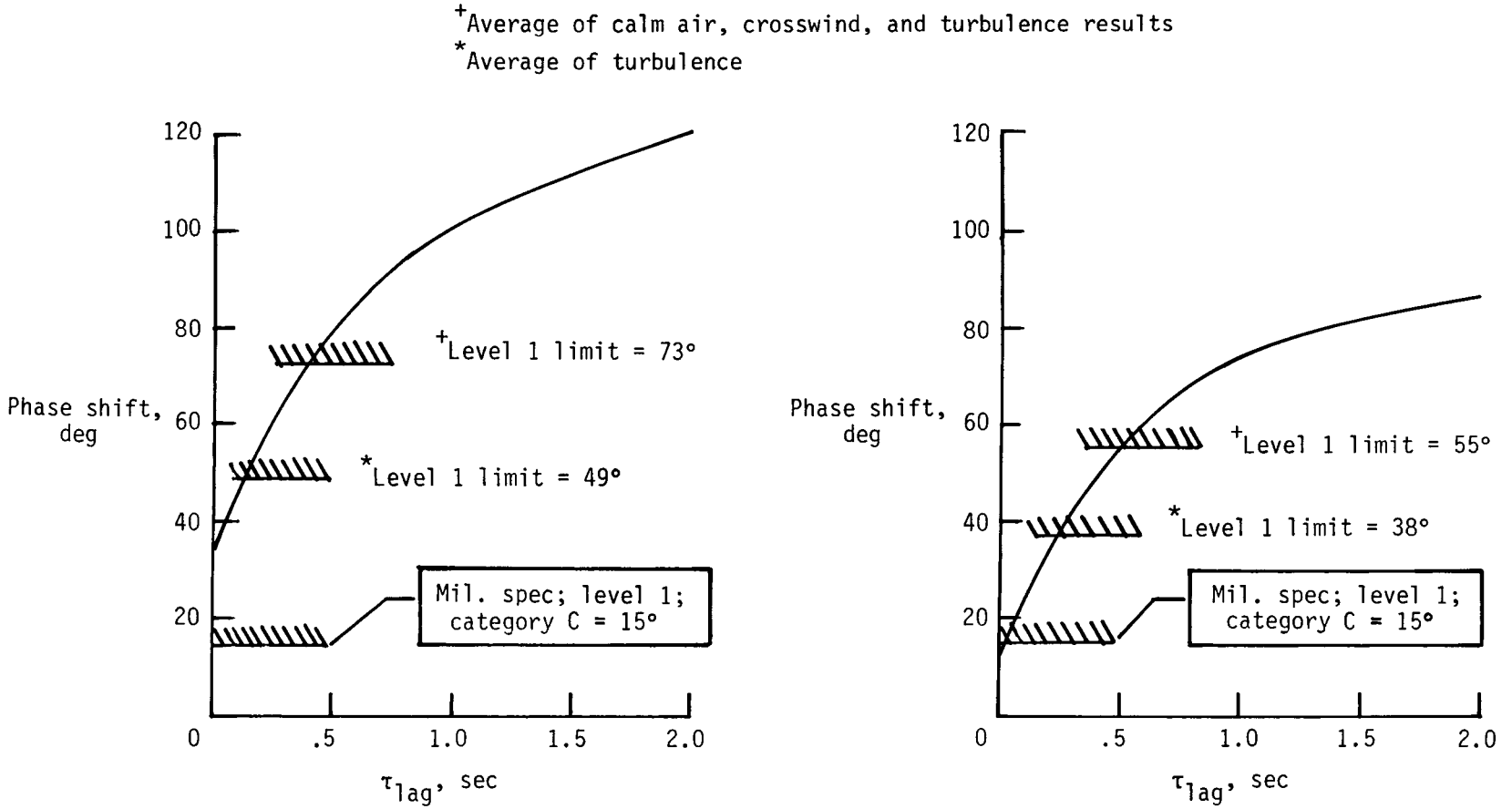

(a) Column-elevator control system characteristics.

(b) Wheel-aileron control system characteristics.

Figure 26. Phase shift between cockpit input and control surface deflection from Langley tests. $f = 1.96$ rad/sec.

Standard Bibliographic Page

1. Report No.	2. Government Accession No.	3. Recipient's Catalog No.
NASA TP-2652		

4. Title and Subtitle	5. Report Date
Piloted Simulator Study of Allowable Time Delays in Large-Airplane Response	February 1987
	6. Performing Organization Code: 505-66-01-01
7. Author(s): William D. Grantham, Paul M. Smith, Lee H. Person, Jr., Robert T. Meyer, and Stephen A. Tingas	8. Performing Organization Report No.: L-16149
9. Performing Organization Name and Address: NASA Langley Research Center, Hampton, VA 23665-5225	10. Work Unit No.
	11. Contract or Grant No.
12. Sponsoring Agency Name and Address: National Aeronautics and Space Administration, Washington, DC 20546-0001	13. Type of Report and Period Covered: Technical Paper
	14. Sponsoring Agency Code

15. Supplementary Notes

William D. Grantham and Lee H. Person, Jr.: Langley Research Center, Hampton, Virginia.
Paul M. Smith: PRC Kentron, Inc., Hampton, Virginia.
Robert T. Meyer and Stephen A. Tingas: Lockheed-Georgia Company, Marietta, Georgia.

16. Abstract

A piloted simulation was performed to determine the permissible time delay and phase shift in the flight control system of a specific large transport-type airplane. The study was conducted with a six-degree-of-freedom ground-based simulator and a math model similar to an advanced wide-body jet transport. Time delays in discrete and lagged form were incorporated into the longitudinal, lateral, and directional control systems of the airplane. Three experienced pilots flew simulated approaches and landings with random localizer and glide slope offsets during instrument tracking as their principal evaluation task. Results of the present study suggest a level 1 (satisfactory) handling qualities limit for an effective time delay of 0.15 sec in both the pitch and roll axes, as opposed to a 0.10-sec limit of the present specification (MIL-F-8785C) for both axes. Also, the present results suggest a level 2 (acceptable but unsatisfactory) handling qualities limit for an effective time delay of 0.82 sec and 0.57 sec for the pitch and roll axes, respectively, as opposed to 0.20 sec of the present specifications for both axes. In the area of phase shift between cockpit input and control surface deflection, the results of the present study, flown in turbulent air, suggest less severe phase shift limitations for the approach and landing task—approximately 50° in pitch and 40° in roll—as opposed to 15° of the present specifications for both axes.

17. Key Words (Suggested by Authors(s))	18. Distribution Statement
Flying qualities (low speed) Time delays Control system design Ground-based simulation	Unclassified—Unlimited Subject Category 08

19. Security Classif.(of this report)	20. Security Classif.(of this page)	21. No. of Pages	22. Price
Unclassified	Unclassified	67	A04

For sale by the National Technical Information Service, Springfield, Virginia 22161

NASA-Langley, 1987